Chapter Three

Supramolecular Daisy Chains

"Can you do addition," the White Queen asked, "What's one and one and one and one and one and one and one and one and one and one?" – Lewis Carroll

The research described in this **Chapter** is based upon two publications:

Ashton, P. R.; Baxter, I.; **Cantrill, S. J.**; Fyfe, M. C. T.; Glink, P. T.; Stoddart, J. F.; White, A. J. P.; Williams, D. J. *Angew. Chem., Int. Ed.* **1998**, *37*, 1294–1297.

Cantrill, S. J.; Stoddart, J. F.; Williams, D. J. *Am. Chem. Soc., Polym. Prepr.* **1999**, *40(2),* 1130–1131.

Table of Contents

Abstract: Two series of self-complementary daisy chain monomers—in which a secondary ammonium ion-containing arm is grafted onto a macrocycle with either a [24]- or [25]crown-8 constitution—have been synthesized. In the solid- and 'gas'-phases, the parent [24]crown-8 based monomer forms dimeric superstructures, as revealed by X-ray crystallography and mass spectrometry, respectively. Elucidation of the complicated solution phase behavior of this compound was facilitated by the synthesis and study of both deuterated, and fluorinated, analogues. These investigations revealed that the cyclic dimeric superstructure also dominates in solution, except for when extremes of either concentration (low), temperature (high), or solvent polarity (highly polar, *e.g.*, DMSO) are employed. Whereas, upon aggregation, the [24]crown-8 based daisy chain monomers have the capacity to form stereoisomeric superstructures—further complicating the study of this series of compounds—the assembly of [25]crown-8-based monomers gives only achiral superstructures. Unfortunately, however, the weaker association exhibited between secondary ammonium ions and crown ethers with a [25]crown-8 constitution, resulted in limited oligomerization—only dimeric and trimeric superstructures were formed at experimentally attainable concentrations—of [25]crown-8 based daisy chain monomers.

3.1. Introduction

The foundations of covalent polymer science were laid[1] in the early part of the 20th Century by the German chemist Hermann Staudinger.[2] Subsequently, the practical—and therefore industrial—significance of such high molecular weight materials was soon realized,[3] most notably by a group of DuPont researchers led by Wallace Carothers. Although cut tragically short,[4] his remarkable industrial career served to establish the polymer industry – an astounding legacy of immeasurable proportions. Since then, our everyday lives have become increasingly reliant upon polymeric materials. Nowadays, synthetic polymers are ubiquitous[5] in contemporary societies. However, the rise of supramolecular chemistry[6]—and its precise exploitation of delicate noncovalent interactions—has spurred investigations[7] into alternative approaches for polymer synthesis, challenging[8] the covalent bond's monopoly of the macromolecular world.

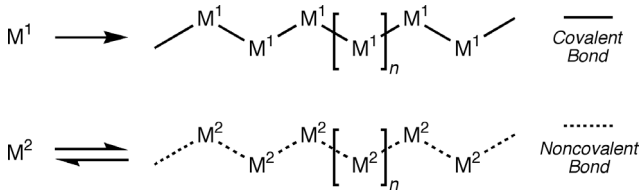

Figure 3.1. Top: A schematic representation of the covalent polymerization of monomer M^1. Bottom: A schematic representation of the noncovalent polymerization of a different monomer, M^2.

Whereas *molecular* polymerization relies upon the formation (Figure 3.1, Top) of *covalent* bonds between monomeric building blocks, the propagation step in a *supramolecular* polymerization proceeds *via* the formation (Figure 3.1, Bottom) of *noncovalent* bonds. Consequently, it is the inherent reversibility associated with the self-assembly[9] of such a dynamic aggregate that is anticipated[10] to bestow, upon the resulting polymer, properties that are distinct from those observed for traditional covalently-linked macromolecules. Foremost, polymerization performed under such a thermodynamically-controlled regime allows[7c,10] for a high degree of architectural control; incorrect or unspecific chain extensions are simply reversed in the constantly evolving system as it strives to find a local energy minimum. Therefore, this proof-reading process—in conjunction with a judicious design of monomer—can be exploited in order to exert a high degree of control over the final polymeric assembly. Furthermore, once assembled, the dynamic nature of such an assembly does not cease to be important. In fact, this very attribute remains of paramount importance, and renders such a species extremely sensitive (*i.e.*, responsive) to external environmental factors[10] such as mechanical stress or temperature. Once sheared, a material linked through noncovalent interactions retains—under the appropriate conditions—the capacity to 'heal' itself, reforming those bonds that were broken under the application of mechanical stress. Conversely, no correspondingly simple repair mechanism exists for covalent polymers. Secondly, changes in temperature should

affect[11] directly (and reversibly) the degree of polymerization (DP) exhibited by a supramolecular polymer, and in turn, may be used to attenuate bulk properties such as viscosity and/or rheology. In contrast, although potentially significant,[12] temperature effects upon covalent polymers are generally less dramatic, and are rarely[13] utilized in order to alter, reversibly, the degree of polymerization. Therefore, although in its infancy, the field of supramolecular polymerization offers much potential, and is expected to produce materials that have properties very different to those exhibited by their covalently-bonded cousins.

Although both (i) metal-ligand,[11,14] and (ii) π–π stacking[15] interactions have been utilized as the 'glue' with which monomers have been strung together to form supramolecular polymers, hydrogen bonding interactions have been exploited[10,16-20] far more widely. This preference arises as a consequence of the easily tunable—and, therefore, favorable—thermodynamic and kinetic parameters associated with hydrogen bonding interactions. Whereas the reversibility of some metal-ligand interactions is limited, and the strength of π–π stacking interactions is not sufficient enough to produce polymers with high DPs, hydrogen bonding interactions can be fine-tuned to deliver the desired properties. Although single,[16] double,[17] and triple[18] hydrogen bond manifolds have been employed in the construction of supramolecular polymers, the most successful has been that involving a quadruple[19] couple. Meijer and coworkers have exploited the strong dimerization[21] (Figure 3.2) of 2-ureido-4-pyrimidone

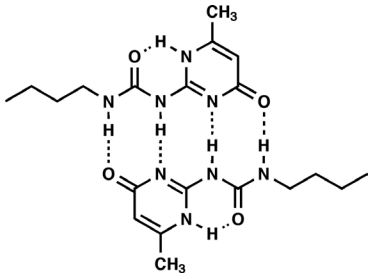

Figure 3.2. The hydrogen-bond-mediated dimerization of 2-butylureido-6-methyl pyrimidone.

derivatives—with K_a values in excess of 10^6 M^{-1} in $CHCl_3$—for the reversible formation[19] of hydrogen bonded supramolecular polymers and networks (a linear example is illustrated in Figure 3.3). Remarkably, the Eindhoven group were able to achieve DPs of *ca*. 700 in only a 40 mM solution, which corresponds to the formation of polymers having an average molar mass of ~5 x 10^5 g mol^{-1}. Therefore, by utilizing such a well-defined dimerization, a self-complementary monomer—incapable of undergoing intramolecular cyclization as a consequence of geometrical constraints—was shown to assemble, in a highly precise manner, into aggregated systems that exhibited polymer-like behavior in relatively dilute solutions.

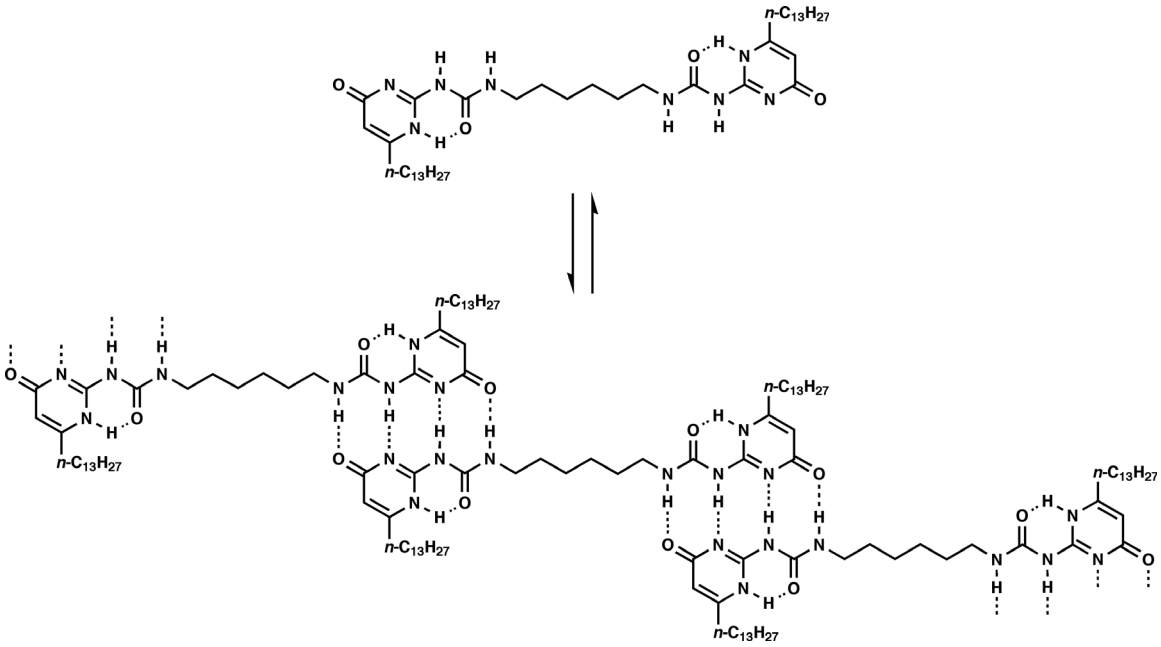

Figure 3.3. Reversible formation of a hydrogen-bonded linear supramolecular polymer formed from a monomer bearing two 2-ureido-4-pyrimidone end groups.

Rather than the simple face-to-face association (*vide supra*) of monomers, however, more complex topological interactions may be contrived. The concept (Figure 3.4) of threading a *rod*-shaped molecule through the macrocyclic cavity of another *ring*-shaped one—to

create[22] an interwoven host-guest complex (often referred to as a *pseudorotaxane*[23])—can be applied to the propagation step of a supramolecular polymerization. Covalently coupling the two mutually-recognizing components to one another[24] affords (Figure 3.5) a self-complementary monomer,[25] which has the capacity to self-assemble (Figure 3.6) into either linear[26] or cyclic[27] daisy chain[28] arrays. Furthermore, it can be envisioned that, unlike the supramolecular polymers discussed previously, these aggregates, if appropriately functionalized, can subsequently be trapped kinetically[29]—by undergoing a 'stoppering' reaction (Figure 3.7)—thus capturing an interlocked polymeric architecture, namely a polyrotaxane.[30]

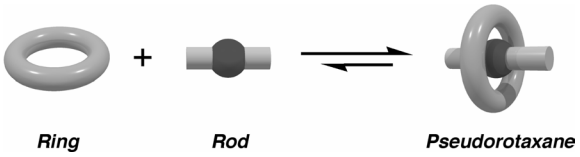

Figure 3.4. A schematic representation depicting the formation of a threaded 1:1 complex (a ***Pseudorotaxane***) between two complementary species wherein the cavity of a suitably-sized ***Ring*** is skewered by a linear ***Rod***.

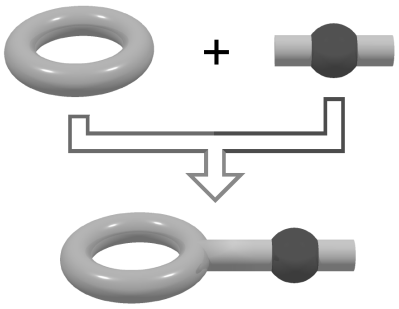

Figure 3.5. Conceptually, when two mutually-recognizing species are merged together, a single self-complementary entity is formed.

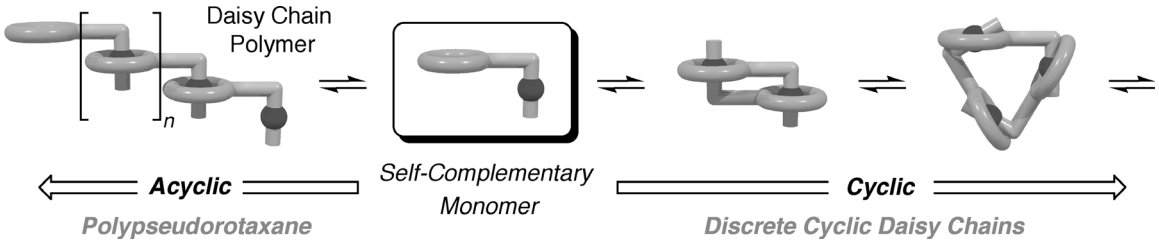

Figure 3.6. A schematic representation depicting how a daisy chain monomer can self assemble to form both cyclic and acyclic interwoven superstructures.

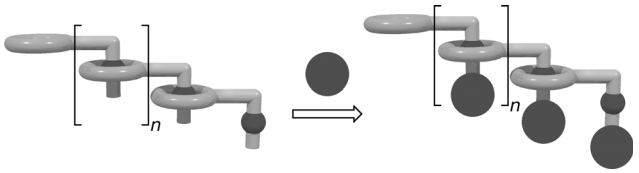

Figure 3.7. A schematic representation depicting the post-assembly kinetic capture—achieved by 'stoppering' of the threaded portions of each monomer with a bulky end group over which the macrocyclic portions cannot pass—of an interwoven acyclic daisy chain.

The research reported in this Chapter focuses upon the study of self-complementary molecules containing both crown ether and dibenzylammonium ion recognition sites. The design, synthesis, characterization, and ultimately aggregation behavior of these daisy chain monomers—which are based upon a well-understood[31] supramolecular interaction —are described.

3.2. [24]Crown-8-Based Systems

Conceptually, the initial target molecule (**1**-H·PF_6) arose as a consequence of splicing (Figure 3.8) both the dibenzo[24]crown-8 (**2**) and dibenzylammonium hexafluorophosphate (**3**-H·PF_6) structural motifs into one and the same molecule. Upon inspection of space-filling molecular models, it was apparent that such a structure satisfied one of the most important design criteria, *i.e.*, that intramolecular self-complexation is geometrically unfavorable – if not impossible.

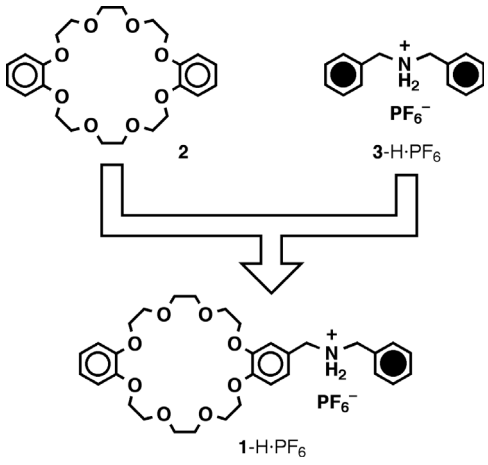

Figure 3.8. Combining the features of both DB24C8 (**2**) and dibenzylammonium hexafluorophosphate (**3**-H·PF_6) into one and the same molecule results in the design a self-complementary daisy chain monomer **1**-H·PF_6.

3.2.1. The Parent Monomer

The synthesis of this self-complementary daisy chain monomer is outlined in Scheme 3.1. Alkylation of 3,4-dihydroxybenzaldehyde (**4**) with the chloride **5** proceeded under basic

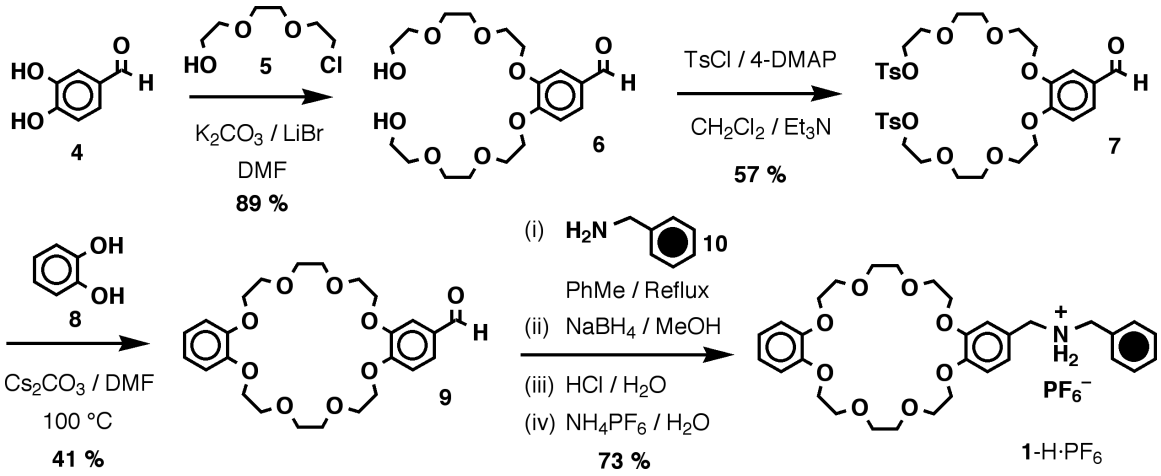

Scheme 3.1. The synthesis of the parent [24]crown-8 daisy chain monomer **1**-H·PF_6.

conditions in DMF to afford the diol **6** in very good yield. Tosylation of **6**, under standard conditions, gave the ditosylate **7**, which was subsequently reacted with catechol (**8**) to give the formyl-substituted DB24C8 derivative **9** in reasonable yield. Condensation of **9** with benzylamine (**10**), followed by borohydride reduction, protonation (HCl), and counterion exchange from Cl^- to PF_6^-, afforded the target compound **1**-H·PF_6 in a 73 % yield.

Mass Spectrometry

The liquid secondary ion (LSI) mass spectrum of the salt **1**-H·PF_6 revealed (Figure 3.9) intense peaks—encountered at m/z = 1281 and 1135—corresponding to the creation of dimeric supermolecules in the 'gas phase'. These peaks can be identified as the supramolecular ions

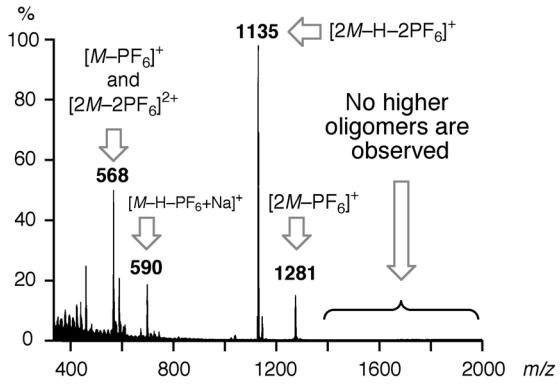

Figure 3.9. The LSI-mass spectrum of **1**-H·PF_6.

$[(\mathbf{1}\text{-H})_2(PF_6)]^+$ and $[(\mathbf{1}\text{-H})(\mathbf{1})]^+$, respectively, and indicate the aggregation of two monomer units. Interestingly, the peak at m/z = 1135 was observed to be the spectrum's base peak—it was approximately twice as intense as the peak located at m/z = 568, which could correspond to the species $[\mathbf{1}\text{-H}]^+$. However, closer inspection of the expanded spectrum revealed that, the isotope peaks—in the area surrounding the '$[\mathbf{1}\text{-H}]^+$' peak—are separated by 0.5 mass units, indicating the presence of a doubly-charged species with a mass corresponding to a dimeric entity, thus providing evidence for the existence of the doubly charged dimer $[(\mathbf{1}\text{-H})_2]^{2+}$. It is also notable that no higher order oligomeric species were detected, inferring that they are either (i) not formed, (ii) do not survive the conditions of the analysis, or (iii) are not amenable to mass spectrometric analysis, *i.e.*, do not ionize as well as their smaller siblings. In conclusion, the mass spectrometric evidence suggests that this self-complementary daisy chain monomer does indeed exist in the 'gas-phase' as a dimeric species. Furthermore, the absence of other, higher order, oligomers seems to indicate an overwhelming preference for dimer formation.

X-Ray Crystallography

Gratifyingly, the trifluoroacetate[32] salt $\mathbf{1}\text{-H}\cdot O_2CCF_3$ crystallized on standing from a mixture of ($EtOAc/C_6H_{14}/CD_3CN$, *ca*. 10:10:1) affording crystals suitable for single crystal X-ray diffraction analysis. The X-ray structural analysis of $\mathbf{1}\text{-H}\cdot O_2CCF_3$ revealed (Figure 3.10) the formation of a C_2 symmetric head-to-tail dimeric structure in which the benzylammonium cationic portions of each component thread simultaneously through the DB24C8 portions of their adjacent counterparts. The pairs of molecules are

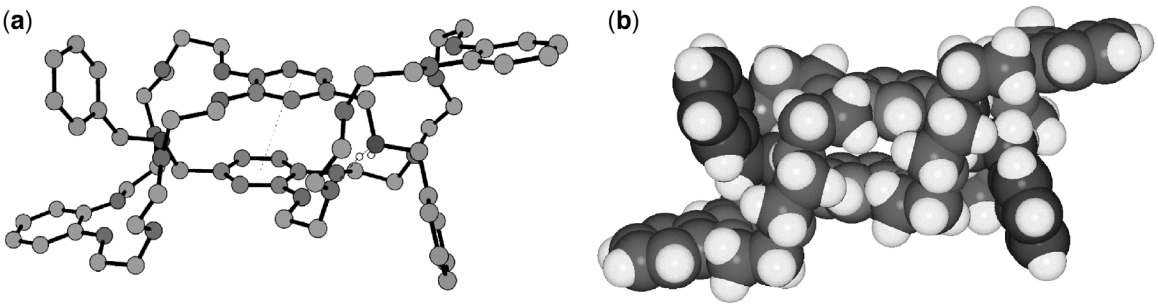

Figure 3.10. (**a**) Ball-and-stick and (**b**) space-filling representations of the C_2 symmetric head-to-tail dimer formed by **1**-H^+.

stabilized by a combination of π–π stacking of the substituted catechol rings (interplanar and centroid-centroid separations of 3.36 and 3.55 Å, respectively) and [N^+–H···O] hydrogen bonds between one of the hydrogen atoms on each NH_2^+ center and a polyether oxygen atom within one of the linkages of each DB24C8 component ([N^+···O], [H···O] distances are 2.91 and 2.02 Å, respectively, with an [N^+–H···O] angle of 170˚). Investigation of the packing of the molecules revealed (Figure 3.11) the formation of a mosaic-like sheet of dimer pairs. This supramolecular sheet self-assembles *via*, in one

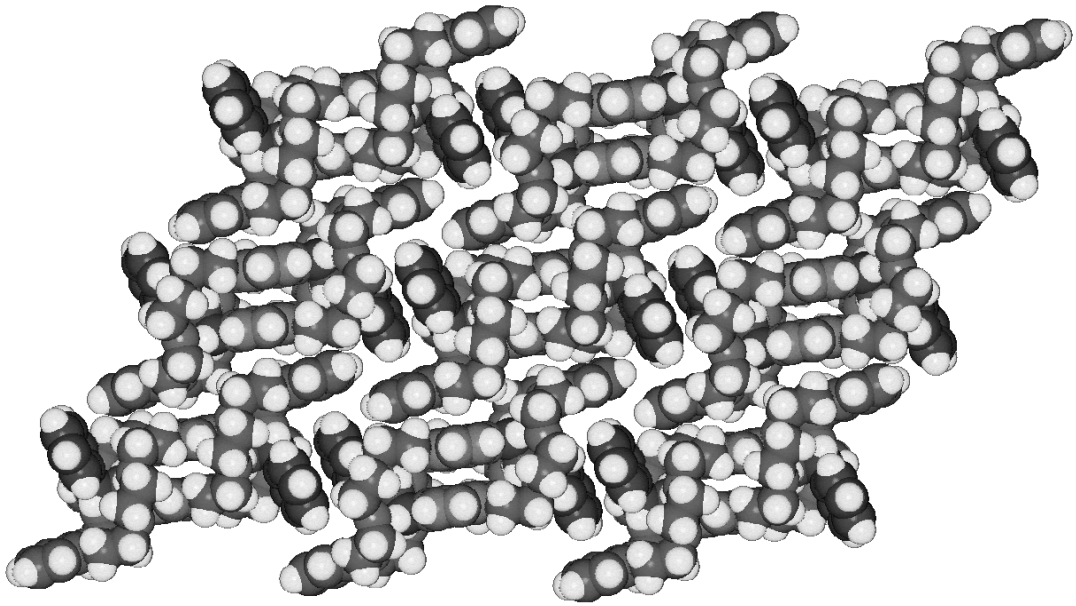

Figure 3.11. The mosaic-like sheet of dimer pairs formed by **1**-H^+.

direction (Figure 3.12), a combination of face-to-face π–π stacking of the terminal phenyl rings of each monomer (interplanar and centroid-centroid separations of 3.62 and 3.73 Å, respectively) and edge-to-face aromatic interactions between these pairs of interacting terminal rings and the immediately adjacent unsubstituted catechol rings of neighboring

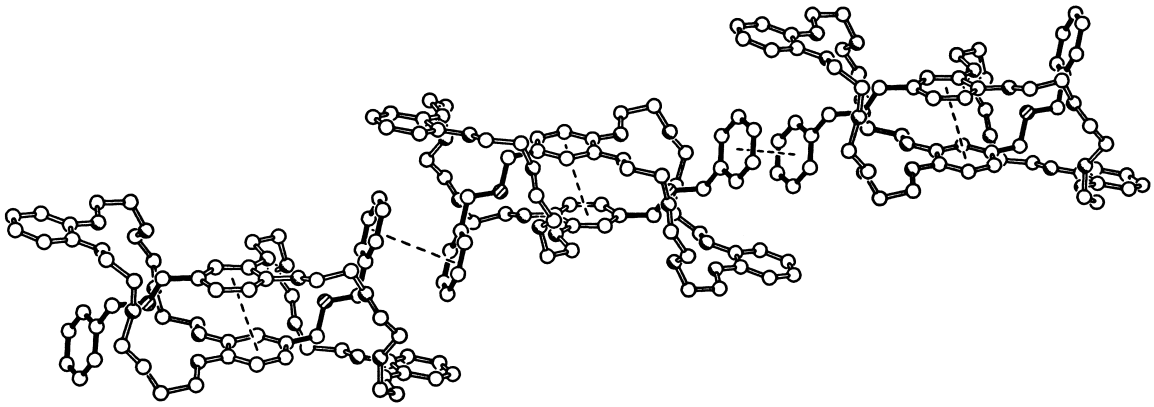

Figure 3.12. The packing of dimers of **1**-H^+, in one direction, *via* face-to-face π-π stacking interactions and edge-to-face aromatic interactions.

dimer pairs (centroid-centroid separation is 5.06 Å, the rings being inclined by 83° to each other). Adjacent rows of supermolecules are aligned such that pairs of *O*-methylene hydrogen atoms within the polyether linkages in one π-stacked row are directed from above and below into the π-faces of the already π–π stacked substituted catechol rings within each dimer, producing the array depicted in Figure 3.13. The [H···π] distances are 2.69 Å and the associated [C–H···π] angles are 161°.

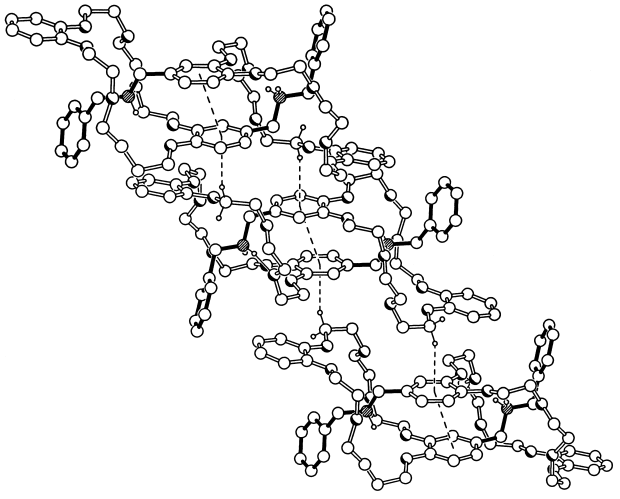

Figure 3.13. The stacking of adjacent rows of dimers of **1**-H^+, *via* C–H···π interactions.

Channels are formed between adjacent sheets, which are populated by trifluoroacetate and trifluoroacetic acid counterions / solvent molecules.

Interestingly, in this instance, the interaction between the two achiral **1**-H$^+$ cations is dissymmetrizing, rendering a chiral association and resulting in the formation (Figure 3.14a,c) of a pair of enantiomeric C_2-symmetric supramolecular stereoisomers. This kind of interaction occurs because the enantiotopic faces of the interacting **1**-H$^+$ cations possess the same prochirality. However, an alternative situation can also be envisaged: a diastereoisomeric '*meso*' supramolecular stereoisomer—endowed with C_i symmetry—would have been created (Figure 3.14b) if the interacting faces of individual **1**-H$^+$ cations had maintained different prochiralities upon crystallization.

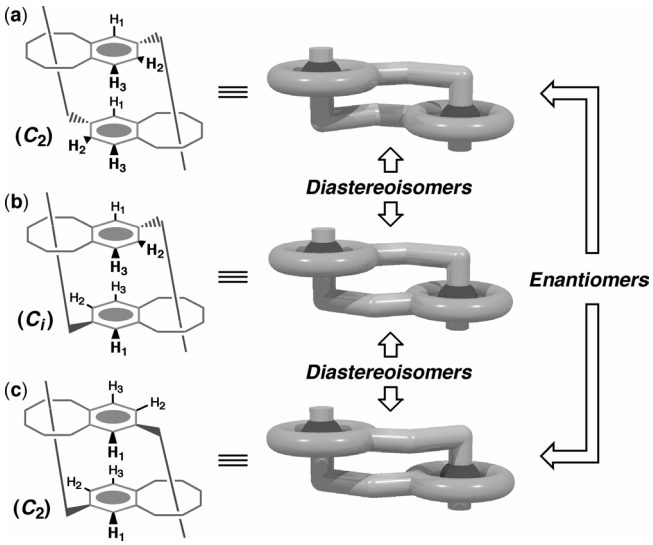

Figure 3.14. The three cyclic stereoisomeric superstructures that can be formed upon dimerization of **1**-H·PF$_6$.

In other words, the noncovalent dimerization of the **1**-H$^+$ cation proceeds diastereoselectively, at least in the solid state, to furnish a racemic mixture of the C_2-symmetric supramolecular stereoisomers.

NMR Spectroscopy

The ^{1}H NMR spectrum (300 MHz, 298 K) of the hexafluorophosphate salt **1**-H·PF$_6$—recorded in CD_3SOCD_3—is shown in Figure 3.15a. The spectrum is relatively

simple, and each of the peaks can be assigned (as annotated in the Figure) as arising from a particular set of protons. In contrast, however, when the ^{1}H NMR spectrum (400 MHz, 273 K) of **1**-H·PF_6 was recorded in CD_3CN, a more complicated spectrum (Figure 3.15b)

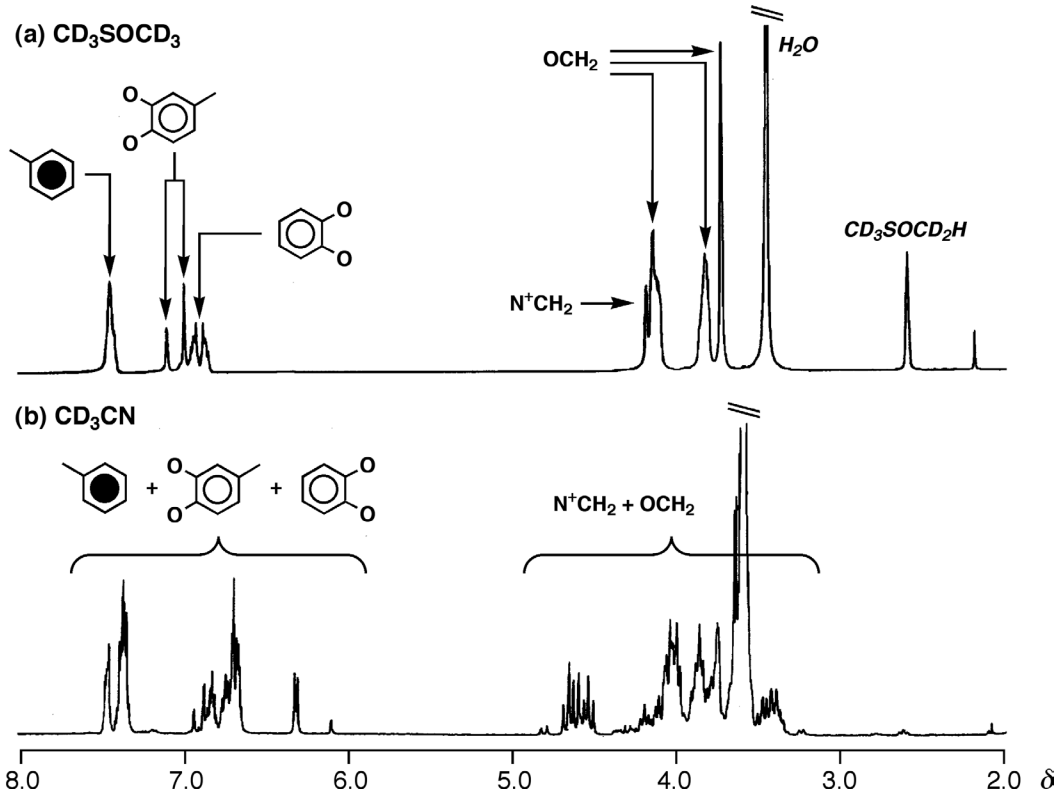

Figure 3.15. The ^{1}H NMR spectra of **1**-H·PF_6 dissolved in (**a**) CD_3SOCD_3 (300 MHz, 298 K), and (**b**) CD_3CN (400 MHz, 273 K).

was observed. Signals arising from the resonances of the OCH_2 and N^+CH_2 protons are now smeared across the region δ = 3.0–5.0 ppm, and dramatic changes are also seen in the aromatic region of the spectrum. It can be appreciated easily that the spectrum obtained in CD_3SOCD_3 is far simpler than that observed in the case of the CD_3CN. Indeed, this simpler spectrum can be rationalized by ascribing it to the 'monomeric' daisy chain species, *i.e.*, no complexation is occurring. As expected,[33] in the more polar CD_3SOCD_3,

solvation of the ammonium center occurs preferentially by the solvent molecules rather than by the macrocyclic polyether component, thus precluding intermolecular association of the daisy chain monomers. Conversely, in the less polar CD_3CN solution, the preference for complexation of the ammonium center by the solvent is less overwhelming,[33] and hence ammonium ion complexation ensues. Consequently the formation of numerous oligomeric species—all in slow exchange[34] with one another—could result in the complicated spectrum observed for **1**-H·PF_6 in CD_3CN solution.

Unfortunately, the only well-resolved peaks in this spectrum, are two doublets (Figure 3.16)—with coupling constants of ~1.5 and 8.0 Hz, respectively—that have been shifted upfield from the remainder of the signals associated with the aromatic protons. The magnitude of the *J* values, in addition to the chemical shifts of these signals (δ = 6.17 and 6.43, respectively), can be used to infer which protons are responsible for these characteristic peaks. With regard to aromatic proton spin systems, coupling constants of 1.5 and 8.0 Hz suggest *meta* (^4J) and *ortho* (^3J) coupling, respectively. Therefore, such coupling patterns, as well as δ values, are unlikely to arise from the protons of the terminal benzyl ring – the protons of such an electron

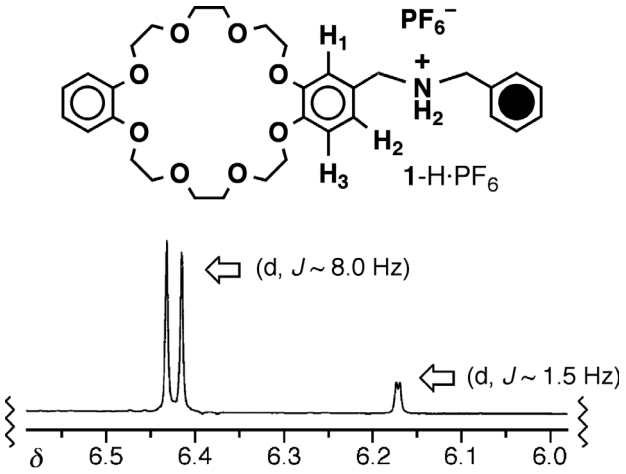

Figure 3.16. An expansion of the two upfield-shifted aromatic doublets that appear in the ^{1}H NMR spectrum (400 MHz, CD_3CN, 273 K) of **1**-H·PF_6.

neutral (neither especially electron poor or rich) aromatic ring would be expected to produce signals with δ values of ~7.1–7.6 ppm, as well as give rise to a more complicated splitting pattern. Similar logic leads to the same conclusion for the protons of the 'catechol' ring (*i.e.*, the *o*-$C_6H_4O_2$ aromatic residue) of **1**-H·PF_6. Although an electron rich ring, the resonances of protons attached to 1,2-dioxy-substituted benzene rings generally[35] give rise to second-order multiplets (or occasionally broad singlets) centered around δ ~6.8–7.0 ppm. The most plausible explanation—which is reinforced later in Section 3.3.2—is one based upon the protons attached to the central aromatic ring of **1**-H·PF_6, namely: H_1, H_2, and H_3. An *ortho*-coupled doublet is anticipated for H_3, and a *meta*-coupled doublet is expected for H_1. The corresponding doublet of doublets for H_2 is seemingly buried amongst other resonances, most likely those associated with the signals arising from the resonances of the protons of the 'catechol' ring – once again, see Section 3.3.2. Furthermore, the relative upfield shift of these distinctive doublets, could result from the offset face-to-face stacking of two of these central aromatic units, as would be anticipated—based upon observations of the solid state superstructure (*vide supra*)—for a cyclic head-to-tail dimer. Moreover, the ratio of the intensities of these doublets is ~5:1, indicating that they most likely originate from two different aggregated species. Therefore, one possible rationalization could be that, in a cyclic dimer superstructure, H_1 lies in close proximity to the shielding zone of another aromatic ring, whereas in a cyclic trimeric system, H_3 is the proton that is influenced more strongly, or *vice versa*. However, are the central aromatic residues of **1**-H·PF_6 likely to stack in such a fashion when constrained into a cyclic trimer superstructure? Inspection of space-filling molecular models suggests that this scenario is unlikely. Perhaps a more plausible

explanation is that both of the distinctive upfield-shifted doublets result as a consequence of *different* cyclic dimeric superstructures. As noted previously, three possible stereoisomeric head-to-tail dimers (recall Figure 3.14) can be formed – an enantiomeric pair and a third diastereoisomeric '*meso*' form. Despite the presence of only the racemate in the solid-state superstructure, this inherently kinetic crystallization process does not rule out the possibility that the '*meso*' diastereoisomer is also present in solution. Hence, one dimeric diastereoisomer may[36] position H_3 within a shielding zone, and the other, H_1. In a substantial portion of the remainder of this Chapter evidence will be presented in support of this 'dimer' hypothesis. First of all, however, examining (i) acid/base, (ii) temperature, and (iii) concentration effects upon the solution phase behavior of this dynamic self-complementary aggregating system will be appraised.

Acid/Base Effects

The spectrum of the amine **1** is shown in Figure 3.17a. Upon addition of an excess of CF_3CO_2D (10 mol equiv.) to the NMR tube, the spectrum shown in Figure 3.17b was obtained. The complexity of this spectrum is reminiscent of that exhibited (Figure 3.15b) by the hexafluorophosphate salt **1**-H·PF_6. Subsequently, addition of an excess of Et_3N (20 mol equiv.) to the same NMR tube, followed by spectroscopic analysis, resulted in the spectrum shown in Figure 3.17c, which is essentially the same as that illustrated in Figure 3.17a, except that there are additional peaks arising from the presence of $[Et_3NH]^+[CF_3CO_2]^-$ and an excess of Et_3N. These observations suggest that, addition of CF_3CO_2D to the amine **1** results in deuteration to give the trifluoroacetate salt

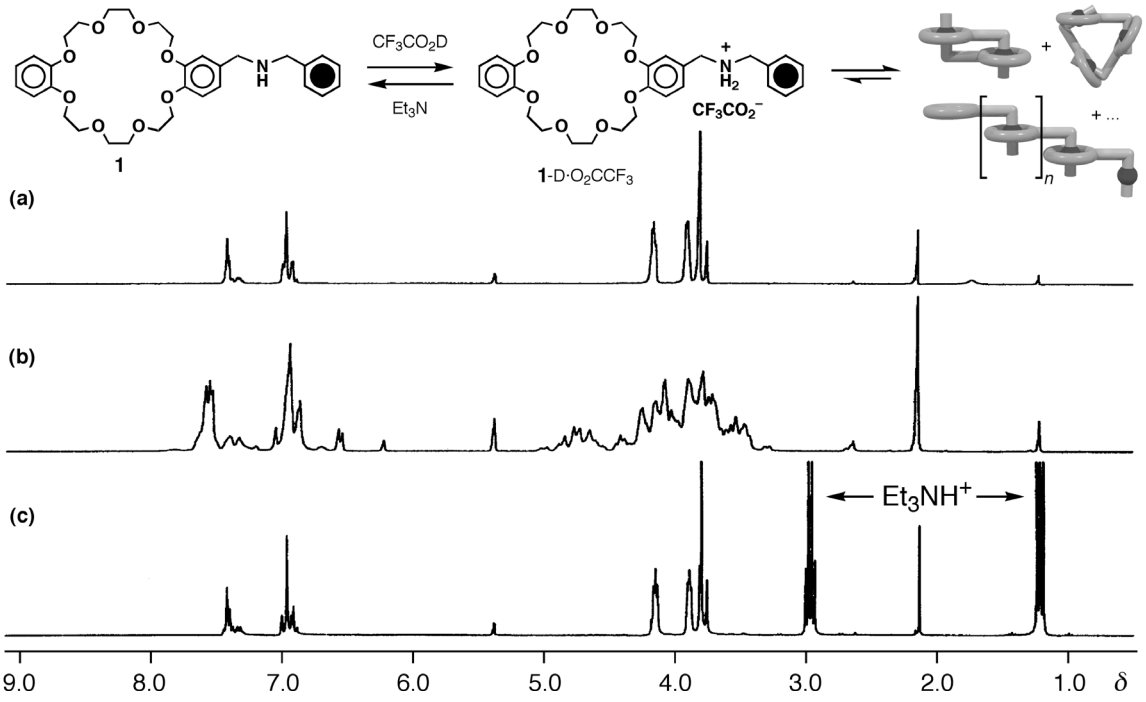

Figure 3.17. ^{1}H NMR Spectra of (**a**) the amine **1**, followed by sequential addition of (**b**) CF_3CO_2D (10 mol equiv) and (**c**) Et_3N (20 mol equiv).

1-D·O_2CCF_3, which aggregates in a manner similar to the hexafluorophosphate salt **1**-H·PF_6. Subsequent addition of Et_3N deprotonates the ammonium center, thus reversing—and subsequently preventing—any aggregation.

Temperature Effects

As with all equilibrium processes, the reversible association of two or more molecules depends markedly upon the temperature at which the process is occurring. In the case[33] of the model secondary ammonium ion/crown ether binding interaction, at room temperature the negative ΔS for threading the dibenzylammonium cation through the DB24C8 macrocycle is more than compensated for by the negative ΔH associated with all of the stabilizing interactions that result from that process. Subsequently, both ΔS and

ΔH vary with temperature, but an entropy/enthalpy compensation assures that ΔG varies only slightly (<1 kcal mol^{-1}) over the temperature range 200-350 K. Nevertheless, since ln K_a is inversely proportional to $-T$ (from $\Delta G = -RT\ln K_a$), the association constant (K_a)—for this particular system—decreases as T increases.

The temperature-dependent ^{1}H NMR spectra (400 MHz) of a 98:2 CD_3CN/D_2O solution of **1**-H·PF_6 show (Figure 3.18) how increasing the temperature of the sample simplifies significantly the spectroscopic behavior. At 358 K, the aromatic region of the spectrum is very similar to that obtained (Figure 3.15a) when analyzing a CD_3SOCD_3 solution of **1**-H·PF_6 at room temperature. By analogy, it seems reasonable to conclude therefore, that at 358 K in this CD_3CN/D_2O mixture, there is negligible association of daisy chain monomers. However, as the temperature decreases, other signals in the spectrum—most notably the two upfield shifted doublets described above—start to 'grow', indicative of the formation of aggregated species. The lower the temperature becomes, the larger these peaks grow, a trend consistent with such a temperature-dependent assembly/disassembly.

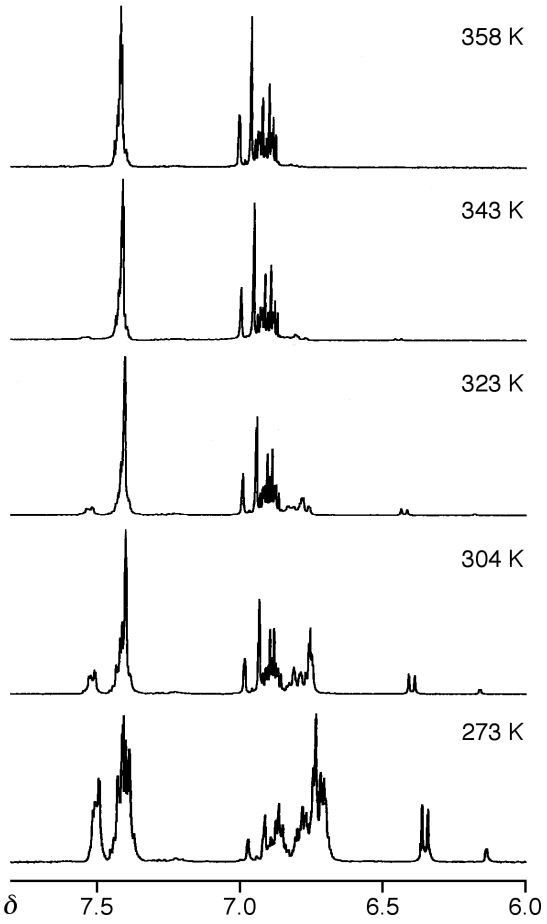

Figure 3.18. The temperature-dependent (273–358 K) partial ^{1}H NMR spectra of a CD_3CN/D_2O (98:2) solution of **1**-H·PF_6.

Simply put, in this particular system (with its own enthalpic and entropic nuances) the K_a value increases as the temperature decreases, resulting in a greater degree of aggregation at these lower temperatures.

Concentration Effects

The extent of aggregation (*i.e.*, DP) exhibited by any particular self-complementary daisy chain monomer depends considerably upon the overall concentration of monomeric species that is dissolved in solution. Generally speaking, as the concentration increases, larger and larger aggregates assemble. Conversely, as solutions are diluted, the monomer eventually dominates. To investigate its concentration dependent behavior, a 46.6 mmol CD_3CN solution of **1**-H·PF_6 was prepared,[37] and subjected to ^{1}H NMR spectroscopic analysis (400 MHz, 298 K). This solution was diluted repeatedly with known amounts of CD_3CN, and ^{1}H NMR spectra were recorded (partial region shown in Figure 3.19) at each particular concentration. As the solution becomes more and more dilute, eventually (at 0.026 mmol) the spectrum simplifies into one that is reminiscent of that obtained (Figure 3.15a) for a 10 mM solution of **1**-H·PF_6 dissolved in CD_3SOCD_3. In conclusion, therefore, at this very low

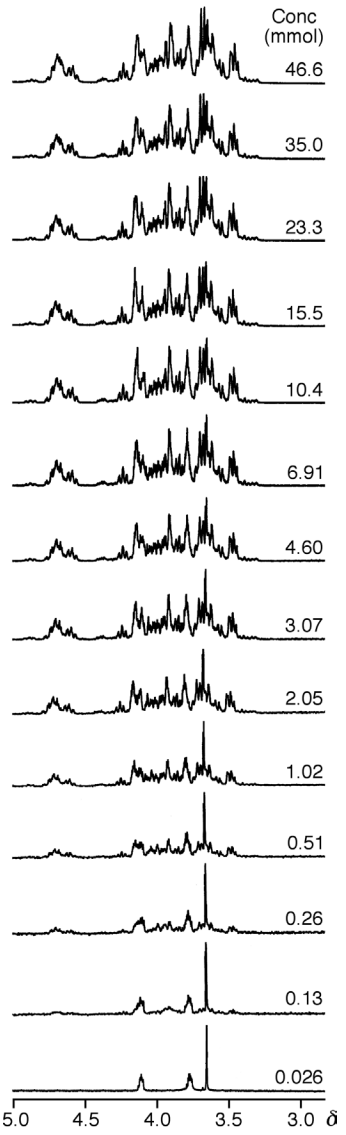

Figure 3.19. The concentration-dependent partial ^{1}H NMR spectra obtained from CD_3CN solutions of **1**-H·PF_6.

monomer concentration, the only species present in solution is the free (non-aggregated) daisy chain monomer. At higher concentrations, however, the region from δ = 3.5–4.3 ppm becomes ever more complicated, presumably as a result of the formation of aggregated species. Furthermore, at higher concentrations, signals clustered around δ = 4.7 ppm—a chemical shift value that is characteristic of DB24C8-encircled NH_2^+-adjacent benzylic methylene protons—begin to appear, thus suggesting the formation of intermolecularly threaded aggregates, *i.e.*, daisy chains. In addition, the characteristic *ortho*- and *meta*-coupled aromatic doublets (not shown) associated with dimer formation (*vide supra*) disappear at low concentration, but grow in intensity at higher concentrations. Despite these observations, however, little more can be said other than that **1**-H·PF_6—under the appropriate conditions of solvent polarity, concentration and temperature—forms, reversibly, aggregated species that are presumed to have the threaded daisy chain architectures outlined in Figure 3.6.

In order to appreciate the dramatic effects concentration can play in the assembly of these daisy chain superstructures, an Excel spreadsheet was written (see Appendix for details) in order to plot concentration profiles for daisy chain assemblies (up to, and including, trimers), based upon assumed values of K_a for the appropriate equilibria. Also, at this juncture, a shorthand method for annotating different daisy chain species is introduced: *a* denotes acyclic, whereas *c* denotes cyclic; and, in each case, the numerical suffix refers to the value of DP, *i.e.*, a dimer is 2, a trimer is 3, *etc*. The model employed (Figure 3.20) for these calculations assumes[38] that no oligomers larger than trimers are formed, thus limiting the resulting algorithm to a cubic equation (rather than a potentially insoluble

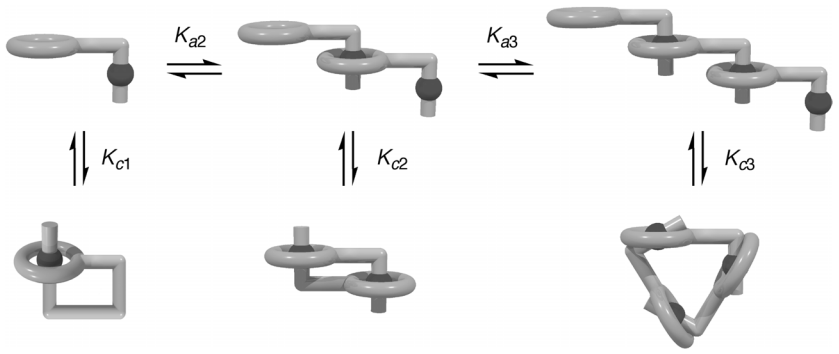

Figure 3.20. A schematic representation of the dynamic assembly of both acyclic and cyclic daisy chain superstructures (up to, and including, trimers) from a self-complementary monomer.

quartic—or even higher order—equation). The expressions for equilibrium (K_a) values (Equations 1–5) are simply rearranged (with appropriate substitution of terms) to give expressions (Equations 6–10) for the concentration of each aggregated daisy chain species in terms of [$a1$]. The total dissolved monomer concentration ([M]) is given simply by Equation 11, into which the results of Equations 6–10 can be substituted to give an expression (Equation 12), which is subsequently rearranged to give a cubic equation (Equation 13) which can be solved for [$a1$]. Subsequently, this value of [$a1$] can be

$$K_{c1} = [c1] / [a1] \quad (1) \qquad \therefore \quad [c1] = K_{c1}[a1] \quad (6)$$

$$K_{c2} = [c2] / [a2] \quad (2) \qquad \therefore \quad [c2] = K_{c2}K_{a2}[a1]^2 \quad (7)$$

$$K_{c3} = [c3] / [a3] \quad (3) \qquad \therefore \quad [c3] = K_{c3}K_{a3}K_{a2}[a1]^3 \quad (8)$$

$$K_{a2} = [a2] / [a1]^2 \quad (4) \qquad \therefore \quad [a2] = K_{a2}[a1]^2 \quad (9)$$

$$K_{a3} = [a3] / ([a1][a2]) \quad (5) \qquad \therefore \quad [a3] = K_{a3}K_{a2}[a1]^3 \quad (10)$$

[M] = concentration of monomer dissolved in solution

$$[M] = [a1] + [c1] + 2[a2] + 2[c2] + 3[a3] + 3[c3] \quad (11)$$

$$[M] = (3K_{c3}K_{a3}K_{a2} + 3K_{a3}K_{a2})[a1]^3 + (2K_{c2}K_{a2} + 2K_{a2})[a1]^2 + (1 + K_{c1})[a1] \quad (12)$$

$$(3K_{c3}K_{a3}K_{a2} + 3K_{a3}K_{a2})[a1]^3 + (2K_{c2}K_{a2} + 2K_{a2})[a1]^2 + (1 + K_{c1})[a1] - [M] = 0 \quad (13)$$

substituted back into Equations 6–10, to give the concentrations of each of the aggregated daisy chain species. By assuming reasonable K_a values for each equilibrium process

shown in Figure 3.20, it is then possible to plot how the percentage concentration of any given species in solution varies (Figure 3.21) depending upon how much daisy chain monomer (M) is initially dissolved. Initially (Figure 3.21i), K_{a2} was assumed to be 320 M^{-1} (the same K_a value[39] as that obtained in CD_3CN for the threading of the dibenzylammonium cation through DB24C8), and K_{a3} was given a slightly lower value of 210 M^{-1}. The K_a values for cyclization (K_{c1}, K_{c2}, and K_{c3}), were chosen as 0, 640, and 480, respectively, reflecting the fact that intramolecular self-complexation is not possible, but that dimerization is further favored by the π–π stacking of the central aromatic rings of **1**-H^+, and that there may also be a degree of cooperativity in cyclic trimerization.

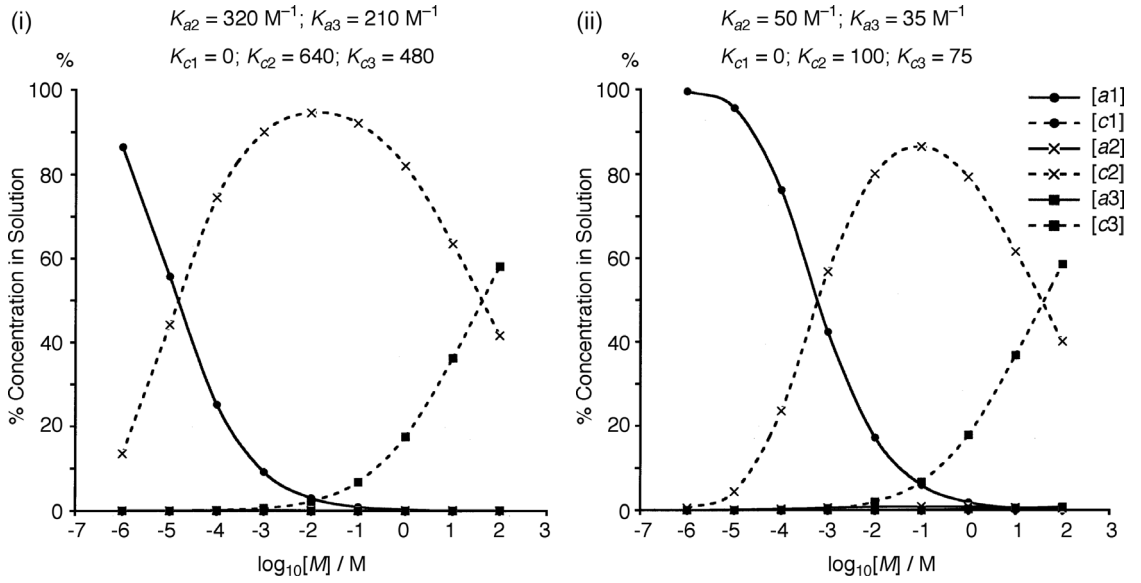

Figure 3.21. Concentration profiles—plotted using an Excel spreadsheet—that demonstrate how, based upon assumed K_a values, the concentration of daisy chain species in solution (expressed as a % of the total concentration of all species in solution) varies with the initial concentration of dissolved monomer (M).

Given these values, it can be seen (Figure 3.21i) that, over a wide concentration range (10^{-4}–10 M), the cyclic dimeric daisy chain ([*c*2]) predominates in solution. Based upon the dilution studies described above, however, it has been observed that, at 0.026 mM,

only daisy chain monomer is observed in CD_3CN solution. To fit this observed data, the estimates of K_a values were reduced[40] (Figure 3.21ii) to give a new concentration profile. Using these values, a plot is obtained which still shows that cyclic dimer dominates in solution from 10^{-3}–10 M, but at significantly lower concentration, *i.e.*, 0.026 mmol, the daisy chain monomer is now the most abundant species. Therefore, although only an approximation, this spreadsheet can be used—in conjunction with experimental data—to estimate the equilibrium values for cyclization/oligomerization in such self-complementary aggregating systems.

3.2.2. A Deuterated Monomer

It has just been revealed that the ^{1}H NMR spectroscopic behavior of **1**-H·PF_6 in solution is quite complicated. The only distinctive signals in the ^{1}H NMR spectrum of a CD_3CN solution of this compound indicate the formation of two different aggregated species, both thought to be cyclic dimeric superstructures. However, the formation of other higher order aggregates—either linear or cyclic—cannot be ruled out at this stage. It is possible that trimeric, tetrameric, or even larger structures, do not give rise to signals in the ^{1}H NMR spectrum with such dramatic chemical shifts, *i.e.*, just because the two distinctive doublets between 6.0–6.5 ppm have been assigned tentatively as cyclic dimers, signals corresponding to larger aggregates may be lurking elsewhere in the forest of peaks observed in the ^{1}H NMR spectrum of **1**-H·PF_6 (recall Figure 3.15b). In order to clarify the situation, it was decided to simplify the 'aromatic' portion of the spectrum by reducing the number of signals that resonate in that region. With this objective in mind, evidence so far indicates that the important protons to focus upon are those situated on

the central aromatic ring, *i.e.*, H_1, H_2, and H_3. Less important are the other aromatic protons, those associated with the benzyl group, and those on the 'catechol' ring. Although the signals arising from the resonances of the benzyl aromatic protons do not overlap with any signals from the important probe protons designated above, the protons of the catechol-derived aromatic ring *do* produce resonances in the same region of the spectrum as these diagnostic protons. Therefore, in an attempt to facilitate the interpretation of spectra obtained from this compound, **1**-H·PF_6 was 'resynthesized' using the tetradeuterated catechol-derivative[41] **12**, giving rise to a compound (**11**-H·PF_6) in which the resonances arising from H_1, H_2, and H_3 are not obscured by other, less significant, ones.

The tetradeuterated catechol-derivative **12** was synthesized[41] (Scheme 3.2) from catechol (**8**) using D_2SO_4. The synthesis of the deuterium-masked daisy chain monomer **11**-H·PF_6 was carried out (Scheme 3.3) in the same manner as that which was employed in the synthesis of the parent (all ^1H) monomer. The extent to which the catechol ring had been deuterated—93% of all catechol ^1H atoms were replaced by ^2H atoms—was calculated based upon the integrals observed in the ^1H NMR spectrum (Figure 3.22) of the

Scheme 3.2. The synthesis of catechol-d_4 (**12**) from catechol (**8**).

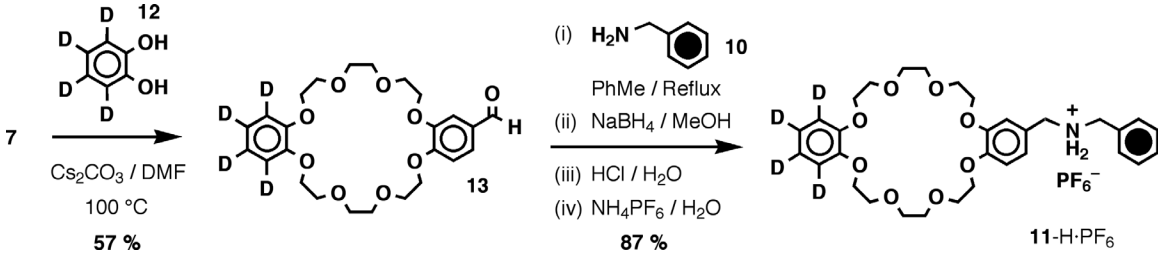

Scheme 3.3. The synthesis of the deuterium-labeled daisy chain monomer **11**-H·PF_6.

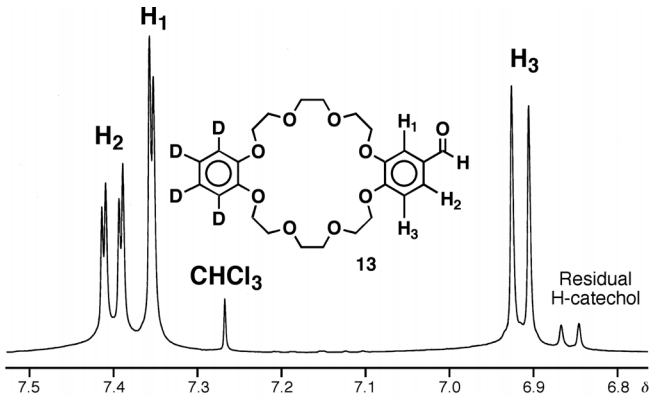

Figure 3.22. The partial ^{1}H NMR spectrum (400 MHz, $CDCl_3$) of **13**, showing the residual peaks arising from the remaining H-resonances of the 'catechol' rings that were not 100 % deuterated.

d_4-formyl-substituted macrocycle **13**. Subsequently, the ^{1}H NMR spectrum (400 MHz, 300 K) of **11**-H·PF_6 (20 mM) in CD_3CN revealed (Figure 3.23) the presence of *only* two different species in solution. As expected, the two characteristic upfield shifted doublets (*) are present. However, in this case, the corresponding signals for the appropriately-coupled protons can be observed—for both major (‡) and minor (†) species—in the region from δ = 6.7–7.0 ppm. This observation suggests that there are only two significant species in

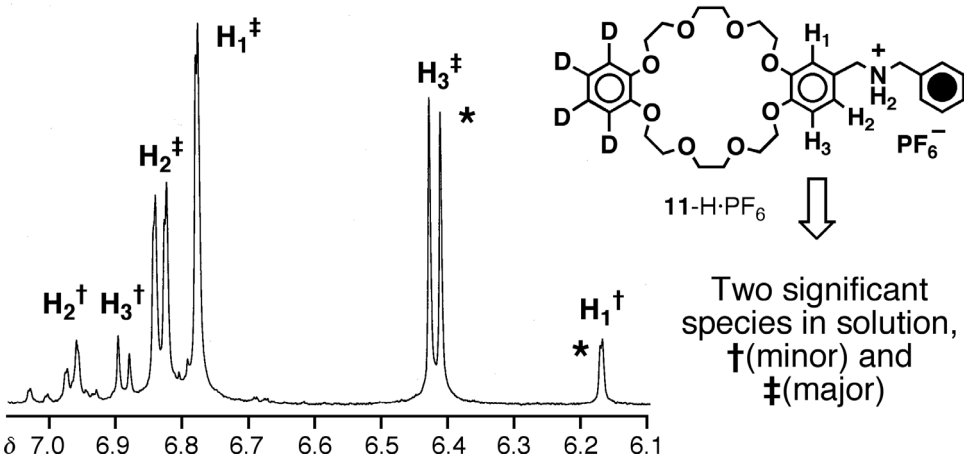

Figure 3.23. The partial ^{1}H NMR spectrum (400 MHz, 300 K) of a CD_3CN solution of the deuterium-labeled daisy chain monomer **11**-H·PF_6. Two sets (‡ and †) of signals are observed for the resonances of the protons (H_1, H_2, and H_3) of the central aromatic ring.

solution, which—based upon previous arguments—are likely to be the chiral and *meso* [*c*2]daisy chains (Figure 3.24). This outcome is also consistent with the estimated

concentration profiles (Figure 3.21) which predict that cyclic dimeric superstructures (*i.e.*, [*c*2]daisy chains) will dominate the solution phase behavior at this particular concentration (20 mM).

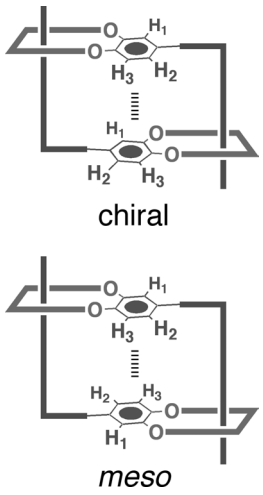

Figure 3.24. The chiral and achiral (*meso*) [*c*2]daisy chain superstructures that can be formed upon dimerization of a [24]crown-8 based monomer such as **11**-H·PF_6.

3.2.3. Two Fluorinated Monomers

We have witnessed previously how atom-substitution was used to mask a spectral response for this daisy chain system. In this Section, however, the use of fluorine atom labeling—to provide an additional spectroscopic probe *via* which a greater understanding of the solution phase behavior of this system could be achieved—is described. The reason for placing fluorine atoms judiciously at strategic locations in the daisy chain monomer was so that ^{19}F NMR spectroscopy could be employed in the solution phase analysis of these systems. Whereas the resonances of numerous different protons in the structure would give rise—upon complexation—to many different signals in the ^{1}H NMR spectrum, one, or maybe two, fluorine atoms located in the structure, would be expected to give a more simplistic—and hence interpretable—^{19}F NMR spectroscopic response.

p-F Systems

To test the viability of this fluorine substitution strategy, a model system was first of all investigated. A bis-*p*-fluoro-substituted dibenzylammonium hexafluorophosphate salt **14**-H·PF_6 was prepared (Scheme 3.4) starting from 4-fluorobenzaldehyde (**15**) and 4-fluorobenzylamine (**16**). Imine formation—employing a Dean-Stark apparatus to trap

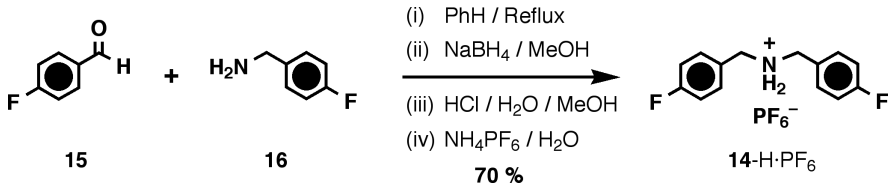

Scheme 3.4. The synthesis of bis(4-fluorobenzyl)ammonium hexafluorophosphate (**14**-H·PF_6).

water generated during the reaction—followed by borohydride reduction, protonation, and counterion exchange, gave the desired F-labeled compound in good yield. The binding of this F-substituted dibenzylammonium salt by DB24C8 was then investigated, in the usual manner, by recording a ^{1}H NMR spectrum (400 MHz, 300 K) of a 1:1 mixture of the two components dissolved in CD_3CN. The aliphatic region of the spectrum shows (Figure 3.25) the expected[42] doubling of signals, with one set of peaks arising from the free (non-interacting) species and the other set arising from the [2]pseudo-

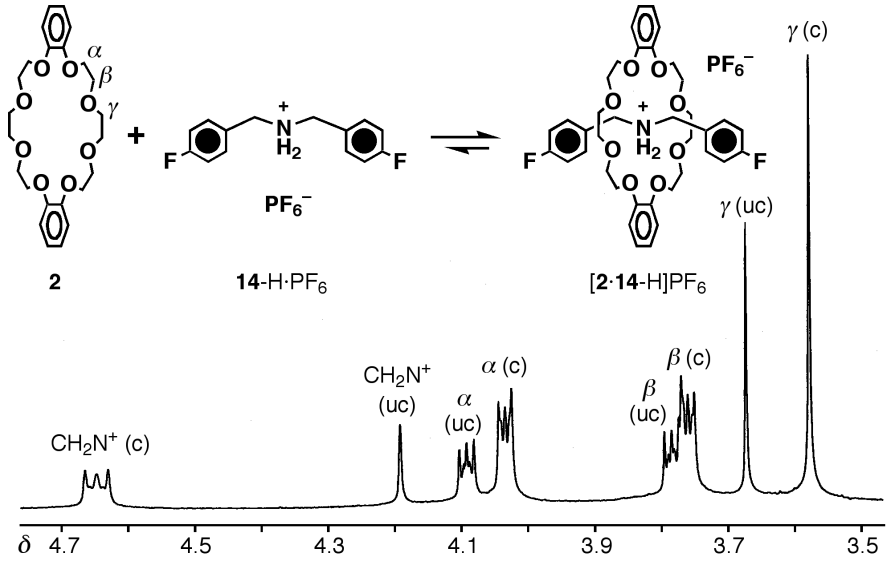

Figure 3.25. The partial ^{1}H NMR spectrum (400 MHz, 300 K) of a CD_3CN solution containing a 1:1 mixture of DB24C8 (**2**) and the *p*-F-substituted dibenzylammonium salt **14**-H·PF_6.

rotaxane [**2**·**14**-H]PF_6. Particularly diagnostic—as always[33,43]—are the signals that correspond to the resonances of the NH_2^+-adjacent methylene protons of the

dibenzylammonium cation. When 'free', these protons give rise to a single peak at δ = 4.19 ppm. However, when encircled by DB24C8, a second-order multiplet—centered around δ = 4.65 ppm—is observed. Subsequently, the K_a value for the association of [**2**·**14**-H]PF_6 and DB24C8 at 300 K was calculated—using the single point method[44]—to be 875 M^{-1}. The true test of this system, however, lay in the recording of the ^{1}H-decoupled-^{19}F NMR spectrum of the same sample. In particular, would the chemical environment of the F atom differ significantly when it is part of either a bound or unbound cation and so give rise to two different signals in the ^{19}F NMR spectrum? Furthermore, would integration of these two signals give the same value for the association constant (K_a) value as was determined by examining the ^{1}H NMR spectrum? Gratifyingly, the ^{19}F NMR spectrum (376 MHz, 300 K) revealed (Figure 3.26) the presence of two aromatic F peaks —separated by $\delta \sim 0.9$ ppm— corresponding to (i) 'free' **14**-H·PF_6, and (ii) bound **14**-H·PF_6, which, when integrated, gave values that resulted in the calculation of a K_a value exactly the same (875 M^{-1}) as that already determined using the ^{1}H NMR spectrum. Therefore, the success of this experiment prompted the synthesis (Scheme 3.5) of a fluoro-labeled daisy chain monomer, namely **17**-H·PF_6 in which the terminal phenyl ring carries a fluorine atom in the *para* position—in the hope that ^{19}F

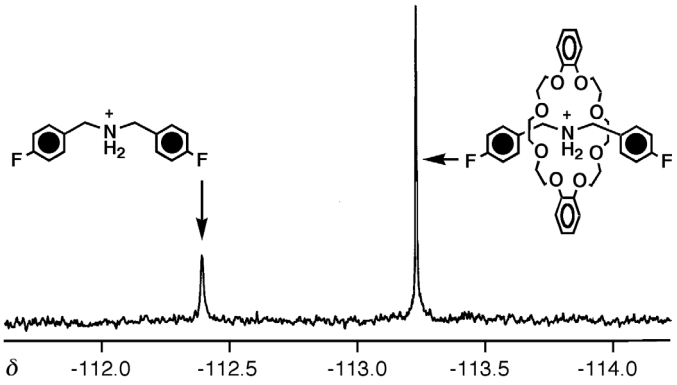

Figure 3.26. The partial ^{19}F NMR spectrum (376 MHz, 300 K) of a CD_3CN solution containing a 1:1 mixture of DB24C8 (**2**) and the *p*-F-substituted dibenzylammonium salt **14**-H·PF_6.

NMR spectroscopic analysis will prove much more enlightening than had previous ^{1}H NMR spectroscopic investigations on the unlabeled analogue.

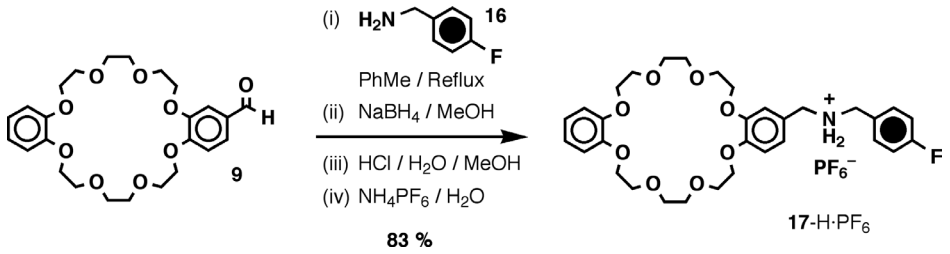

Scheme 3.5. The synthesis of the *p*-F-substituted daisy chain monomer **17**-H·PF_6.

The synthesis (Scheme 3.5) of **17**-H·PF_6 began with the common CHO-substituted macrocycle precursor **9**. In the standard way, imine formation was followed by (i) reduction, (ii) protonation, and finally, (iii) counterion exchange to afford the F-substituted daisy chain monomer **17**-H·PF_6 in a very good yield. Except for variations in the aromatic region—as a consequence of the AA'BB' spin system of the terminal *p*-F substituted phenyl ring—the ^{1}H NMR spectrum of a 10 mM solution of **17**-H·PF_6 dissolved in CD_3CN was reminiscent of that obtained for the unsubstituted parent daisy chain monomer. Despite the complexity of the ^{1}H NMR spectrum, however, the ^{19}F NMR spectrum contained (Figure 3.27, Bottom) only three peaks (**A**, **B**, and **C**) that corresponded to the resonances of aromatic F atoms. In an effort to assign these peaks to either complexed or uncomplexed species, a 10 mM CD_3SOCD_3 solution of **17**-H·PF_6 was added portionwise to the original CD_3CN sample, and ^{1}H and ^{19}F NMR spectra were recorded after each addition. Therefore, this experiment allowed the change in solution phase behavior to be monitored as the polarity of the solvent system was gradually increased. It is important to note, however, that in this process the sample is not diluted: since as the CD_3SOCD_3 solution contains a 10 mM concentration of **17**-

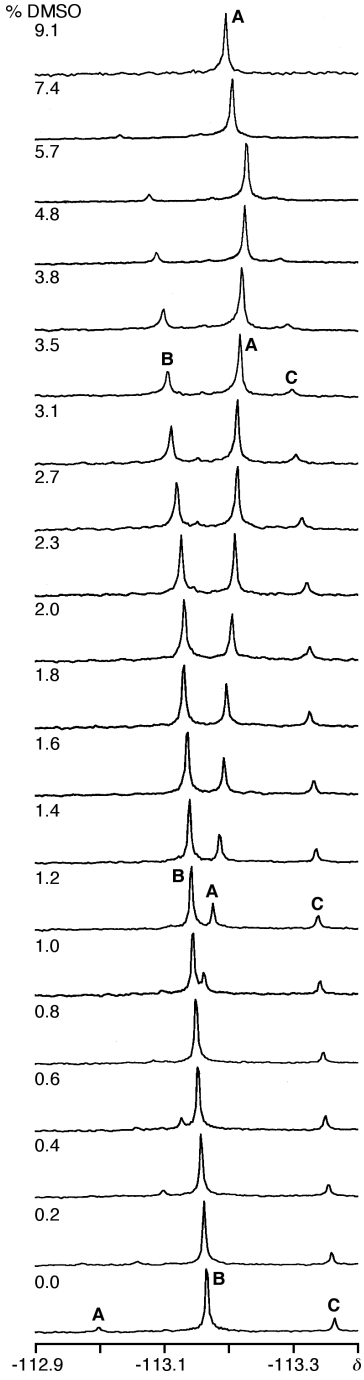

Figure 3.27. The partial ^{19}F NMR spectra (376 MHz, 300 K) of a 10 mM solution of **17**-H·PF_6 dissolved in varying mixtures of CD_3CN/CD_3SOCD_3.

H·PF_6, the resulting solutions always maintains a 10 mM concentration of daisy chain monomer despite changes in volume. This fact is important, as now changes in the species present in solution—as monitored spectroscopically—can be attributed solely to solvent polarity, rather than to concentration effects. As the percentage CD_3SOCD_3 content of the CD_3CN solution of **17**-H·PF_6 increases (Figure 3.27), the peaks **B** and **C** begin to reduce in intensity as signal **A** grows in intensity. Ultimately, when just over 9 % of the solvent mixture is CD_3SOCD_3, only one peak (**A**) remains. The corresponding ^1H NMR spectrum of this sample reveals (Figure 3.28, Top) that **17**-H·PF_6 is present only in the monomeric form under these conditions – as indicated by the simple nature of the spectrum. These experiments lead to the conclusion that peaks **B** and **C** arise as a consequence of aggregated species, *i.e.*, daisy chains. In a nutshell, in CD_3CN, ammonium ion binding is favorable and intermolecular association occurs, resulting in the formation of species that give rise to signals **B** and **C**). However, as the solvent polarity is increased upon addition of CD_3SOCD_3, the NH_2^+ sites become solvated by these solvent molecules, resulting in the deaggregation of daisy

chains to form monomer, *i.e.*, the species responsible for signal **A**. Furthermore, the presence of only two different aggregated species is in agreement with the behavior observed for the parent daisy chain systems (Section 3.2.2). Coincidentally, the ratio of peaks **B** and **C** is ~5:1, the same proportion as that observed for the two upfield shifted aromatic doublets which are so distinctive in the ^{1}H NMR spectra of both this analogue and the parent system. It seems reasonable, therefore, to propose that the two signals **B** and **C**—observed in the ^{19}F NMR spectrum under aggregation-promoting conditions—originate from the two diastereoisomerically different [*c*2]daisy chains. This conclusion finds further support in so far as the presence of significant amounts of acyclic daisy chains—which would give rise to different patterns in the ^{19}F NMR spectrum to those that are observed—can be ruled out. For example, in the case of the [*a*2]daisy chain, each F-atom lies in a different chemical environment, thus potentially resulting in two equal intensity peaks appearing in the spectrum. Based upon the model two-component system (*vide supra*)—in which 'free' and bound F-containing thread-like molecules give rise to signals ~0.9 ppm apart—it is unlikely that the resonances of the two different F atoms in the acyclic dimer would be isochronous. Obviously, a linear trimer would have F atoms occupying three different F

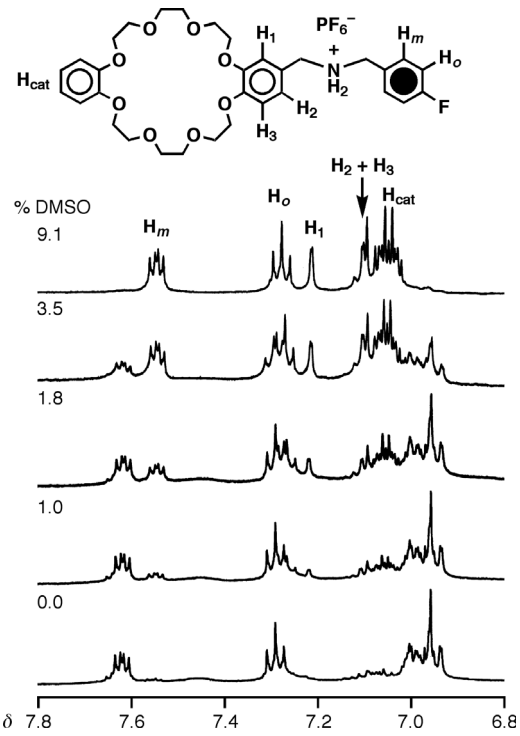

Figure 3.28. The partial ^{1}H NMR spectra (400 MHz, 300 K) of a 10 mM solution of **17**-H·PF_6 dissolved in varying mixtures of CD_3CN/ CD_3SOCD_3.

environments, and so on. Therefore, based upon all the evidence gathered so far, the 'dimer hypothesis' is still the most likely one. In conclusion, although a corresponding simplification of the ^{1}H NMR spectrum is witnessed (Figure 3.28) during the course of the experiment, only the ^{19}F NMR spectrum is simple enough for an interpretation of the data to be made with confidence. Thus investigating a fluorinated analogue has helped to shed light on the solution phase behavior of these daisy chain systems. The next question was to see if moving the F atom closer to the recognition site would improve the $\Delta\delta$ separation between the 'free' and bound F-containing species.

3,5-F_2 Systems

When located in the *para* position of the terminal phenyl ring, the F atom occupies a position that is as far away from the recognition site (the NH_2^+ center) as possible. By placing F atoms in each of the *meta* positions, it was hoped that the influence of binding upon the environment of a fluorine substituent would be increased, resulting in a greater separation in the chemical shifts of the signals arising from the resonances of the F atoms attached to the 'free' and bound species, respectively. Therefore, the initial aim was to study a model system employing this substitution pattern—namely, bis(3,5-difluorobenzyl) ammonium hexafluorophosphate (**18**-H·PF_6). This salt was prepared (Scheme 3.6) starting from 3,5-difluorobenzaldehyde (**19**) and 3,5-difluorobenzylamine

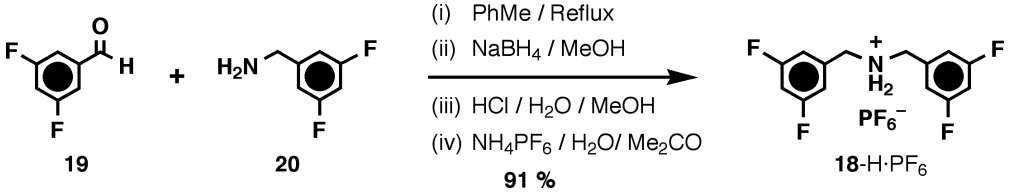

Scheme 3.6. The synthesis of bis(3,5-difluorobenzyl)ammonium hexafluorophosphate (**18**-H·PF_6).

(**20**). Imine formation—using a Dean-Stark apparatus to trap water generated during the reaction—followed by borohydride reduction, protonation, and counterion exchange, gave the desired F-labeled compound in very good yield. The binding of this F-substituted dibenzylammonium salt by DB24C8 was then investigated, in the usual manner, by recording a ^{1}H NMR spectrum (400 MHz, 300 K) of a 1:1 mixture of the two components dissolved in $CDCl_3/CD_3CN$ (3:1). Initially, the spectrum exhibited only peaks for each of the two free species—as if it was simply an overlay of the spectra of the two independent compounds—indicating that no complexation had occurred. In order to monitor the sample reliably over a longer time period, the NMR tube was sealed to ensure that the solvent ratio and solute concentrations remained constant. ^{1}H NMR Spectra were recorded over the following weeks, revealing (Figure 3.29) the formation of a complex, albeit very slowly. The diagnostic multiplet at δ = 4.6 increased in intensity with time while the ratio of 'free':bound thread can be most easily followed by monitoring the signals arising from the resonances of the γ protons of 'free' and bound DB24C8. Unfortunately, however, careful inspection of the corresponding ^{19}F NMR

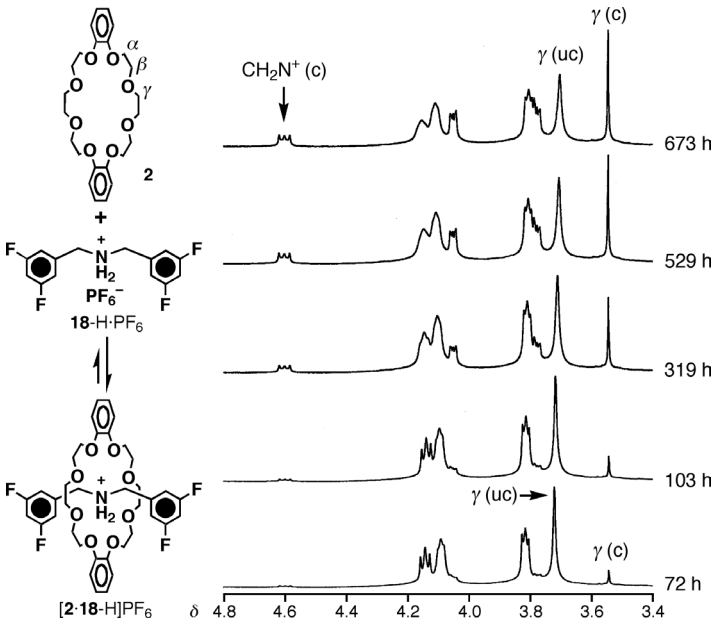

Figure 3.29. Partial ^{1}H NMR spectra (400 MHz, 300 K) recorded over time of a $CDCl_3/CD_3CN$ (3:1) solution containing a 1:1 mixture of DB24C8 (**2**) and the bis(3,5-difluoro)-substituted dibenzylammonium ion salt **18**-H·PF_6 in a sealed NMR tube.

spectra revealed (Figure 3.30) that the sample was undergoing decomposition during the course of the analysis. Although more and more of the cation was slowly finding its way into DB24C8 macrocycles, the PF_6^- anion was—after ~100 h—no longer present. Interestingly, a new doublet—shifted upfield from the PF_6^- doublet by ~12 ppm—appears, and then fades away with time as well. One possible explanation lies in the decomposition[45] of PF_6^- to give PF_5,[46] which—with a boiling point of –75 °C[47]—although, initially dissolved in solution, is drawn into the partial vacuum above the liquid that is formed upon sealing[48] the NMR tube. Therefore, even although the system appears to be undergoing equilibration, the uncertainty surrounding the identity of the corresponding anion[49] ended the experiment abruptly and prematurely. Nonetheless, the synthesis of the corresponding 3,5-F_2-substituted daisy chain monomer was undertaken, safe in the knowledge that, although slow in their passage, 3,5-F_2-substituted phenyl rings *will pass* through the macrocyclic cavity of DB24C8. Furthermore, the slow kinetics of threading/unthreading

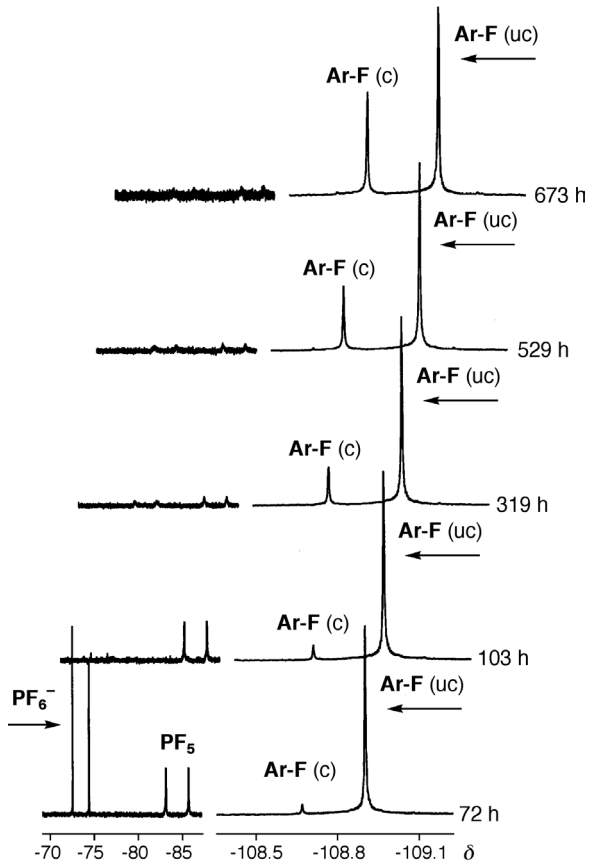

Figure 3.30. Partial ^{19}F NMR spectra (376 MHz, 300 K) recorded over time of a $CDCl_3/CD_3CN$ (3:1) solution containing a 1:1 mixture of DB24C8 (**2**) and the bis(3,5-difluoro)-substituted dibenzylammonium ion salt **18**-H·PF_6 in a sealed NMR tube, reveal that the PF_6^- anion decomposes in a matter of days under these conditions.

did not necessarily constitute a problem since they could potentially provide an opportunity to follow the assembly of daisy chain species on the human, rather than the NMR, timescale.

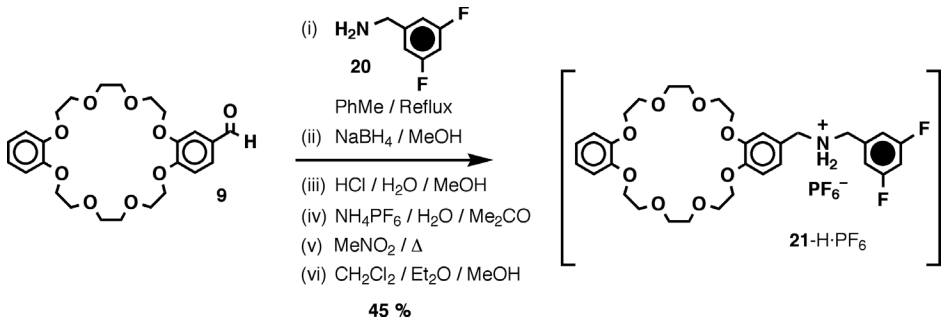

Scheme 3.7. The synthesis of the 3,5-difluorophenyl-terminated [24]crown-8 daisy chain monomer **21**-H·PF_6.

The synthesis (Scheme 3.7) of **21**-H·PF_6 began with the common formyl-substituted macrocycle precursor **9**. In the standard fashion, imine formation was followed by (i) reduction, (ii) protonation, and finally, (iii) counterion exchange. Rather than precipitate from aqueous solution as a solid at this point (which is usually the case[50] with dibenzylammonium-based hexafluorophosphate salts), **21**-H·PF_6 formed an oily residue and so it was extracted into $MeNO_2$. After evaporation to dryness, the semi-solid material was redissolved in CH_2Cl_2 and filtered to remove a small amount of NH_4PF_6. Addition of Et_2O to this solution caused the precipitation of a sticky solid, which redissolved upon the addition of a small amount of MeOH. On standing, **21**-H·PF_6 finally precipitated from this methanolic solution as a while solid. Once again, the initial spectroscopic analysis was performed in CD_3SOCD_3 in an effort to determine whether or not the compound was pure, *i.e.*, since aggregation does not occur in this solvent, the purity of the sample can be assessed rather easily. Therefore, the ^{1}H NMR (400 MHz, 300 K) spectrum of **21**-H·PF_6 (Figure 3.31) was greeted with some surprise. Instead of a

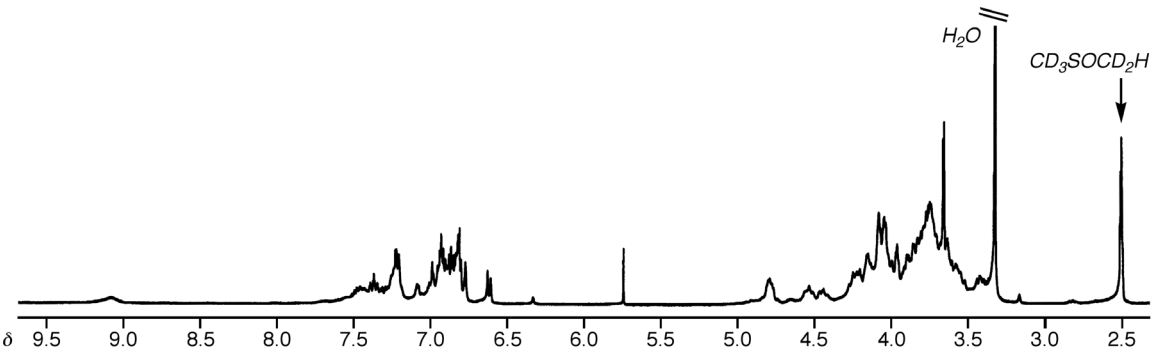

Figure 3.31. Surprisingly, the ^{1}H NMR spectrum (400 MHz, 300 K) of **21**-H·PF$_6$, obtained immediately after its dissolution in CD_3SOCD_3, indicated the presence of aggregated daisy chain superstructures.

simple spectrum—representing only the daisy chain monomer—a spectrum reminiscent of that obtained when a self-complementary daisy chain monomer is dissolved in aggregation-promoting CD_3CN was observed. Not only are the peaks in the aliphatic region smeared out across a wide chemical shift range, but the two distinctive upfield-shifted aromatic doublets (assigned tentatively up to now as arising from [*c*2]daisy chains) are also present. Furthermore, the ^{19}F NMR spectrum (*vide infra*) contained more than one aromatic ^{19}F peak, which is all that should be expected if the monomeric species is the only one present in solution. Not only was this initial spectrum a surprise but it was also transient! Upon re-running the spectrum the next day, both the ^{1}H and ^{19}F NMR spectra had changed significantly. This observation prompted a more in-depth analysis of this compound – one in which a sample of **21**-H·PF$_6$ was dissolved in CD_3SOCD_3 and monitored spectroscopically at more frequent intervals. The ^{19}F NMR spectra recorded over a period of 6 d revealed (Figure 3.32) that, although initially two peaks (**A** and **B**) are present in the spectrum, eventually these signals disappear and give rise to one singlet, which—upon inspection of the corresponding simple ^{1}H NMR spectrum—can be assigned to a monomeric species. Therefore, it appears that **21**-H·PF$_6$

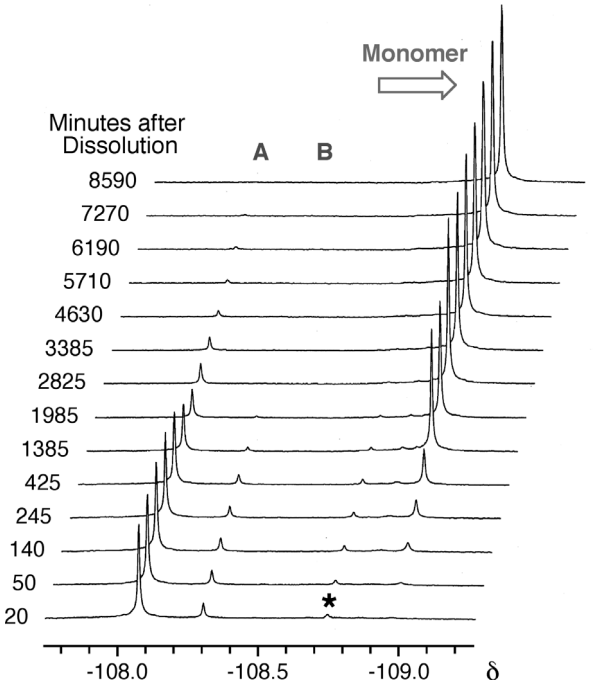

Figure 3.32. Partial ^{19}F NMR spectra (376 MHz, 300 K) recorded over time of a CD_3SOCD_3 solution of **21**-H·PF_6. For an explanation of the peak-labels **A**, **B**, and *, see text.

was isolated as a mixture of two aggregated daisy chain species—one giving rise to signal **A**, and the other, signal **B**—which, upon dissolution in CD_3SOCD_3, dissociate extremely slowly to give the daisy chain monomer.

At this point, however, an important question should be raised: if it takes weeks for the bis(3,5-difluorobenyzl)-ammonium cation to thread—to an appreciable extent—through DB24C8 (*vide supra*), how is it possible that a reasonable yield of aggregated daisy chain species are isolated in the case of **21**-H·PF_6? The answer to this question most likely lies in the manner in which **21**-H·PF_6 was isolated. When the crude $MeNO_2$ solution containing **21**-H·PF_6 is evaporated to dryness, it is both heated (water-bath temperature ~60 °C) and concentrated. Since, intermolecular aggregation becomes more favored as the monomer concentration increases and, even although it is a slow process at room temperature, the rate at which a 3,5-difluorophenyl group threads through a DB24C8 macrocycle will be much greater[51] at 60 °C. Such a slippage-like process,[52] however, is not necessarily responsible for the isolation of complexed species in this case. Indeed, the sample of **21**-H·PF_6 was isolated upon precipitation from solution *over a period of weeks*. Thus, not only is this process a very slow one—perhaps allowing enough time for sufficient

threading to occur—but also, the kinetic precipitation event would drive any solution phase equilibrium to give more of the species that precipitates. Subsequently, once this solid is redissolved in CD_3SOCD_3—a solvent in which there is no thermodynamic preference for crown ether/ammonium ion recognition—aggregated species are not immediately dismembered since unthreading requires the passage of the 3,5-difluorophenyl terminated arms of **21**-H·PF_6 through DB24C8-sized macrocycles, which is, relatively speaking, kinetically slow at room temperature. In summary, therefore, it is obvious that the isolated solid is not simply the daisy chain monomer—as this substance is what the sample in question transforms into when dissolved in CD_3SOCD_3—but rather, it is a mixture of two aggregated species, as demonstrated (*vide infra*) by ^{19}F NMR spectroscopy. The nature of these aggregated species can be identified, based upon spectroscopic comparisons with previous systems.

Although complicated, the initial ^1H NMR spectrum contains the two diagnostic upfield shifted aromatic doublets that are be indicative (*vide supra*) of the formation of the two possible diastereoisomeric [*c*2]daisy chains. Furthermore, the ^{19}F NMR spectrum contains, initially, two signals (**A** and **B**), with an intensity ratio of ~5:1 – a feature which is reminiscent of that observed for the *p*-F daisy chain system (**17**-H·PF_6). This observation suggests that there are *two different* F atom environments arising from *two different* F-containing aggregated species. Based upon all of the evidence to hand, it is reasonable to conclude that these two aggregated species are indeed the two diastereoisomeric [*c*2]daisy chains. This conclusion is further supported by FAB mass spectrometric investigations that were subsequently performed on this compound.

The FAB mass spectrum of the isolated solid—*i.e.*, prior to dissolution in CD_3SOCD_3—reveals (Figure 3.33i) the presence of dimeric species. The signals at *m/z* values of 1207.9 and 1353.9, respectively, correspond to unipositive dimeric structures – the larger value arises as a consequence of an associated PF_6^- anion. Furthermore, the cluster of isotopic peaks centered around *m/z* = 604.4, are spaced by 0.5 mass units, indicating the presence of the doubly-charged dimeric superstructure. This result suggests that no higher order daisy chain oligomers (*i.e.*, trimers, tetramers, etc.) are to be found in the isolated sample, and that it consists solely of dimeric superstructures, of which there are only three – (i) the *two* diastereoisomeric [*c*2]daisy chains and (ii) the linear [*a*2]daisy chain. The second of these possibilities can be excluded based upon the simplicity (only two peaks, **A** and **B** in a ratio of *ca*. 5:1) of the initial ^{19}F NMR spectrum. The reason is that, such an unsymmetric species would give rise to two equal intensity singlets, one each for a bound 3,5-difluorophenyl ring, and an unbound one – the same argument that was applied in explaining the ^{19}F NMR spectra observed in the case of the *p*-F daisy chain system **17**-H·PF_6. Subsequently, the proposed composition of the six-day old CD_3SOCD_3 solution of **21**-H·PF_6 was confirmed (Figure 3.33ii) following FAB mass spectrometric analysis of this solution. Only a single peak (at *m/z* = 604.3) is observed in the spectrum and, since the adjacent isotope peaks are separated by unity, only the

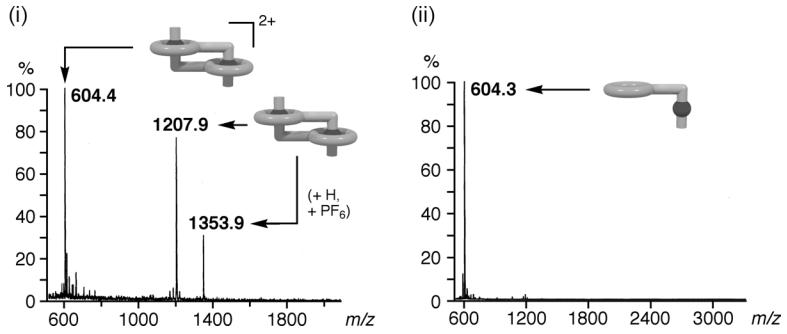

Figure 3.33. The FAB-mas spectra of **21**-H·PF_6 (i) prior to dissolution in CD_3SOCD_3, and (ii) after sitting in CD_3SOCD_3 solution for 6 d.

monomeric daisy chain species remains, *i.e.*, there are no longer any aggregated assemblies present.

There is, however, one feature of the spectra illustrated in Figure 3.32, that remains to be explained. A small signal (*) is evident at $\delta = -108.7$. Initially, it grows ever so slightly in intensity, and then 'shrinks back' into the baseline of the spectrum until it is no longer visible at the end of the experiment. Perhaps, finally, we are 'seeing' a little of the [*a*2]daisy chain. When the [*c*2]daisy chains dissociate to give the monomeric structure, unless both 3,5-difluorophenyl terminated arms dethread simultaneously, some of the [*a*2]daisy chain will inevitably be formed (Figure 3.34). Such a structure contains both 'free' and bound ammonium ion-containing arms, each of which is terminated by a 3,5-difluoro-phenyl group. The [*a*2]daisy chain would be expected to give rise to two equal intensity peaks in the ^{19}F NMR spectrum. It is likely that the peak at $\delta = -108.7$ corresponds to the resonance of the F atoms of the 'free' ammonium ion-containing arm of the [*a*2]daisy chain, while the corresponding signal for the bound arm remains hidden under the either peak **A** or **B**. As the intensity of this peak never 'grows' to any significant proportions, such an explanation would require that the transformation from [*c*2]daisy chain into [*a*2]daisy chain proceeds at a slower rate than does the conversion of [*a*2]daisy chain into [*a*1]daisy chain, *i.e.*, the monomer. It is not unreasonable to propose that the more tangled nature of

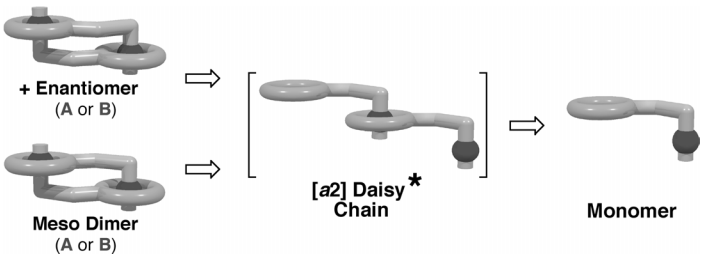

Figure 3.34. A schematic representation depicting the pathway *via* which a [*c*2]daisy chain superstructure is expected to disassemble to give, initially, the [*a*2]daisy chain, and then, ultimately, the monomeric species ([*a*1]daisy chain).

the cyclic superstructure, with less degrees of translational and rotational freedom, as compared with the linear [*a*2]daisy chain superstructure, may offer an explanation for this observation. At this point, therefore, there is no doubt regarding the absence of higher order daisy chain superstructures in the initial solution. For example, the presence of a [*c*3]daisy chain would—in the process of its CD_3SOCD_3-induced dismemberment —generate [*a*2]- and [*a*3]daisy chains (the latter complex having *three* distinct F atom environments), almost certainly giving rise to a more complicated set of spectra than those observed experimentally. Obviously the situation would be considerably more complicated for even larger daisy chain complexes.

Finally, the slow kinetics of threading/dethreading a 3,5-difluorophenyl end group through a DB24C8 macroring were exemplified in another set of mass spectrometric investigations. Upon mixing equimolar quantities of the parent daisy chain monomer (**1**-

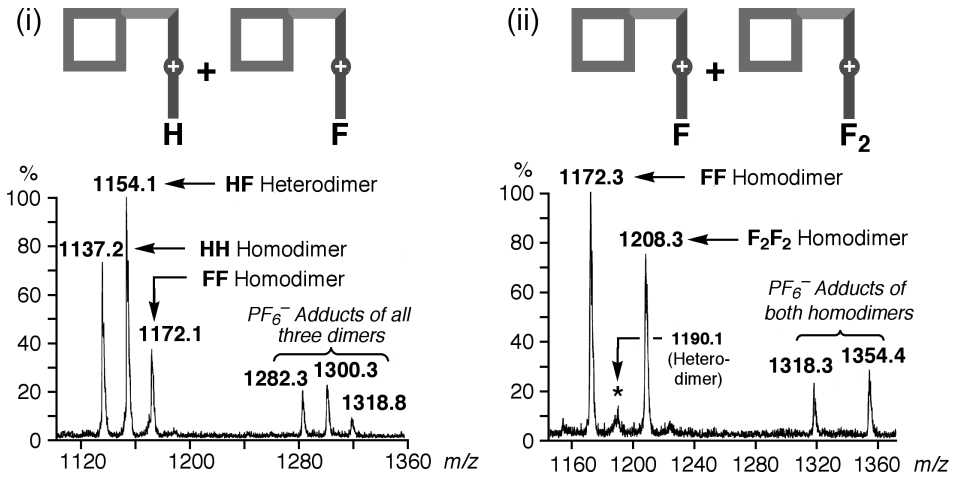

Figure 3.35. The FAB mass spectra of (i) an equimolar mixture of **1**-H·PF_6 {**H**} and **17**-H·PF_6 {**F**}, and (ii) an equimolar mixture of **17**-H·PF_6 {**F**} and **21**-H·PF_6 {$\mathbf{F_2}$}.

H·PF_6, {**H**}) and the *p*-F analogue (**17**-H·PF_6, {**F**}) in MeCN, subsequent FAB mass spectrometric analysis of this solution revealed (Figure 3.35i) the formation, in the 'gas

phase' of all three possible dimeric superstructures – namely (i) the **HH** and **FF** homodimers, and (ii) the **HF** heterodimer. In contrast, when the *p*-F daisy chain (**17**-H·PF_6, {**F**}) was mixed with **21**-H·PF_6 ($\mathbf{F_2}$), only a very minor amount of heterodimerization was observed—as evidenced by the signal at *m/z* = 1190.1—with the major signals in the spectrum (Figure 3.35ii) corresponding to the homodimers **FF** and $\mathbf{F_2F_2}$, respectively. Therefore, the lack of mixing of these two F-substituted daisy chain monomers reflects the slow kinetics of threading and dethreading associated with the DB24C8/3,5-difluorophenyl couple.

3.3. [25]Crown-8-Based Systems

It is clear that gaining an appreciation of the aggregation behavior of [24]crown-8 based daisy chain systems is hampered by the formation of stereoisomeric superstructures. In an effort to remove this stereochemical ambiguity, monomers based upon a [25]crown-8 macrocycle were investigated as candidates for the formation of aggregated daisy chains. Although crown ethers with a [25]crown-8 constitution have been shown[53] to have much lower affinities for secondary ammonium ions than their DB24C8-based counterparts, the more highly symmetric nature of the proto-typical [25]crown-8 daisy chain monomer (**22**-H·PF_6)—as compared to the [24]crown-8 monomer (**1**-H·PF_6)—means that, upon assembly (Figure 3.36), only one unique

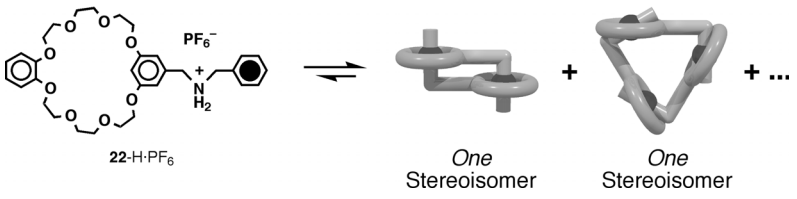

Figure 3.36. The inherent symmetry of a [25]crown-8-based daisy chain monomer means that only one unique [*c*2]daisy chain can be formed upon aggregation. Similarly, only one [*c*3]-, one [*c*4]-, and one [*c*5]daisy chain, *etc*... can be formed.

[*c*2]daisy chain is formed. Furthermore, only one form of each of the higher order aggregates, *i.e.*, [*c*3]daisy chain, [*c*4]daisy chain, *etc.*, is possible. In summary, therefore, if conditions can be optimized—*e.g.*, very concentrated solutions employed—so that daisy chain oligomerization is observed in such a less strongly bound [25]crown-8 based system, interpreting the spectroscopic data should, in theory, be much easier than in the case of the more stereochemically complicated [24]crown-8-based systems.

3.3.1. The Parent Monomer

The synthesis of this [25]crown-8-based self-complementary daisy chain monomer is outlined in Scheme 3.8. Tosylation of the known[54] diol **23**, under standard conditions, gave the ditosylate **24**, which was subsequently reacted with 3,5-dihydroxybenzyl alcohol (**25**) to give the hydroxymethyl-substituted BMP25C8 derivative **26** in reasonable

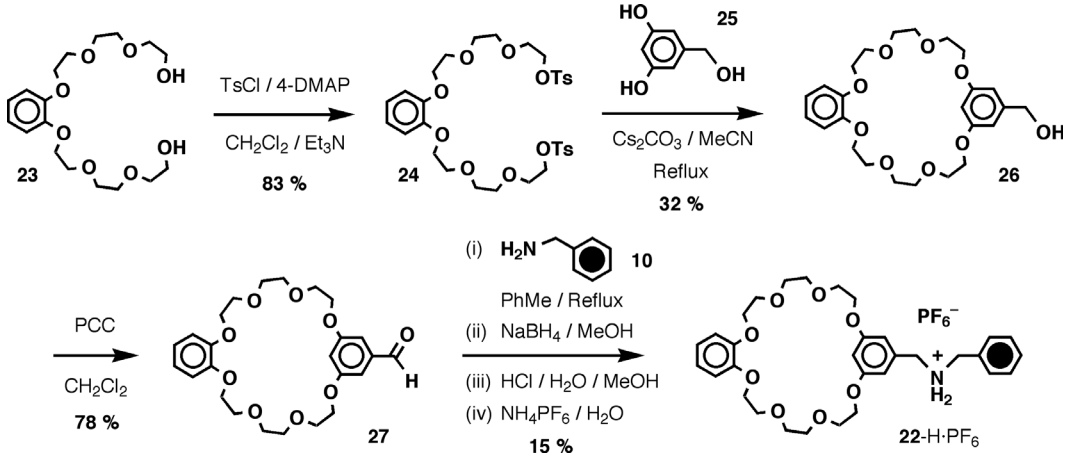

Scheme 3.8. The synthesis of the parent [25]crown-8-based daisy chain monomer **22**-H·PF_6.

yield. Oxidation of the hydroxyl group of **26** with PCC gave the corresponding formyl-substituted macrocycle **27** in good yield. Subsequent condensation of **27** with

benzylamine (**10**), followed by borohydride reduction, protonation (HCl), and counterion exchange from Cl^- to PF_6^-, afforded the target compound **22**-H·PF_6 in a 15 % yield.

Unlike the [24]crown-8 daisy chain analogues, **22**-H·PF_6 was found to be soluble in CD_2Cl_2—perhaps the optimal solvent[33] for the crown ether/ammonium ion interaction—and, therefore, subsequent ^{1}H NMR investigations were conducted in this solvent. Unfortunately, as expected,[55] the kinetics associated with the threading/dethreading of a phenyl ring through a [25]crown-8 sized macrocycle are such that neither a slow- nor a fast-exchange regime operates. Consequently, ^{1}H NMR spectra obtained from solutions of **22**-H·PF_6 over a range (0.05–28.5 mM) of concentrations consist (Figure 3.37) of broad peaks that are difficult to assign to any particular species. The spectroscopic changes observed over a given concentration range indicate that aggregation—to some extent—does occur with this [25]crown-8-based monomer.

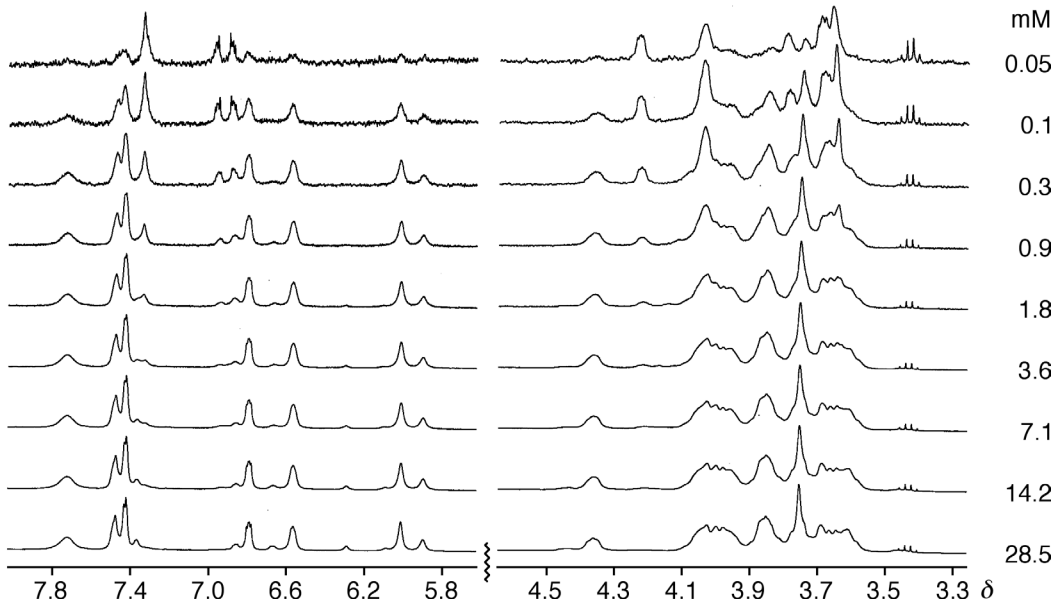

Figure 3.37. The concentration-dependent partial ^{1}H NMR spectra (400 MHz, 300 K) of CD_2Cl_2 solutions of the parent [25]crown-8 daisy chain monomer **22**-H·PF_6.

Furthermore, the FAB mass spectrum of **22**-H·PF_6 contains a peak—albeit very small (*ca*. 3 % of the peak arising from the monomer)—corresponding to a dimeric assembly.

3.3.2. A Fluorinated Monomer

The limited information garnered from the study of the parent [25]crown-8 daisy chain prompted the search for a system that would be more amenable to analysis. Not only would a slowly-exchanging system be preferable spectroscopically, but, as observed in the [24]crown-8 series, it was felt that a ^{19}F probe might prove helpful. One candidate immediately sprang to mind – namely, the 3,5-difluorophenyl group – which had been shown to pass very slowly through a DB24C8 sized macrocycle. Might it also prove useful in the [25]crown-8-based system? Before proceeding with the synthesis of a 3,5-difluorophenyl terminated [25]crown-8 daisy chain monomer, the appropriate model system was investigated. A CD_3CN solution containing a 1:1 mixture of bis(3,5-

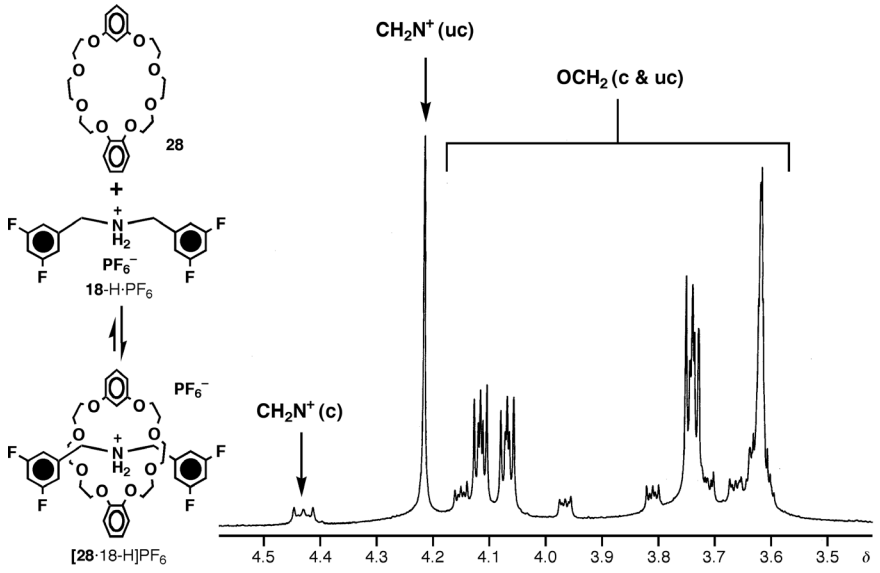

Figure 3.38. The partial ^1H NMR spectrum (400 MHz, 300 K) of a CD_3CN solution containing a 1:1 mixture of BMP25C8 (**28**) and the 3,5-difluorophenyl-substituted dibenzylammonium salt **18**-H·PF_6.

difluorobenzyl)ammonium hexafluorophosphate (**18**-H·PF_6) and BMP25C8 (**28**) was subjected to both ^{1}H and ^{19}F NMR spectroscopic analyses. The ^{1}H NMR spectrum (Figure 3.38) was characteristic of a slowly exchanging crown ether/dibenzylammonium ion system. Signals were observed for all three species present in solution, namely (i) 'free' BMP25C8, (ii) 'free' **18**-H·PF_6, and (iii) the [2]pseudorotaxane [**28**·**18**-H]PF_6. Consequently, this spectrum was used to calculate—using the single point method[44]—a K_a value (at 300 K in CD_3CN) of 25 M^{-1} for the association of these two species. Further-more, the ^{19}F NMR spectrum revealed (Figure 3.39) the presence of two aromatic F singlets, one each for the 'free' and bound bis(3,5-difluorobenzyl)ammonium cation. Crucially, the K_a value—when calculated based upon the intensities of these two peaks—was the same as that already obtained from the data extracted from the ^{1}H NMR spectrum. The slow passage—on the NMR timescale—of a 3,5-difluorophenyl ring through the cavity of BMP25C8 prompted the synthesis (Scheme 3.9) of the correspondingly substituted daisy chain analogue, namely **29**-H·PF_6.

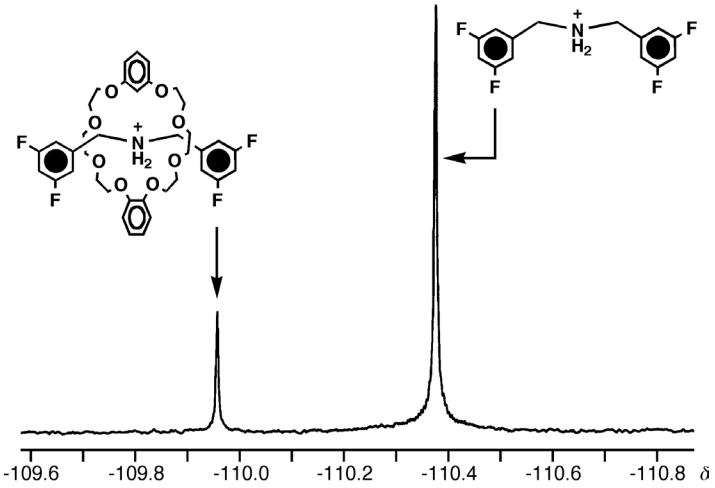

Figure 3.39. The partial ^{19}F NMR spectrum (376 MHz, 300 K) of a 1:1 mixture of BMP25C8 (**28**) and **18**-H·PF_6 reveals the presence of two aromatic F signals, one corresponding to free **18**-H·PF_6, and the other to the [2]pseudorotaxane [**28**·**18**-H]PF_6.

The synthesis (Scheme 3.9) of **29**-H·PF_6 started from the formyl-substituted macrocycle precursor **27**. In standard fashion, imine formation was followed by (i) reduction, (ii)

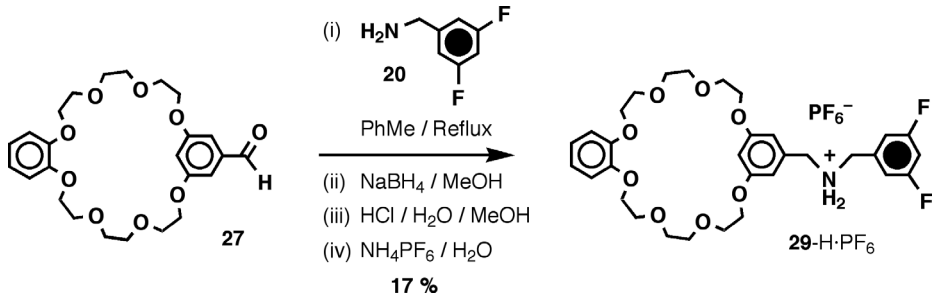

Scheme 3.9. The synthesis of the 3,5-difluorophenyl-terminated [25]crown-8 daisy chain monomer.

protonation, and finally, (iii) counterion exchange, to afford the 3,5-difluorophenyl-substituted daisy chain monomer **29**-H·PF_6 in a 17 % yield. The initial ^{1}H and ^{19}F NMR spectroscopic character-ization, which was carried out in CD_3SOCD_3, revealed the daisy chain monomer to be pure – a simple, easily assignable, ^{1}H NMR spectrum was obtained and the ^{19}F NMR spectrum contained a single peak corresponding to the aromatic F atoms, in addition to the doublet for the PF_6^- anion. Mass spectrometry (FAB) revealed the formation, in the 'gas phase', of dimeric superstructures, as evidenced by the presence of signals corresponding to both the uni- and di-positive dimers. More interesting, however, were the concentration-dependent ^{19}F NMR spectroscopic investigations conducted[56] in CD_3CN solution.

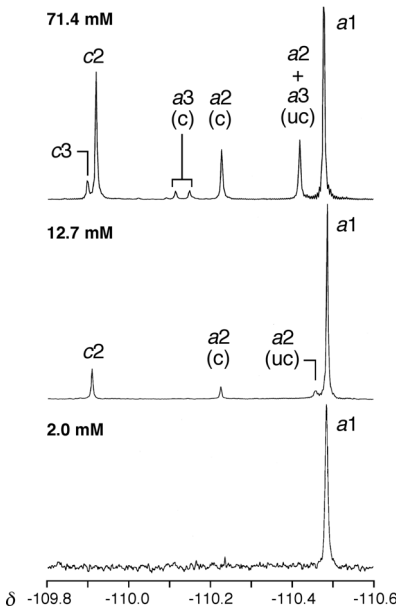

Figure 3.40. The concentration dependent partial ^{19}F NMR spectra (376 MHz, 298 K, CD_3CN) of **29**-H·PF_6.

The ^{19}F NMR spectra obtained from three samples containing different concentrations of **29**-H·PF_6 (2.0, 12.7, and 71.4 mM, respectively) revealed (Figure 3.40) a dramatic concentration dependence. The least concentrated sample (2.0 mM) gave rise to a ^{19}F

NMR spectrum containing a single aromatic F signal. Inspection of the corresponding ^{1}H NMR spectrum—which was reminiscent of that obtained when **29**-H·PF_6 was dissolved in CD_3SOCD_3—confirmed that the single F resonance could be attributed to the monomeric species, *i.e.*, the [*a*1]daisy chain. The ^{19}F NMR spectrum arising from the sample of intermediate concentration (12.7 mM) contained three additional aromatic F signals. From these extra peaks, it can be inferred that—at this higher concentration—intermolecular aggregation is starting to occur and results in the formation of new species. The presence of two small equal-intensity peaks (δ = –110.46 and –110.22, respectively) suggest the presence of an [*a*2]daisy chain in which one of the 3,5-difluorophenyl-terminated ammonium ion-containing arms is complexed, and the other one is not. One peak has a chemical shift similar to that observed for the monomeric species, whereas the other one is shifted downfield – consistent with complex formation, as was observed in the case of the model BMP25C8/**18**-H·PF_6 system. Even further downfield shifted is another singlet (δ = –109.90), which, most likely, corresponds to the [*c*2]daisy chain in which all of the F atoms reside in equivalent environments. The ^{19}F NMR spectrum, obtained from the most concentrated sample (71.4 mM) investigated in this study, is, appropriately, the most complicated. At this concentration, a new peak is observed to appear just downfield of that assigned to the [*c*2]daisy chain, and can, therefore, be attributed to the [*c*3]daisy chain. Correspondingly, peaks that can be attributed to the acyclic trimer ([*a*3]daisy

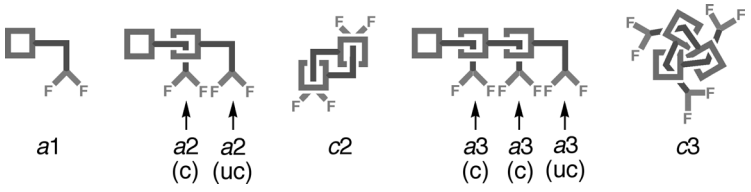

Figure 3.41. A schematic representation depicting the 'free' and bound ammonium ion-containing arms of aggregated (up to, and including, trimeric) daisy chain superstructures.

chain) are also annotated on the spectrum. Two small equal-intensity peaks (δ = –110.12 and –110.15, respectively) are observed in the same region of the spectrum as the peak (δ = –110.22) corresponding to the resonance of the F atoms on the complexed arm of the [*a*2]daisy chain. The [*a*3]daisy chain is expected (Figure 3.41) to give rise to three equal intensity signals, two corresponding to the F atom resonances of bound arms and one arising from the resonance of the F atoms in the 'free' arm. It is not unreasonable to propose that the peak associated with this latter resonance overlaps with the peak arising corresponding resonance of the 'free' arm of the [*a*2]daisy chain. This hypothesis gains further support when it is considered that the signal labeled '*a*2 + *a*3 (uc)' has an intensity equal to the sum of the intensities of the peak corresponding to *a*2 (c) and one of the *a*3 (c) peaks. Although these assignments cannot be made with 100 % certainty, they are consistent with (i) the anticipated solution phase behavior—upon increasing concentration—of an aggregating self-complementary system, (ii) the number and intensity ratios of peaks that would be expected to arise from the proposed species, as well as (iii) the relative chemical shift values that would arise for peaks corresponding to the resonances of either 'free' or bound F-containing arms. Assuming the correct interpretation of the spectrum, K_a values for the appropriate assembly steps (recall Figure 3.20) were calculated—employing the single point method—based

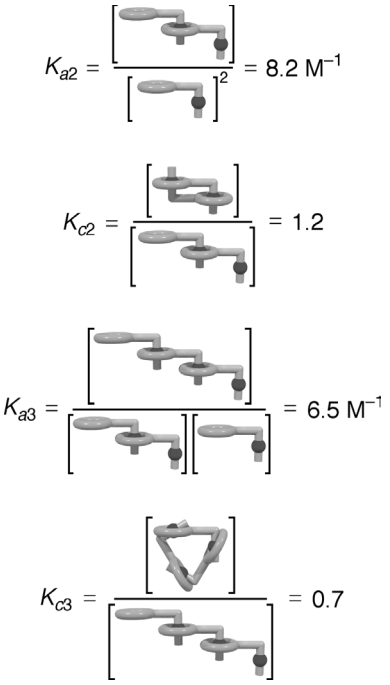

Figure 3.42. The expressions used to calculate the association constants for the aggregation of **29**-H·PF_6 in CD_3CN solution at 298 K.

upon the data contained with the ^{19}F NMR spectrum obtained from the 71.4 mM sample. Although the values obtained (Figure 3.42) are lower than those observed for the model system (K_a = 25 M^{-1}), this outcome is consistent with observations made in the [24]crown-8 series. In that case, concentration-dependent ^{1}H NMR spectroscopic studies—in conjunction with a mathematical model—also indicate that the association constants for daisy chain aggregation are lower[40] than those observed in a model two component system. Using the K_a values determined for the self-aggregation of **29**-H·PF_6 at 71.4 mM, the concentration profile of this system can be plotted (Figure 3.43) using the Excel spreadsheet (See Apendix). This plot not only reveals that significant amounts of [*a*3]- and [*c*3]daisy chain are only expected to form at relatively high monomer concentrations (> 1 M), but it also serves to confirm the ^{19}F NMR spectroscopic observations made on 2.0 and 12.7 mM solutions of **29**-H·PF_6, respectively. The ^{19}F NMR spectrum, obtained from the 12.7 mM solution, contained peaks (recall Figure 3.40) corresponding to the presence of [*a*1]-, [*a*2]-, and [*c*2]daisy chains with percentage concentrations of 87.8, 5.6, and 6.6, respectively. The percentage concentrations of these species, as predicted from the concentration profile shown in Figure 3.43, are 85.0, 6.5, and 7.8, respectively, values which are within experimental error of those observed experimentally. Furthermore, the

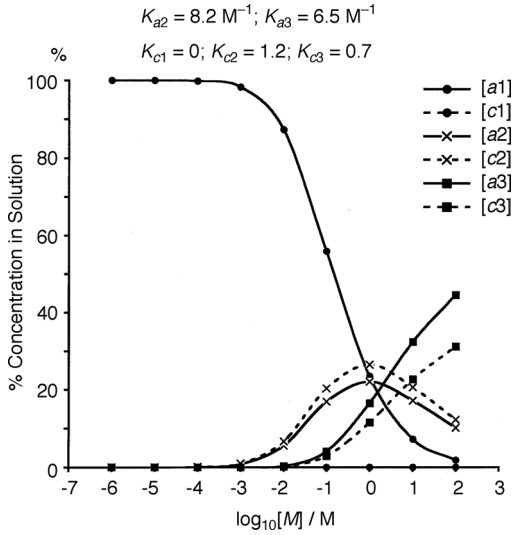

Figure 3.43. A concentration profile can be constructed for **29**-H·PF_6 based upon the K_a values determined from the ^{19}F NMR spectroscopic studies.

[*a*3]- and [*c*3]daisy chains are predicted to account for 0.4 and 0.3 %, respectively, of the total concentration of all species in solution, a result that explains why signals for these species are not observed in the 12.7 mM spectrum. When considering the most dilute solution (2.0 mM), only one signal—arising from the [*a*1] monomer—is observed. Once again, this result can be rationalized by using the concentration profile plotted in Figure 3.43. It predicts that ~97 % of the 2.0 mM solution is anticipated to be the monomeric species, with only ~1.5 % of both [*a*2]- and [*c*2]daisy chains being present. Unless it is a remarkable coincidence, the good agreement between theory and experiment is surely a testament to both (i) the assignment of peaks in the concentration-dependent ^{19}F NMR spectra of **29**-H·PF_6 and (ii) the validity of the model employed in the construction of the concentration profiles.

For such a self-assembling system, it is possible to define (Figure 3.44) *overall* cyclic dimerization and cyclic trimerization constants – namely K_{Dim} and K_{Tri}, respectively. By utilizing variable temperature ^{19}F NMR spectroscopy (Figure 3.45), values for these association constants were calculated at different temperatures. An increase in the temperature of the solution resulted in a decrease in the amount of dimeric and trimeric species observed. Such a trend is reflected in the ever-decreasing values of K_{Dim} and K_{Tri} as the temperature rises. By constructing a van't Hoff plot for each of these species (Figure 3.46), the enthalpic and entropic contributions to the formation of these species can be determined. Straight lines,

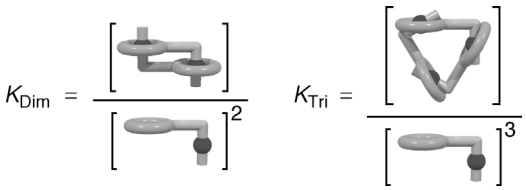

Figure 3.44. Expressions for the overall cyclic dimerization and trimerization constants in a self-complementary daisy chain system.

each with a good fit, can be approximated to the experimental data, revealing that (i) the formation of the [*c*3]daisy chain is more *enthalpically* favorable than the assembly of the [*c*2]daisy chain, whereas (ii) entropy factors favor the formation of the cyclic dimeric, rather than the trimeric, superstructure. These results are not unexpected: assembly of the [*c*3]daisy chain proceeds with the creation of more noncovalent interactions than does the formation of the [*c*2]daisy chain, but it requires the assembly of three separate components rather than two. One important point to note is that the enthalpic gain upon cyclic trimerization is almost twice as much as that calculated for cyclic dimerization. Based upon the fact that the formation of a [c3]daisy chain results from three crown ether/ammonium ion interactions, and two such interactions are responsible for [c2]daisy chain formation, why do the enthalpic terms not reflect this 3:2 ratio? Furthermore, in the case of the [24]crown-8 daisy chains, the stacking of the central aromatic rings appears to account for a significant stabilization of the [*c*2] superstructure, resulting in their domination of both the solution- and solid-state properties. If extrapolated to the [25]crown-8-based systems, this additional π–π derived stabilization would surely result in an even smaller ratio of the enthalpy changes observed for cyclic trimerization *vs* dimerization. Perhaps the fact that

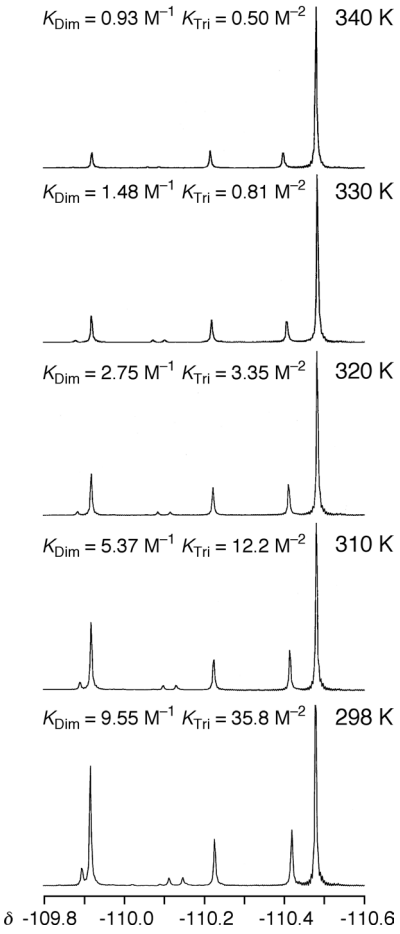

Figure 3.45. The temperature-dependent partial ^{19}F NMR spectra (376 MHz, CD_3CN) of **29**-H·PF_6.

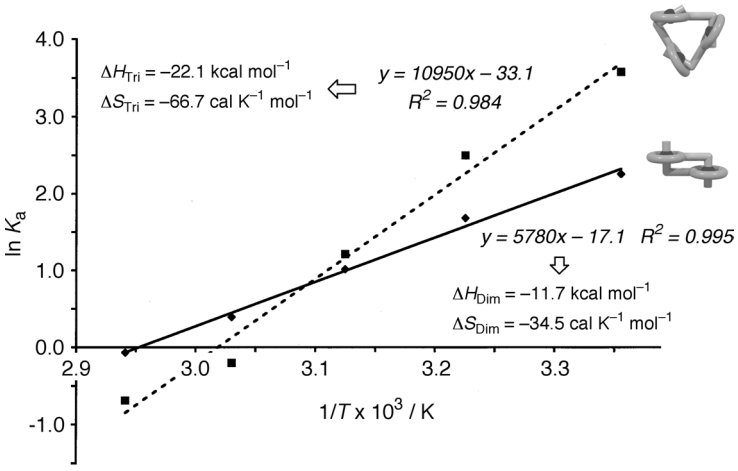

Figure 3.46. The van't Hoff plot obtained upon plotting ln K_a *vs* 1/T for the K_a values determined from the partial ^{19}F NMR spectra illustrated in Figure 3.45.

such an effect is not observed, means that, in the [25]crown-8 series the [*c*2] superstructure does not represent such an island of stability as it does in the case of the [24]crown-8 analogues. In retrospect, this observation is also reflected in the values of K_{a2} and K_{c2} obtained for **29**-H·PF$_6$. Whereas K_{a2} is over six times larger than K_{c2} in the [25]crown-8 series, the trend—if not the magnitude—is believed to be reversed in the [24]crown-8 series.

3.4. Conclusions

It has been shown that self-complementary dibenzylammonium ion substituted crown ethers—with either a [24]- or [25]crown-8 constitution—will aggregate to give daisy chain assemblies under the appropriate conditions of concentration, temperature and solvent polarity. Unfortunately, these supramolecular aggregates fall far short of the suprapolymeric systems described in the Introduction of this Chapter. Although intramolecular self-complexation is not an option for these daisy chain molecules, a growing chain quickly finds its own tail and cyclizes, preventing any further chain propagation. In the case of the [24]crown-8 systems, there is overwhelming evidence to suggest that—over a wide concentration range—the [*c*2]daisy chain is by far the most

favorable assembly. This conclusion was not reached easily or lightly. It required the application of deuterium- as well as fluorine-labeling – in conjunction with extensive concentration- and temperature-dependent spectroscopic studies. Furthermore, the interpretation of the spectroscopic data collected for these compounds is complicated by the formation of stereoisomeric aggregates. In an attempt to alleviate this subtle stereochemical nuance, more symmetrical daisy chain monomers based upon [25]crown-8 macrocycles were prepared and studied. Not only is the spectroscopic behavior of these modified daisy chain monomers considerably simpler, but the [*c*2]daisy chain superstructure no longer represents a dead-end for chain growth. Unfortunately, however, the weaker interaction between secondary dialkylammonium ions and [25]crown-8-based macrocycles undermines the effectiveness of this supramolecular ssytem. Although trimeric aggregates are observed in solution, these species are not predicted to rise to significant levels at concentrations < 1 M. Consequently, the concentration at which a species considered to be supramolecular polymer would be formed is likely to far exceed the solubility limits of these salts. In summary, although not precursors for interwoven supramolecular polymers, the compounds reported in this Chapter represent interesting examples of interwoven supermolecules that than could be utilized—with appropriate modification—in the formation (*vide infra*) of mechanically-interlocked polymers.

3.5. Future Directions

The overwhelming preference for [24]crown-8-based daisy chain systems to form cyclic dimeric superstructures has, thus far, precluded the formation of extended polymeric

arrays. Both enthalpic and entropic considerations seem to favor the formation of discrete [*c*2]daisy chains in preference to the assembly of extended polymeric structures.

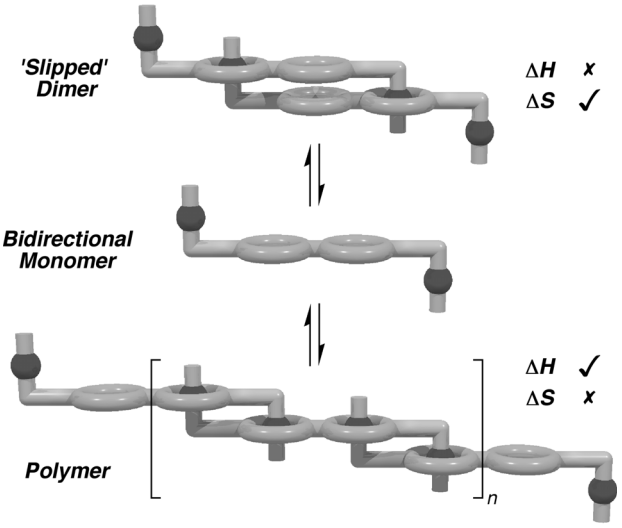

Figure 3.47. A schematic representation depicting the possible ways in which a bidirectional quadratopic daisy chain monomer may self-assemble to form aggregated superstructures.

By changing the design of the monomeric building block, however, this feature could, potentially, still be utilized in the construction of interwoven macromolecules. Conceptually, a bidirectional quadratopic monomer (illustrated in Figure 3.47) has the potential to aggregate in many different ways.[57] However, although the formation of discrete 'slipped' dimers is—compared to polymerization—entropically favorable,[58] the assembly of such a superstructure is anticipated to be enthalpically disfavored. Upon formation of a 'slipped' dimer only half of all the recognition sites are satisfied, in violation of the principle of maximal site occupancy.[59] In contrast, the polymerization pathway depicted in Figure 3.47 represents an enthalpically-favorable option for the self assembly of this bidirectional monomer. Although the formation of either superstructure will depend upon a delicate balance between enthalpic and entropic factors, unlike the original daisy chain monomers, these two effects now work in opposition, and can, potentially be exploited to generate the desired product. Currently, a system with this architecture—based upon pyrido-crown ether/secondary ammonium ion recognition sites[60]—is being investigated in the Stoddart group.

Another way in which the cyclic dimerization of these systems could be exploited is shown schematically in Figure 3.48. This approach involves the assembly of a [*c*2]daisy

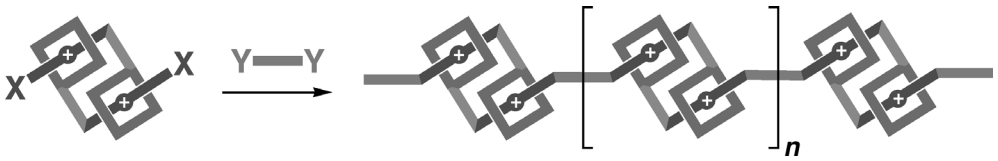

Figure 3.48. A schematic representation depicting the covalent polymerization of a discrete [*c*2]daisy chain superstructure to afford an interlocked macromolecule.

chain that possesses, at its termini, reactive functional groups (**X**). Subsequently, a traditional covalent polymerization, with a bifunctional (**Y**) spacer unit, will afford a mechanically interlocked polymer. This unique polymeric architecture has no continuous covalent backbone, which may result in such a material exhibiting unusual physical properties.[61] This project[62] is currently underway, employing a system in which the reactive **X** groups are hydroxymethyl functions, and the bifunctional spacer units are inserted using diisocyanate linkers.

3.6. Experimental

General: Chemicals were purchased from Aldrich and Lancaster Synthesis Ltd and used as received unless indicated otherwise. Compounds **12**[41] and **23**[54] were prepared according to literature procedures. The synthesis and characterization data for BMP25C8 (**28**) are reported in Chapter 2 of this Thesis. Solvents were dried according to literature procedures.[63] Thin-layer chromatography was carried out using aluminium sheets pre-coated with silica gel 60F (Merck 5554). The plates were inspected by UV light and, if required, developed in I_2 vapor. Column chromatography was carried out using silica gel 60F (Merck 9385, 0.040–0.063 mm). Melting points were determined on an Electrothermal 9100 apparatus and are uncorrected. ^{1}H and ^{13}C NMR spectra were recorded on either a Bruker AC300 (300

and 75 MHz, respectively), Bruker ARX400 (400 and 100 MHz, respectively), or Bruker ARX500 (500 and 125 MHz, respectively) spectrometer, using residual solvent as the internal standard. ^{1}H-Decoupled ^{19}F NMR spectra were recorded on a Bruker ARX400 (376 MHz) spectrometer, and were referenced to C_6F_6 (–163.0 ppm) present as a CH_2Cl_2 solution in an internal capillary tube. All chemical shifts are quoted on the δ scale, and all coupling constants are expressed in Hertz (Hz). Liquid secondary ion (LSI) mass spectra were obtained on a VG Zabspec mass spectrometer, equipped with a cesium ion source and utilizing a *m*-nitrobenzyl alcohol matrix. Fast atom bombardment (FAB) mass spectra were obtained using a ZAB-SE mass spectrometer, equipped with a krypton primary atom beam, utilizing a *m*-nitrobenzyl alcohol matrix. Cesium iodide or poly(ethylene glycol) were employed as reference compounds. Electron impact mass spectra (EIMS) were obtained from a VG Prospec mass spectrometer. Microanalyses were performed by either the University of North London Microanalytical Service (UK) or Quantitative Technologies, Inc (USA).

3,4-Bis{2-[2-(2-hydroxyethoxy)ethoxy]ethoxy}benzaldehyde (**6**). 3,4-Dihydroxybenzaldehyde (**4**) (15.1 g, 0.11 mol), K_2CO_3 (37.3 g, 0.27 mol), and LiBr (9.5 g, 0.11 mol) were placed in a 2 L round-bottomed flask fitted with a condenser and a pressure equalized dropping funnel. The system was flushed with N_2 and anhydrous DMF (500 mL) was introduced into the flask. 2-[2-(2-Chloroethoxy)ethoxy]ethanol (**5**) (40.6 g, 0.24 mol) was dissolved in DMF (100 mL) and added to the dropping funnel, again through a flow of nitrogen. The suspension in the flask was heated to 100 °C whilst stirring, and the solution of **5** was added dropwise over 1 h. The reaction mixture was stirred at 100 °C for a further 3 d under a continuous flow of N_2. After this time, the reaction mixture was filtered (in order to remove inorganic salts), evaporated to dryness, and the residue partitioned between CH_2Cl_2 (300 mL) and 10 % w/v K_2CO_3 solution (300 mL). The organic layer was further washed with 10 % w/v K_2CO_3 solution (3 x 100 mL). The organic phase was dried ($MgSO_4$) and the solvents removed *in vacuo* to yield **6** as a brown oil (39.1 g, 89 %). This oil was used in subsequent reactions without further purification. An analytically pure sample was obtained as a pale yellow oil after chromatography (SiO_2 : gradient elution with CH_2Cl_2/MeOH, 100:0 to 96:4); ^{1}H NMR (300 MHz, $CDCl_3$): δ = 3.32 (br s, 2H), 3.52–3.74 (m, 16H), 3.83–3.90

(m, 4H), 4.14–4.23 (m, 4H), 6.94 (d, J = 8.1 Hz, 1H), 7.35–7.42 (m, 2H), 9.77 (s, 1H); ^{13}C NMR (75 MHz, $CDCl_3$): δ = 61.5, 68.5, 69.2, 69.3, 70.2, 70.7, 70.8, 72.6, 111.5, 112.2, 126.7, 130.1, 148.9, 154.0, 190.8; MS (EI): *m/z* (%): 402 (37) $[M]^+$; $C_{19}H_{30}O_9$ (402.4): calcd C 56.71, H 7.51; found C 56.88, H 7.41.

3,4-Bis(2-{2-[2-(*p*-toluenesulfonyloxy)ethoxy]ethoxy}ethoxy)benzaldehyde (**7**). Diol **6** (26.6 g, 66.0 mmol), Et_3N (66.8 g, 660 mmol) and a catalytic amount of 4-dimethylaminopyridine were dissolved in CH_2Cl_2 (400 mL) and this solution was stirred and cooled (0–5 °C). A solution of *p*-toluenesulfonyl chloride (62.9 g, 330 mmol) in CH_2Cl_2 (200 mL) was then added dropwise over a period of 3 h, maintaining the reaction temperature below 5 °C. Subsequently, the reaction mixture was allowed to warm up to ambient temperature and left to stir for a further 8 h under a continuous flow of N_2. The reaction mixture was acidified with 5M HCl solution (250 mL) and the organic layer was washed with 2M HCl solution (200 mL) and saturated brine (2 x 200 mL). The organic layer was dried ($MgSO_4$) and the solvents removed *in vacuo*. The residue was purified by column chromatography (SiO_2 : gradient elution with EtOAc/C_6H_{14}, 50:50 to 80:20) to yield the desired compound **7** as a pale yellow oil (26.8 g, 57 %); ^{1}H NMR (300 MHz, $CDCl_3$): δ = 2.38 (s, 6H), 3.53–3.67 (m, 12H), 3.78–3.86 (m, 4H), 4.08–4.21 (m, 8H), 6.96 (d, J = 8.1 Hz, 1H), 7.29 (d, J = 8.5 Hz, 4H), 7.36–7.43 (m, 2H), 7.74 (d, J = 8.5 Hz, 4H), 9.78 (s, 1H); ^{13}C NMR (75 MHz, $CDCl_3$): δ = 21.8, 68.9, 69.4, 69.6, 69.7, 70.9, 71.5, 111.5, 112.0, 112.7, 126.9, 128.1, 130.0, 130.4, 133.1, 145.0, 149.3, 154.5, 191.0; MS (FAB): *m/z* (%): 711 (21) $[M]^+$; $C_{19}H_{30}O_9$ (710.8): calcd C 55.76, H 5.96; found C 55.74, H 5.75.

(2-Formyl)dibenzo[24]crown-8 (**9**)**.** Cesium carbonate (19.3 g, 59.3 mmol) was placed in a 1 L round-bottomed flask fitted with condenser and pressure equalized dropping funnel. The system was flushed with N_2 and anhydrous DMF (200 mL) was added to the flask. The ditosylate **7** (8.43 g, 11.9 mmol) and catechol (**8**) (1.31 g, 11.9 mmol) were dissolved in DMF (500 mL) and added to the dropping funnel, again through a flow of N_2. The suspension in the flask was heated up to 100 °C whilst stirring, and the ditosylate/catechol solution was added dropwise over 24 h. This mixture was stirred at 100 °C—under an N_2

atmosphere—for a further 7 d. Subsequently, the solvent was removed *in vacuo* and the residue partitioned between PhMe (300 mL) and 10 % w/v K_2CO_3 solution (300 mL). The aqueous layer was further extracted with PhMe (3 x 200 mL) and the combined organic layers were washed with 10 % w/v K_2CO_3 solution (300 mL). The organic phase was dried ($MgSO_4$) and the solvents removed *in vacuo*. The residue was subjected to column chromatography (SiO_2 : gradient elution with EtOAc/MeOH, 100:0 to 95:5) to yield an off-white solid which was recrystallized from EtOAc/C_6H_{14} to yield the desired compound **9** as a white solid (2.31 g, 41 %); m.p. 105–107 °C; ^{1}H NMR (300 MHz, $CDCl_3$): δ = 3.82–3.85 (m, 8H), 3.89–3.97 (m, 8H), 4.12–4.24 (m, 8H), 6.83–6.90 (m, 4H), 6.93 (d, J = 8.1 Hz, 1H), 7.37 (d, J = 1.8 Hz, 1H), 7.42 (dd, J = 1.8, 8.1 Hz, 2H), 9.81 (s, 1H); ^{13}C NMR (75 MHz, $CDCl_3$): δ = 69.4, 69.5, 69.7, 70.0, 71.3, 71.4, 71.5, 111.1, 111.9, 114.0, 121.4, 126.8, 130.2, 148.9, 149.2, 154.3, 190.9; MS (FAB): *m/z* (%): 477 (100) $[M+H]^+$, 494 (13) $[M+NH_4]^+$, 499 (24) $[M+Na]^+$, 515 (5) $[M+K]^+$; $C_{25}H_{32}O_9$ (476.5): calcd C 63.01, H 6.77; found C 63.12, H 6.54.

(2-Benzylaminomethyl)dibenzo[24]crown-8 (**1**). A solution of the formyl crown ether **9** (1.50 g, 3.15 mmol) and benzylamine **10** (337 mg, 3.15 mmol) was heated under reflux for 30 h in PhMe (150 mL) using a Dean-Stark apparatus. On allowing the reaction mixture to cool down to ambient temperature, an aliquot (*ca*. 1 mL) was removed, and the solvent evaporated *in vacuo* to give a yellow oily residue which was shown by ^{1}H NMR to be the imine; ^{1}H NMR (300 MHz, $CDCl_3$): δ = 3.85–3.98 (m, 16H), 4.13–4.23 (m, 8H), 4.81 (s, 2H), 6.85–6.95 (m, 5H), 7.16-7.45 (m, 7H), 8.28 (s, 1H). The reaction mixture was diluted with dry MeOH (100 mL) and then $NaBH_4$ (1.19 g, 31.5 mmol) was added portionwise to the stirring solution over a period of 1 h. Stirring was maintained under ambient conditions for a further 24 h, after which time 5M HCl solution (250 mL) was added to the reaction mixture. The solvents were removed *in vacuo* and the residue was partitioned between 2M NaOH solution (250 mL) and CH_2Cl_2 (250 mL). The aqueous layer was extracted with CH_2Cl_2 (2 x 100 mL) and the combined organic extracts were dried ($MgSO_4$). The solvents were removed *in vacuo* yielding a crude product which was subjected to column chromatography (SiO_2 : Me_2CO) to yield the title compound **1** as a pale yellow oil (1.42 g, 79 %); ^{1}H NMR (300 MHz, $CDCl_3$): δ = 3.71 (s, 2H), 3.77 (s, 2H), 3.82 (s, 8H), 3.88–3.93 (m, 8H), 4.11–4.17 (m,

8H), 6.78–6.91 (m, 5H), 7.20–7.34 (m, 7H); ^{13}C NMR (75 MHz, $CDCl_3$): δ = 52.9, 53.2, 69.5, 69.6, 70.0, 71.3, 114.0, 114.2, 121.0, 121.5, 127.0, 128.3, 128.5, 133.7, 140.4, 147.9, 149.0; MS (LSI): *m/z* (%): 568 (15) $[M+H]^+$ and $[2M+2H]^{2+}$, 1135 (100) $[2M+H]^+$; $C_{32}H_{41}NO_8$ (567.7): calcd C 67.71, H 7.28, N 2.47; found C 67.75, H 7.29, N 2.39.

(2-Benzylammoniummethyl)dibenzo[24]crown-8 Hexafluorophosphate (**1**-H·PF_6). Amine **1** (470 mg 0.83 mmol) was dissolved in 5M HCl solution (50 mL) and the resulting solution was evaporated to dryness. The residue was dissolved in hot water (*ca*. 15 mL) and a saturated aqueous solution of NH_4PF_6 was added until no further precipitation occurred. The white precipitate was collected, washed with copious amounts of H_2O and dried to yield the hexafluorophosphate salt **1**-H·PF_6 as a white powder (552 mg, 93 %); m.p. >210 °C (decomp.); ^{1}H NMR (300 MHz, CD_3SOCD_3): δ = 3.68 (s, 8H), 3.74–3.83 (m, 8H), 4.04–4.16 (m, 12H), 6.86–6.99 (m, 4H), 7.02 (s, 2H), 7.13 (s, 1H), 7.47 (br s, 5H), 9.09 (br s, 2H); ^{13}C NMR (75.5 MHz, CD_3SOCD_3): δ = 49.9, 50.0, 68.7, 69.0, 69.1, 70.4, 113.5, 114.0, 115.4, 121.1, 123.0, 124.2, 128.7, 129.0, 129.9, 132.0, 148.2, 148.4, 148.9; MS (LSI): *m/z* (%): 568 (51) $[M-PF_6]^+$ and $[2M-2PF_6]^{2+}$, 590 (21) $[M-H-PF_6+Na]^+$, 700 (19) $[M-H-PF_6+Cs]^+$, 1135 (100) $[2M-H-2PF_6]^+$, 1281 (16) $[2M-PF_6]^+$; $C_{32}H_{42}NO_8PF_6$ (713.6): calcd C 53.86, H 5.93, N 1.96; found C 53.60, H 5.84, N 2.05.

(2-Benzylammoniummethyl)dibenzo-24-crown-8 Trifluoroacetate (**1**-H·O_2CCF_3)**.** A CH_2Cl_2 solution of the amine **1** was treated with an excess of CF_3CO_2H. Removal of the solvents *in vacuo*, afforded **1**-H·O_2CCF_3 as a pale yellow solid. Single crystals suitable for X-ray crystallographic analysis were obtained when a solution of the salt in EtOAc/C_6H_{14}/MeCN (10:10:1) was allowed to stand at 20 °C for approximately 1 d. Crystal data for $C_{32}H_{42}NO_8{\cdot}CF_3CO_2{\cdot}CF_3CO_2H$: M_r = 795.7, monoclinic, space group *C*2/*c*, *a* = 22.936 (4), *b* = 23.249 (3), *c* = 15.393 (3) Å, β = 112.14 (1)°, *V* = 7603 (2) Å^3, *Z* = 8, ρ_{calcd} = 1.39 g cm^{-3}, μ ($Mo_{K\alpha}$) = 1.22 cm^{-1}, *F*(000) = 3328. Crystal dimensions 0.33 x 0.33 x 0.80 mm (needles), Siemens P4 diffractometer, graphite-monochromated $Mo_{K\alpha}$ radiation, ω-scans, *T* = 203 K. Of 6449 independent reflections measured ($2\theta \leq 50°$), 2715 had $I_o > 2\sigma(I_o)$ and were considered to be observed. The structure was solved by direct methods and the non-hydrogen atoms refined anisotropically. The positions of the NH_2^+ hydrogen atoms were located from

a ΔF map and refined isotropically subject to an N–H distance constraint. The remaining hydrogen atoms were placed in calculated positions, assigned isotropic thermal parameters U(H) = 1.2 U_{eq}(C), and allowed to ride on their parent atoms. Refinement was by full-matrix least-squares, based on F^2 to give R_1 = 0.092, wR_2 = 0.222. Computations were carried out using the SHELXTL 5.03 package.[64] CCDC 100961.[65]

(2-Formyl)dibenzo{catechol-d_4}[24]crown-8 (13). Cesium carbonate (46.5 g, 143 mmol) was placed in a 2 L round-bottomed flask fitted with condenser and pressure equalized dropping funnel. The system was flushed with N_2 and anhydrous DMF (500 mL) was added to the flask. The ditosylate **7** (8.43 g, 11.9 mmol) and d_4-catechol[41] (**12**) (3.26 g, 28.6 mmol) were dissolved in DMF (1 L) and added to the dropping funnel, again through a flow of N_2. The suspension in the flask was heated to 100 °C whilst stirring, and the ditosylate/d_4-catechol solution was added dropwise over 48 h. This mixture was stirred at 100 °C—under an N_2 atmosphere—for a further 3 d. Upon cooling down, the reaction mixture was filtered, the solvent removed *in vacuo*, and the residue partitioned between PhMe (300 mL) and 10 % w/v K_2CO_3 solution (300 mL). The aqueous layer was further extracted with PhMe (4 x 300 mL) and the combined organic layers were washed with 10 % w/v K_2CO_3 solution (300 mL). The organic phase was dried ($MgSO_4$) and the solvents removed *in vacuo*. The residue was subjected to column chromatography (SiO_2 : gradient elution with EtOAc/MeOH, 100:0 to 96:4) to yield a white solid which was recrystallized from EtOAc/C_6H_{14} to yield the desired compound **13** as a white solid (7.79 g, 57 %); m.p. 108–109 °C; ^{1}H NMR (400 MHz, $CDCl_3$): δ = 3.81–3.85 (m, 8H), 3.89–3.96 (m, 8H), 4.11–4.22 (m, 8H), 6.92 (d, J = 8.0 Hz, 1H), 7.36 (d, J = 2.0 Hz, 1H), 7.40 (dd, J = 2.0, 8.0 Hz, 1H), 9.80 (s, 1H); ^{13}C NMR (100 MHz, $CDCl_3$): δ = 69.4, 69.5, 69.6, 69.7, 69.8, 70.0, 71.4, 71.5, 71.6, 111.1, 112.0, 113.1–114.0 (^{2}H-coupled multiplet), 120.6–121.4 (^{2}H-coupled multiplet), 126.9, 130.3, 148.9, 149.3, 139.8, 154.4, 191.0; MS (FAB): *m/z* (%): 481.4 (100) $[M+H]^+$; HRMS (FAB): calcd for $[M]^+$ ($C_{25}H_{28}D_4O_9$) 480.2297, found 480.2319; $C_{25}H_{28}D_4O_9$ (480.5): calcd C 62.49, H+D 7.55; found C 62.61, "H" 6.83. Note: Combustion analysis does not discriminate between H_2O, HOD, and D_2O, therefore, the theoretical values (%) for C and H will not be observed in the analysis of a pure sample of this compound. After combustion, all water vapor detected (on a

thermal conductivity, *not* a mass, basis) passing through the GC column is assumed to be H_2O (rather than other, heavier, isotopic forms), and, as such, a correct composition analysis will reflect the C and H values (%) for the undeuterated analogue of the compound. In this case, the observed values (*vide supra*) are within 0.4 % of those expected (C 63.01, H 6.77) for the unlabeled analogue.

(2-Benzylammoniummethyl)dibenzo{catechol-*d*4}[24]crown-8 Hexafluorophosphate (**11**-H·PF_6). Conversion of **13** (761 mg, 1.58 mmol) into the corresponding d_4-daisy chain monomer **11**-H·PF_6 was achieved using the same procedures as described previously for the non-deuterated analogue. The target compound (**11**-H·PF_6) was obtained as a white solid (280 mg, 87 % over three steps); m.p. 208–211 °C (decomp.); ^{1}H NMR (400 MHz, CD_3SOCD_3): δ = 3.64–3.68 (m, 8H), 3.74–3.81 (m, 8H), 4.03–4.14 (m, 12H), 6.97–7.03 (m, 2H), 7.36 (s, 1H), 7.39–7.51 (m, 5H); ^{13}C NMR (125 MHz, CD_3SOCD_3): δ = 50.2, 50.3, 69.0, 69.1, 69.2, 69.4, 69.5, 70.7, 70.8, 113.5–114.3 (^{2}H-coupled multiplet) overlapping with a singlet at 113.8, 115.8, 120.6–121.3 (^{2}H-coupled multiplet), 123.4, 124.4, 129.1, 129.4, 130.3, 132.2, 148.5, 148.7, 149.3; MS (FAB): *m/z* (%): 572.3 (87) $[M–PF_6]^+$ and $[2M–2PF_6]^{2+}$, 1143.6 (100) $[2M–H–2PF_6]^+$, 1289.8 (37) $[2M–PF_6]^+$; HRMS (FAB): calcd for $[M–PF_6]^+$ ($C_{32}H_{38}D_4NO_8$) 572.3158, found 572.3157; $C_{32}H_{42}NO_8PF_6·0.5H_2O$ (721.1): calcd C 53.19, H 6.00, N 1.94; found C 53.10, H 5.94, N 1.88. Note: As with **13**, the composition analysis assumes the compound to contain only protium, and no deuterium.

Bis(4-fluorobenzyl)ammonium Hexafluorophosphate (**14**-H·PF_6). A solution of 4-fluorobenzylamine (**16**) (5.00 g, 40.0 mmol) and 4-fluorobenzaldehyde (**15**) (4.96 g, 40.0 mmol) in C_6H_6 (150 mL) was heated under reflux for 20 h using a Dean-Stark apparatus. The resulting solution was evaporated to dryness, the residue dissolved in dry MeOH (100 mL), and $NaBH_4$ (7.57 g, 200 mmol) was added portionwise over a period of 10 min. After stirring under ambient conditions for 4 h, the reaction mixture was quenched with an excess of 12M HCl solution. The solvents were removed *in vacuo*, and the residue was partitioned between NaOH solution (5N, 250 mL) and CH_2Cl_2 (250 mL). The aqueous layer was further extracted with CH_2Cl_2 (3 x 250 mL), the combined organic extracts were dried ($MgSO_4$), and the

resulting solution was evaporated to dryness to yield a colorless oil. The oil was subsequently dissolved in MeOH (200 mL) and 12M HCl solution (25 mL) was added carefully. After stirring for *ca*. 10 min, the solvents were removed *in vacuo* to give a white solid, which was then dissolved in hot H_2O. A minor amount of insoluble material was removed by hot filtration, and addition of an excess of saturated aqueous NH_4PF_6 to this solution resulted in the precipitation of the desired compound, which was collected and dried to give a white solid (10.6 g, 70 %); m.p. 229–231 °C (decomp.); ^{1}H NMR (400 MHz, CD_3SOCD_3): δ = 4.23 (s, 4H), 6.99 (br s, 2H), 7.16–7.23 (m, 4H), 7.48–7.54 (m, 4H); ^{19}F NMR (376 MHz, CD_3SOCD_3): δ = –71.9 (d, J = 706 Hz, 6F), –112.4 (s, 2F); ^{13}C NMR (100 MHz, CD_3SOCD_3): δ = 51.5, 116.7 (d, J = 21.8 Hz), 127.3 (d, J = 3.3 Hz), 133.5 (d, J = 8.7 Hz), 164.2 (d, J = 245 Hz); MS (FAB): *m/z* (%): 234.2 (100) $[M–PF_6]^+$; HRMS (FAB): calcd for $[M–PF_6]^+$ ($C_{14}H_{14}NF_2$) 234.1095, found 234.1098; $C_{14}H_{14}NPF_8 \cdot 0.75H_2O$ (392.7): calcd C 42.81, H 3.98, N 3.57; found C 42.56, H 3.54, N 3.38.

(2-[4-Fluorobenzyl]ammoniummethyl)dibenzo[24]crown-8 Hexafluorophosphate (**17**-H·PF_6). A solution of the formyl-substituted crown ether **9** (750 mg, 1.57 mmol) and 4-fluorobenzylamine (**16**) (197 mg, 1.57 mmol) in PhMe (100 mL) was heated under reflux for 16 h using a Dean-Stark apparatus. The resulting solution was evaporated to dryness, the residue dissolved in dry MeOH (75 mL), and $NaBH_4$ (605 mg, 16.0 mmol) was added portionwise over a period of 10 min. After stirring under ambient conditions for 40 h, the reaction mixture was quenched with an excess of 12M HCl solution. The solvents were removed *in vacuo*, and the residue was partitioned between NaOH solution (5N, 250 mL) and CH_2Cl_2 (250 mL). The aqueous layer was further extracted with CH_2Cl_2 (3 x 250 mL), the combined organic extracts were dried ($MgSO_4$), and the resulting solution was evaporated to dryness to yield a colorless oil. The oil was subsequently dissolved in MeOH (50 mL) and 12M HCl solution (5 mL) was added carefully. After stirring for *ca*. 10 min, the solvents were removed *in vacuo* to give an oil, which was then dissolved in hot H_2O. A minor amount of insoluble material was removed by hot filtration, and addition of an excess of saturated aqueous NH_4PF_6 to this solution resulted in the precipitation of a white solid. Upon collection, the solid was washed with copious amounts of H_2O, and finally Et_2O to afford the

desired compound as a powdery white solid (972 mg, 83 %); m.p. 195–199 °C (decomp.); ^{1}H NMR (400 MHz, CD_3SOCD_3): δ = 3.65–3.68 (m, 8H), 3.74–3.81 (m, 8H), 4.04–4.14 (m, 12H), 6.85–6.96 (m, 4H), 7.00 (s, 2H), 7.12 (s, 1H), 7.25–7.32 (m, 2H), 7.50–7.57 (m, 2H), 9.09 (br s, 2H); ^{19}F NMR (376 MHz, CD_3SOCD_3): δ = –69.7 (d, J = 711 Hz, 6F), –112.3 (s, 1F); ^{13}C NMR (125 MHz, CD_3SOCD_3): δ = 49.1, 49.9, 68.7, 68.8, 68.9, 69.4, 69.1, 69.2, 70.4, 70.5, 113.5, 114.1 (d, J = 3.7 Hz), 115.5, 115.7, 121.2, 123.0, 124.2, 128.3 (d, J = 3.1 Hz), 132.4 (d, J = 8.5 Hz), 148.3, 148.5, 149.0, 162.4 (d, J = 244 Hz); MS (FAB): *m/z* (%): 586.5 (90) $[M–PF_6]^+$ and $[2M–2PF_6]^{2+}$, 1172.0 (100) $[2M–H–2PF_6]^+$, 1318.1 (15) $[2M–PF_6]^+$; $C_{32}H_{41}NO_8PF_7$ (731.6): calcd C 52.53, H 5.65, N 1.91; found C 52.55, H 5.43, N 1.69.

Bis(3,5-difluorobenzyl)ammonium Hexafluorophosphate (**18**-H·PF_6). A solution of 3,5-difluorobenzylamine (**20**) (1.01 g, 7.06 mmol) and 3,5-difluorobenzaldehyde (**19**) (1.00 g, 7.04 mmol) in PhMe (100 mL) was heated under reflux for 20 h using a Dean-Stark apparatus. The resulting solution was evaporated to dryness, the residue dissolved in dry MeOH (75 mL), and $NaBH_4$ (2.65 g, 70.1 mmol) was added portionwise over a period of 10 min. After stirring under ambient conditions for 40 h, the reaction mixture was quenched with an excess (~5 mL) of 12M HCl solution. The solvents were removed *in vacuo*, and the residue was partitioned between NaOH solution (2N, 250 mL) and CH_2Cl_2 (250 mL). The aqueous layer was further extracted with CH_2Cl_2 (3 x 250 mL), the combined organic extracts were dried ($MgSO_4$), and the resulting solution was evaporated to dryness to yield a colorless oil. The oil was subsequently dissolved in MeOH (200 mL) and 12M HCl solution (5 mL) was added carefully. After stirring for *ca*. 10 min, the solvents were removed *in vacuo* to give a white solid, which was washed with Et_2O. This solid was dissolved in a 1:1 mixture of Me_2CO/H_2O (400 mL) and an excess (~ 2.0 g) of solid NH_4PF_6 was added to this solution. Whilst this solution was being concentrated under reduced pressure to a volume of *ca*. 200 mL a white precipitate appeared. Subsequent addition of H_2O (300 mL) resulted in more precipitation. After collection and drying, the desired product was obtained as a white solid (2.64 g, 91 %); m.p. 231–233 °C; ^{1}H NMR (400 MHz, CD_3SOCD_3): δ = 4.27 (s, 4H), 7.02–7.20 (m, 8H); ^{19}F NMR (376 MHz, CD_3SOCD_3): δ = –71.7 (d, J = 706 Hz, 6F), –109.1

(s, 4F); ^{13}C NMR (100 MHz, CD_3SOCD_3): δ = 51.2, 106.1 (t, J = 25.5 Hz), 114.1–114.4 (m), 134.6 (t, J = 9.8 Hz), 163.8 (dd, J = 12.9, 247 Hz); MS (FAB): *m/z* (%): 270.2 (100) $[M–PF_6]^+$; HRMS (FAB): calcd for $[M–PF_6]^+$ ($C_{14}H_{12}NF_4$) 270.0906, found 270.0902; $C_{14}H_{12}NPF_{10}$ (415.2): calcd C 40.50, H 2.91, N 3.37; found C 40.55, H 2.79, N 3.26.

(2-[3,5-Difluorobenzyl]ammoniummethyl)dibenzo[24]crown-8 Hexafluorophosphate (**21**-H·PF_6). A solution of the formyl-substituted crown ether **9** (750 mg, 1.57 mmol) and 3,5-difluorobenzylamine (**20**) (225 mg, 1.57 mmol) in PhMe (150 mL) was heated under reflux for 20 h using a Dean-Stark apparatus. The resulting solution was evaporated to dryness, the residue dissolved in dry MeOH (75 mL), and $NaBH_4$ (605 mg, 16.0 mmol) was added portionwise over a period of 5 min. After stirring under ambient conditions for 40 h, the reaction mixture was quenched with an excess (~5 mL) of 12M HCl solution. The solvents were removed *in vacuo*, and the residue was partitioned between NaOH solution (2N, 250 mL) and CH_2Cl_2 (250 mL). The aqueous layer was further extracted with CH_2Cl_2 (3 x 250 mL), the combined organic extracts were dried ($MgSO_4$), and the resulting solution was evaporated to dryness to yield a colorless oil. The oil was subsequently dissolved in MeOH (50 mL) and 12M HCl solution (5 mL) was added carefully. After stirring for *ca*. 10 min, the solvents were removed *in vacuo* to give an oil, which was then dissolved in a 1:1 mixture of Me_2CO/H_2O (400 mL) and an excess (~ 2.0 g) of solid NH_4PF_6 was added to this solution. The solution was concentrated under reduced pressure—until no Me_2CO remained—and the oily H_2O-insoluble residue was extracted into CH_3NO_2 (3 x 50 mL). After drying ($MgSO_4$), the solvent was removed *in vacuo* to afford a sticky semi-solid residue, which was dissolved in CH_2Cl_2 (100 mL). A small amount of CH_2Cl_2-insoluble material was recovered, and determined to be NH_4PF_6. Addition of Et_2O (~100 mL) to the CH_2Cl_2 solution resulted in the precipitation of a sticky solid, which was redissolved upon addition of a small amount of MeOH (~ 10 mL). On leaving this solution to stand, a white solid *slowly* precipitated from solution over the course of the next month, which was collected by filtration and dried. Further treatment of the mother liquor with (i) Et_2O, and (ii) MeOH, caused further slow precipitation. In total, three crops of white solid were collected (535 mg, 45 %); m.p. 213–215 °C. The following NMR spectroscopic data is for the monomeric species, **21**-

H·PF_6, after the isolated material was allowed to de-thread in CD_3SOCD_3 over a period of 7 d. ^{1}H NMR (400 MHz, CD_3SOCD_3): δ = 3.65–3.68 (m, 8H), 3.73–3.81 (m, 8H), 4.04–4.12 (m, 10H), 4.19 (s, 2H), 6.84–6.90 (m, 2H), 6.92–6.96 (m, 2H), 6.98–7.04 (m, 2H), 7.10 (d, J = 1.2 Hz, 1H), 7.22–7.29 (m, 2H), 7.34 (tt, J_{HH} = 2.0 Hz, J_{HF} = 9.6 Hz, 1H), 9.11 (br s, 2H); ^{19}F NMR (376 MHz, CD_3SOCD_3): δ = –69.7 (d, J = 711 Hz, 6F), –108.8 (s, 2F); ^{13}C NMR (100 MHz, CD_3SOCD_3): δ = 48.8, 50.2, 68.7, 68.8, 68.9, 69.1, 69.2, 70.4, 70.5, 104.5 (t, J = 25.5 Hz), 113.1–113.4 (m), 114.0, 114.1, 115.5, 121.2, 123.1, 124.0, 136.0 (t, J = 9.9 Hz), 148.2, 148.5, 149.1, 162.2 (dd, J = 13.2, 245 Hz); MS (FAB): *m/z* (%): (i) of isolated material; 604.4 (100) $[M–PF_6]^+$ and $[2M–2PF_6]^{2+}$, 1207.9 (77) $[2M–H–2PF_6]^+$, 1318.1 (31) $[2M–PF_6]^+$; (ii) of material after DMSO-induced dethreading; 604.3 $[M–PF_6]^+$ *only*; $C_{32}H_{40}NO_8PF_8$ (749.6): calcd C 51.27, H 5.38, N 1.87; found C 51.22, H 5.37, N 1.80.

1,2-Bis(2-{2-[2-(2-*p*-tolylsulfonyloxy)ethoxy]ethoxy}ethoxy)benzene (**24**). Diol **23**[54] (55.0 g, 147 mmol), Et_3N (74.3 g, 734 mmol) and a catalytic amount of 4-dimethyl-aminopyridine were dissolved in CH_2Cl_2 (400 mL) and this solution was stirred and cooled (0-5 °C). A solution of *p*-toluenesulfonyl chloride (61.6 g, 323 mmol) in CH_2Cl_2 (100 mL) was then added dropwise over a period of 2 h, maintaining the reaction temperature below 5 °C. Subsequently, the reaction mixture was allowed to warm up to ambient temperature and left to stir for a further 3 h under a continuous flow of N_2. The reaction mixture was acidified with 5M HCl solution (250 mL) and the organic layer was washed with 2M HCl solution (2 x 200 mL). The organic layer was dried ($MgSO_4$) and the solvents removed *in vacuo*. The residue was purified by filtering through a pad of SiO_2 (gradient elution with EtOAc/C_6H_{14}, 10:90 to 60:40) to yield the desired compound **24** as a pale yellow oil (82.8 g, 83 %); ^{1}H NMR (200 MHz, $CDCl_3$): δ = 2.39 (s, 6H), 3.53–3.81 (m, 16H), 4.08–4.14 (m, 8H), 6.88 (s, 4H), 7.29 (d, J = 8.2 Hz, 4H), 7.75 (d, J = 8.2 Hz, 4H); ^{13}C NMR (50 MHz, $CDCl_3$): δ = 21.6, 68.7, 68.9, 69.4, 69.8, 70.7, 115.0, 121.7, 127.9, 129.9, 133.0, 144.8, 149.0; MS (FAB): *m/z* (%): 682 (26) $[M]^+$; $C_{32}H_{42}O_{12}S_2$ (682.8): calcd C 56.29, H 6.20; found C 56.39, H 6.17.

Benzo(5-hydroxymethylmetaphenylene)[25]crown-8 (**26**). Cesium carbonate (47.7 g, 146 mmol) was placed in a 2 L round-bottomed flask fitted with condenser and pressure

equalized dropping funnel. The system was flushed with N_2 and anhydrous MeCN (700 mL) was added to the flask. The ditosylate **24** (20.0 g, 29.3 mmol) and 3,5-dihydroxybenzylalcohol (**25**) (4.10 g, 29.3 mmol) were dissolved in dry MeCN (600 mL) and added to the dropping funnel, again through a flow of N_2. The suspension in the flask was heated under reflux whilst stirring, and the distosylate/**25** solution was added dropwise over 24 h. This mixture was stirred at reflux—under an N_2 atmosphere—for a further 3 d. Upon cooling down, the reaction mixture was filtered, the solvent removed *in vacuo*, and the residue partitioned between CH_2Cl_2 (300 mL) and 10 % w/v K_2CO_3 solution (300 mL). The aqueous layer was further extracted with CH_2Cl_2 (3 x 300 mL) and the combined organic layers were washed with 10 % w/v K_2CO_3 solution (300 mL). The organic phase was dried ($MgSO_4$) and the solvents removed *in vacuo*. The residue was subjected to column chromatography (SiO_2 : EtOAc/C_6H_{14}, 90:10) to yield a white solid (4.50 g, 32 %); m.p. 68–71 °C; ^{1}H NMR (400 MHz, $CDCl_3$): δ = 3.66–3.71 (m, 8H), 3.77–3.82 (m, 8H), 4.08–4.12 (m, 8H), 4.53 (s, 2H), 6.48 (d, J = 2.3 Hz, 2H), 6.57 (d, J = 2.3 Hz, 1H), 6.84–6.89 (m, 4H); ^{13}C NMR (75 MHz, $CDCl_3$): δ = 65.1, 68.1, 68.9, 69.8, 69.9, 71.0, 101.7, 106.2, 115.1, 121.7, 143.5, 149.0, 160.1; MS (FAB): *m/z* (%): 461 (75) $[M–OH]^+$, 478 (100) $[M]^+$, 501 (6) $[M+Na]^+$; $C_{25}H_{34}O_9$ (478.5): calcd C 62.75, H 7.16; found C 62.73, H 7.04.

Benzo(5-formylmetaphenylene)[25]crown-8 (**27**). PCC (3.68 g, 17.1 mmol) was added to a stirred solution of **26** (3.27 g, 6.83 mmol) in dry CH_2Cl_2 (150 mL). Although initially orange, the solution very quickly went black, and was stirred for a further 75 min. After this time, the reaction mixture was filtered through a small layer of Celite, which was then washed with CH_2Cl_2 (500 mL). The green CH_2Cl_2 filtrate was stirred with 200 mL aliquots of 2N NaOH solution until colorless, subsequently dried ($MgSO_4$), and the solvent removed *in vacuo* to yield a colorless oil. This oil was dissolved in EtOAc and precipitated with C_6H_{14} to afford the desired compound (**27**) as a powdery white solid (2.55 g, 78 %); m.p. 68–69 °C; ^{1}H NMR (500 MHz, $CDCl_3$): δ = 3.69–3.74 (m, 8H), 3.82–3.86 (m, 8H), 4.12–4.21 (m, 8H), 6.86–6.91 (m, 4H), 6.96–7.00 (m, 3H), 9.84 (s, 1H); ^{13}C NMR (125 MHz, $CDCl_3$): δ = 68.6, 69.1, 70.0, 70.1, 71.2, 71.3, 108.9, 109.3, 115.4, 121.9, 138.4, 149.2, 160.7, 192.1; MS

(FAB): *m/z* (%): 476.5 (100) $[M]^+$; $C_{25}H_{32}O_9$ (476.5): calcd C 63.01, H 6.77; found C 62.89, H 6.80.

(5-[Benzylammoniummethyl]*meta*phenylene)[25]crown-8 Hexafluorophosphate (**22**-H·PF_6). A solution of the formyl-substituted crown ether **27** (685 mg, 1.44 mmol) and benzylamine (**10**) (154 mg, 1.44 mmol) in PhMe (50 mL) was heated under reflux for 24 h using a Dean-Stark apparatus. The resulting solution was evaporated to dryness, the residue dissolved in dry MeOH (100 mL), and $NaBH_4$ (272 mg, 7.19 mmol) was added portionwise over a period of 5 min. After stirring under ambient conditions for 24 h, the reaction mixture was evaporated to dryness, and the residue was partitioned between NaOH solution (2N, 200 mL) and CH_2Cl_2 (200 mL). The aqueous layer was further extracted with CH_2Cl_2 (2 x 250 mL), the combined organic extracts were dried ($MgSO_4$), and the resulting solution was evaporated to dryness to yield an off-white solid. The solid was subsequently dissolved in MeOH (100 mL) and 12M HCl solution (10 mL) was added carefully. After stirring for *ca*. 10 min, the solvents were removed *in vacuo* and the residue dissolved in hot H_2O. Addition of an excess of saturated aqueous NH_4PF_6 to this solution resulted in the precipitation of a white solid. Upon collection, the solid was dissolved in CH_2Cl_2, and precipitated with Et_2O to afford the desired compound as a powdery white solid (152 mg, 15 %); m.p. 177–179 °C (decomp.); ^{1}H NMR (400 MHz, CD_3SOCD_3): δ = 3.56–3.62 (m, 8H), 3.69–3.85 (m, 8H), 4.03–4.09 (m, 6H), 4.13–4.17 (m, 6H), 6.65 (d, J = 2.0 Hz, 2H), 6.71 (t, J = 2.0 Hz, 1H), 6.84–6.89 (m, 2H), 6.92–6.98 (m, 2H), 7.36 (s, 1H), 7.39–7.50 (m, 5H), 9.12 (br s, 2H); ^{13}C NMR (125 MHz, CD_3SOCD_3): δ = 50.1, 67.7, 68.1, 69.1, 70.1, 70.2, 102.3, 108.9, 114.3, 121.2, 128.7, 129.1, 130.0, 131.8, 133.7, 148.3, 159.8; MS (FAB): *m/z* (%): 568.4 (100) $[M–PF_6]^+$, 1135.6 (3) $[2M–H–2PF_6]^+$; $C_{32}H_{42}NO_8PF_6$ (713.6): calcd C 53.86, H 5.93, N 1.96; found C 53.47, H 5.85, N 1.86.

(5-[{3,5-Difluorobenzyl}ammoniummethyl]metaphenylene)[25]crown-8 Hexafluorophosphate (**29**-H·PF_6). A solution of the formyl-substituted crown ether **27** (498 mg, 1.05 mmol) and 3,5-difluorobenzylamine (**20**) (150 mg, 1.05 mmol) in PhMe (50 mL) was heated under reflux for 24 h using a Dean-Stark apparatus. The resulting solution was

evaporated to dryness, the residue dissolved in dry MeOH (100 mL), and $NaBH_4$ (198 mg, 5.23 mmol) was added portionwise over a period of 5 min. After stirring under ambient conditions for 24 h, the reaction mixture was evaporated to dryness, and the residue was partitioned between NaOH solution (2N, 200 mL) and CH_2Cl_2 (200 mL). The aqueous layer was further extracted with CH_2Cl_2 (2 x 250 mL), the combined organic extracts were dried ($MgSO_4$), and the resulting solution was evaporated to dryness to yield a colorless oil. This oil was subsequently dissolved in MeOH (100 mL) and 12M HCl solution (10 mL) was added carefully. After stirring for *ca*. 10 min, the solvents were removed *in vacuo* and the residue dissolved in hot H_2O. Addition of an excess of saturated aqueous NH_4PF_6 to this solution resulted in the precipitation of a white solid. Upon collection, the solid was dissolved in CH_2Cl_2, and precipitated with Et_2O to afford the desired compound as a powdery white solid (143 mg, 18 %); m.p. 180–182 °C (decomp.); ^{1}H NMR (400 MHz, CD_3SOCD_3): δ = 3.57–3.62 (m, 8H), 3.69–3.75 (m, 8H), 4.03–4.09 (m, 6H), 4.13–4.17 (m, 4H), 4.20 (s, 2H), 6.65 (d, J = 2.0 Hz, 2H), 6.72 (t, J = 2.0 Hz, 1H), 6.84–6.89 (m, 2H), 6.92–6.98 (m, 2H), 7.21–7.28 (m, 2H), 7.34 (tt, J_{HH} = 2.4 Hz, J_{HF} = 9.6 Hz, 1H), 9.14 (br s, 2H); ^{19}F NMR (376 MHz, CD_3SOCD_3): δ = –69.7 (d, J = 711 Hz, 6F), –108.8 (s, 2F); ^{13}C NMR (100 MHz, CD_3SOCD_3): δ = 49.1, 50.3, 67.7, 68.1, 69.1, 70.1, 70.2, 102.3, 104.6 (t, J = 25.2 Hz), 108.9, 113.2–113.4 (m), 114.3, 121.2, 133.6, 135.9 (t, J = 9.9 Hz), 148.3, 159.9, 162.2 (dd, J = 13.2, 245 Hz); MS (FAB): *m/z* (%): 604.4 (100) $[M–PF_6]^+$ and $[2M–2PF_6]^{2+}$, 1207.8 (76) $[2M–H–2PF_6]^+$, 1353.9 (8) $[2M–PF_6]^+$; $C_{32}H_{40}NO_8PF_8$ (749.6): calcd C 51.27, H 5.38, N 1.87; found C 51.10, H 5.43, N 1.85.

3.7. References and Notes

1. Staudinger, H. *Ber. Dtsch. Chem. Ges.* **1920**, *53*, 1073–1085.
2. Hermann Staudinger's contribution to the field of polymer science was recognized in 1953 when he was awarded the Nobel Prize for Chemistry.
3. Carothers, W. H. *Chem. Rev.* **1931**, *8*, 353–426.
4. If it wasn't for the fact that Wallace Hume Carothers took his own life at the age of 41 in 1937—after only 9 years with DuPont—he would surely have shared the 1953 Nobel Chemistry Prize with Staudinger.

5. This point is reinforced when considering that, at the time of writing this Thesis, the most recent Nobel Prize in Chemistry (2000) was awarded to Alan Heeger, Alan MacDiarmid, and Hideki Shirakawa, for their work on the discovery and development of conductive polymers.
6. (a) Lehn, J.-M. *Supramolecular Chemistry*; VCH: Weinheim, 1995. (b) *Comprehensive Supramolecular Chemistry*; Atwood, J. L.; Davies, J. E. D.; MacNicol, D. D.; Vögtle, F., Eds.; Pergamon: Oxford, 1996; 11 vols.
7. (a) Archer, R. D. *Coord. Chem. Rev.* **1993**, *128*, 49–68. (b) Rehahn, M. *Acta Polymer.* **1998**, *49*, 201–224. (c) Moore, J. S. *Curr. Opin. Colloid Interface Sci.* **1999**, *4*, 108–116. (d) *Supramolecular Polymers*; Ciferri, A., Ed.; Marcel Dekker, Inc.: New York, 2000.
8. Zimmerman, N.; Moore, J. S.; Zimmerman, S. C. *Chem. Ind.* **1998**, 604–610.
9. (a) Philp, D.; Stoddart, J. F. *Synlett* **1991**, 445–458. (b) Whitesides, G. M.; Mathias, J. P.; Seto, C. T. *Science*, **1991**, *154*, 1312–1319. (c) Lawrence, D. S.; Jiang, T.; Levett, M. *Chem. Rev.* **1995**, *95*, 2229–2260. (d) Philp, D.; Stoddart, J. F. *Angew. Chem., Int. Ed. Engl.* **1996**, *35*, 1154–1196. (e) Stang, P. J.; Olenyuk, B. *Acc. Chem. Res.* **1997**, *30*, 502–518. (f) Cusack, L.; Rao, S. N.; Wenger, J.; Fitzmaurice, D. *Chem. Mater.* **1997**, *9*, 624–631. (g) Conn, M. M.; Rebek, Jr., J. *Chem. Rev.* **1997**, *97*, 1647–1668. (h) Linton, B.; Hamilton, A. D. *Chem. Rev.* **1997**, *97*, 1669–1680. (i) Fujita, M. *Chem. Soc. Rev.* **1998**, *27*, 417–425. (j) Breen, T. L.; Tien, J.; Oliver, S. R. J.; Hadzic, T.; Whitesides, G. M. *Science* **1999**, *284*, 948–951. (k) Tomalia, D. A.; Wang, Z. G.; Tirrel, M. *Curr. Opin. Colloid Interface Sci.* **1999**, *4*, 3–5. (l) Emrick, T.; Fréchet, J. M. J. *Curr. Opin. Colloid Interface Sci.* **1999**, *4*, 15–23. (m) Sijbesma, R. P.; Meijer, E. W. *Curr. Opin. Colloid Interface Sci.* **1999**, *4*, 24–32.
10. Sijbesma, R. P.; Beijer, F. H.; Brunsveld, L.; Folmer, B. J. B.; Ky Hirschberg, J. H. K.; Lange, R. F. M.; Lowe, J. K. L.; Meijer, E. W. *Science* **1997**, *278*, 1601–1604.
11. The degree of polymerization (DP) depends critically upon the association constant (K_a) for two monomer units, (see: Michelsen, U.; Hunter, C. A. *Angew. Chem., Int. Ed.* **2000**, *39*, 764–767), and can be approximated by using the following expression: DP $\approx \sqrt{(K_a[\text{monomer}])}$. Consequently, since $K_a = (T\Delta S - \Delta H)/RT$, changing the temperature can alter dramatically the value of K_a, and hence also that of DP.
12. For recent examples of thermo-responsive polymers, see: (a) Everlof, G. J.; Jaycox, G. D. *Polymer* **2000**, *41*, 6527–6536. (b) Bignotti, F.; Penco, M.; Sartore, L.; Peroni, I.; Mendichi, R.; Casolaro, M.; D'Amore, A. *Polymer* **2000**, *41*, 8247–8256. (c) Pan, H.-Z.; Yan, Y.; Tang, Li.; Wu, Z.-Q.; Li, F.-M. *Macromol. Rapid Commun.* **2000**, *21*, 567–573. (d) Kurisawa, M.; Yokoyama, M.; Okano, T. *J. Controlled Release* **2000**, *69*, 127–137. (e) Kim, S. Y.; Cho, S. M.; Lee, Y. M.; Kim, S. J. *J. Appl. Polym. Sci.* **2000**, *78*, 1381–1391.
13. The exception to this statement relates to equilibrium polymerizations, in which dynamic covalent chemistry is employed for the reversible formation of covalently-bonded polymers. For a general background on this topic, see: (a) Sawada, H. J. *Macromol. Sci. Revs. Macromol. Chem.* **1972**, *C8*, 235–288. For specific examples describing how temperature effects can be used to control the DP

in a given polymer system, see: (b) Chikaoka, S.; Takata, T.; Endo, T. *Macromolecules* **1991**, *24*, 6557–6562. (c) Marsella, M. J.; Maynard, H. D.; Grubbs, R. H. *Angew. Chem., Int. Ed. Engl.* **1997**, *36*, 1101–1103. (d) Lowe, T. L.; Tenhu, H. *Macromolecules* **1998**, *31*, 1590–1594.

14. (a) Constable, E. C. *Chem. Commun.* **1997**, 1073–1080. (b) Kelch, S.; Rehahn, M. *Macromolecules* **1997**, *30*, 6185–6193. (c) Kelch, S.; Rehahn, M. *Macromolecules* **1999**, *32*, 5818–5828. (d) Gardner, M.; Guerin, A. J.; Hunter, C. A.; Michelsen, U.; Rotger, C. *New J. Chem.* **1999**, 309–316. (e) Wojaczynski, J.; Latos-Grazynski, L. *Coord. Chem. Rev.* **2000**, *204*, 113–171. (f) Ogawa, K.; Kobuke, Y. *Angew. Chem., Int. Ed.* **2000**, *39*, 4070–4073. (g) Ellis, W. W.; Schmitz, M.; Arif, A. A.; Stang, P. J. *Inorg. Chem.* **2000**, *39*, 2547–2557. In contrast with these metallo-supramolecular polymers—which exhibit macromolecular properties in solution—much research has been done on the crystal engineering of solid-state coordination networks that are also referred to as 'polymers', see: (h) Hirsch, K. A.; Wilson, S. R.; Moore, J. S. *Inorg. Chem.* **1997**, *36*, 2960–2968. (i) Blake, A. J.; Champness, N. R.; Hubberstey, P.; Li, W. S.; Withersby, M. A.; Schroder, M. *Coord. Chem. Rev.* **1999**, *183*, 117–138. (j) Shimizu, G. K. H.; Enright, G. D.; Rego, G. S.; Ripmeester, J. A. *Can. J. Chem.* **1999**, *77*, 313–318. (k) Carlucci, L.; Ciani, G.; Proserpio, D. M. *Chem. Commun.* **1999**, 449–450. (l) Groeneman, R. H.; MacGillivray, L. R.; Atwood, J. L. *Inorg. Chem.* **1999**, *38*, 208–209. (m) Gudbjartson, H.; Biradha, K.; Poirier, K. M.; Zaworotko, M. J. *J. Am. Chem. Soc.* **1999**, *121*, 2599–2600. (n) Kleina, C.; Graf, E.; Hosseini, M. W.; De Cian, A.; Fischer, J. *Chem. Commun.* **2000**, 239–240. (o) Hong, M.; Zhao, Y.; Su, W.; Cao, R.; Fujita, M.; Zhou, Z.; Chan, A. S. C. *Angew. Chem., Int. Ed.* **2000**, *39*, 2468–2470. (p) Robson, R. *J. Chem. Soc., Dalton Trans.* **2000**, 3735–3744. (q) Biradha, K.; Fujita, M. *J. Chem. Soc., Dalton Trans.* **2000**, 3805–3810. (r) Sharma, A. C.; Borovik, A. S. *J. Am. Chem. Soc.* **2000**, *122*, 8946–8955.

15. (a) Alcock, N. W.; Barker, P. R.; Haider, J. M.; Hannon, M. J.; Painting, C. L.; Pikramenou, Z.; Plummer, E. A.; Rissanen, K.; Saarenketo, P. *J. Chem. Soc., Dalton Trans.* **2000**, 1447–1461. (b) Hirschberg, J. H. K. K.; Brunsveld, L.; Ramzi, A.; Vekemans, J. A. J. M.; Sijbesma, R. P.; Meijer, E. W. *Nature* **2000**, *407*, 167–170.

16. (a) Bladon, P.; Griffin, A. C. *Macromolecules* **1993**, *26*, 6604–6610. (b) Alexander, C.; Jariwala, C. P.; Lee, C. M.; Griffin, A. C. *Macromol. Symp.* **1994**, *77*, 283–294. (c) Lee, C. M.; Jariwala, C. P.; Griffin, A. C. *Polymer* **1994**, *35*, 4550–4554. (d) St Pourcain, C. B.; Griffin, A. C. *Macromolecules* **1995**, *28*, 4116–4121. (e) Lee, C. M.; Griffin, A. C. *Macromol. Symp.* **1997**, *117*, 281–290.

17. (a) Ducharme, Y.; Wuest, J. D. *J. Org. Chem.* **1988**, *53*, 5787–5789. (b) Lillya, C. P.; Baker, R. J.; Hutte, S.; Winter, H. H.; Lin, Y. G.; Shi, J. F.; Dickinson, L. C.; Chen, J. C. W. *Macromolecules* **1992**, *25*, 2076–2080. (c) Abed, S.; Boileau, S.; Bouteiller, L. *Macromolecules* **2000**, *33*, 8479–8487.

18. (a) Kotera, M.; Lehn, J.-M.; Vigneron, J.-P. *J. Chem. Soc., Chem. Commun.* **1994**, 197–199. (b) Russell, K. C.; Lehn, J.-M.; Kyritsakas, N.; DeCian, A.; Fischer, J. *New J. Chem.* **1998**,

123–128. (c) Choi, I. S.; Li, X.; Simanek, E. E.; Akaba, R.; Whitesides, G. M. *Chem. Mater.* **1999**, *11*, 684–690. (d) Klok, H.-A.; Jolliffe, K. A.; Schauer, C. L.; Prins, L. J.; Spatz, J. P.; Möller, M.; Timmerman, P.; Reinhoudt, D. N. *J. Am. Chem. Soc.* **1999**, *121*, 7154–7155.

19. (a) Folmer, B. J. B.; Cavini, E.; Sijbesma, R. P.; Meijer, E. W. Chem. Commun. 1998, 1847–1848. (b) Hirschberg, J. H. K. K.; Beijer, F. H.; van Aert, H. A.; Magusim, P. C. M. M.; Sijbesma, R. P.; Meijer, E. W. *Macromolecules* **1999**, *32*, 2696–2705. (c) Lange, R. F. M.; Van Gurp, M.; Meijer, E. W. *J. Polym. Sci., Part A: Polym. Chem.* **1999**, *37*, 3657–3670. (d) Folmer, B. J. B.; Sijbesma, R. P.; Versteegen, R. M.; van der Rijt, J. A. J.; Meijer, E. W. *Adv. Mater.* **2000**, *12*, 874–878. (e) Boileau, S.; Bouteiller, L.; Lauprêtre, F.; Lortie, F. *New J. Chem.* **2000**, 845–848.

20. (a) Castellano, R. K.; Rudkevich, D. M.; Rebek, Jr., J. *Proc. Natl. Acad. Sci. USA* **1997**, *94*, 7132–7137. (b) Castellano, R. K.; Rebek, Jr., J. *J. Am. Chem. Soc.* **1998**, *120*, 3657–3663. (c) Castellano, R. K.; Rebek, Jr., J. *Polym. Mater. Sci. Eng.* **1999**, *80*, 16–17. (d) Castellano, R. K.; Nuckolls, C.; Eichhorn, S. H.; Wood, M. R.; Lovinger, A. J.; Rebek, Jr., J. *Angew. Chem., Int. Ed.* **1999**, *38*, 2603–2606.

21. (a) Beijer, F. H.; Kooijman, H.; Spek, A. L.; Sijbesma, R. P.; Meijer, E. W. *Angew. Chem., Int. Ed.* **1998**, *37*, 75–78. (b) Beijer, F. H.; Sijbesma, R. P.; Kooijman, H.; Spek, A. L.; Meijer, E. W. *J. Am. Chem. Soc.* **1998**, *120*, 6761–6769. (c) El-ghayoury, A.; Peeters, E.; Schenning, A. P. H. J.; Meijer, E. W. *Chem. Commun.* **2000**, 1969–1970. For other recent examples of self-complementary quadruple hydrogen-bonded dimers—yet to be utilized in the construction of larger aggregates—see: (d) Corbin, P. S.; Zimmerman, S. C. *J. Am. Chem. Soc.* **1998**, *120*, 9710–9711. (e) Davis, A. P.; Draper, S. M.; Dunne, G.; Ashton, P. R. *Chem. Commun.* **1999**, 2265–2266.

22. For recent examples, see: (a) Jeon, Y. M.; Whang, D.; Kim, J.; Kim, K. *Chem. Lett*. **1996**, 503–504. (b) Mirzoian, A.; Kaifer, A. E. *Chem. Eur. J.* **1997**, *3*, 1052–1058. (c) Sleiman, H.; Baxter, P. N. W.; Lehn, J.-M.; Airola, K.; Rissanen, K. *Inorg. Chem.* **1997**, *36*, 4734–4742. (d) Loeb, S. J.; Wisner, J. A. *Angew. Chem., Int. Ed.* **1998**, *37*, 2838–2840. (e) Smith, A. C.; Macartney, D. H. *J. Org. Chem.* **1998**, *63*, 9243–9251. (f) Asakawa, M.; Ashton, P. R.; Balzani, V.; Boyd, S. E.; Credi, A.; Mattersteig, G.; Menzer, S.; Montalti, M.; Raymo, F. M.; Ruffilli, C.; Stoddart, J. F.; Venturi, M.; Williams, D. J. *Eur. J. Org. Chem.* **1999**, 985–994. (g) Cantrill, S. J.; Fyfe, M. C. T.; Heiss, A. M.; Stoddart, J. F.; White, A. J. P.; Williams, D. J. *Org. Lett.* **2000**, *2*, 61–64. (h) Chang, T.; Heiss, A. M.; Cantrill, S. J.; Fyfe, M. C. T.; Pease, A. R.; Rowan, S. J.; Stoddart, J. F.; Williams, D. J. *Org. Lett.* **2000**, *2*, 2943–2946. (i) Chang, T.; Heiss, A. M.; Cantrill, S. J.; Fyfe, M. C. T.; Pease, A. R.; Rowan, S. J.; Stoddart, J. F.; White, A. J. P.; Williams, D. J. *Org. Lett.* **2000**, *2*, 2947–2950. (j) Ryan, D.; Rao, S. N.; Rensmo, H.; Fitzmaurice, D.; Preece, J. A.; Wenger, S.; Stoddart, J. F.; Zaccheroni, N. *J. Am. Chem. Soc.* **2000**, *122*, 6252–6257. (k) Chichak, K.; Walsh, M. C.; Branda, N. R. *Chem. Commun.* **2000**, 847–848.

23. These complexes—in which an acyclic component is threaded through a cyclic one—are simply rotaxanes which are lacking the bulky end-groups, and are, therefore, termed *pseudorotaxanes*. In fact, pseudorotaxanes occupy a pivotal position in the chemistry of mechanically-interlocked compounds, as they can serve as intermediates in the syntheses of *both* catenanes and rotaxanes. For recent examples, see: (a) Hansen, J. G.; Feeder, N.; Hamilton, D. G.; Gunter, M. J.; Becher, J.; Sanders, J. K. M. *Org. Lett.* **2000**, *2*, 449–452. (b) Raehm, L.; Hamann, C.; Kern, J.-M.; Sauvage, J.-P. *Org. Lett.* **2000**, *2*, 1991–1994; (c) Safarowsky, O.; Vogel, E.; Vögtle, F. *Eur. J. Org. Chem.* **2000**, 499–505. (d) Cabezon, B.; Cao, J.; Raymo, F. M.; Stoddart, J. F.; White, A. J. P.; Williams, D. J. *Chem. Eur. J.* **2000**, *6*, 2262–2273. (e) Reuter, C.; Vögtle, F. *Org. Lett.* **2000**, *2*, 593–595. (f) Skinner, P. J.; Blair, S.; Kataky, R.; Parker, D. *New J. Chem.* **2000**, *24*, 265–268. (g) Kawaguchi, Y.; Harada, A. *Org. Lett.* **2000**, *2*, 1353–1356. (h) Loeb, S. J.; Wisner, J. A. *Chem. Commun.* **2000**, 845–846. (i) Buston, J. E. H.; Young, J. R.; Anderson, H. L. *Chem. Commun.* **2000**, 905–906. (j) Cantrill, S. J.; Fulton, D. A.; Heiss, A. M.; Pease, A. R.; Stoddart, J. F.; White, A. J. P.; Williams, D. J. *Chem. Eur. J.* **2000**, *6*, 2274–2287. (k) Tachibana, Y.; Kihara, N.; Ohga, Y.; Takata, T. *Chem. Lett.* **2000**, 806–807.

24. An alternative approach requires the self assembly of two homoditopic monomers, *i.e.*, AA and BB building blocks, rather than a self-complementary AB one. See: (a) Yamaguchi, N.; Gibson, H. W. *Angew. Chem., Int. Ed.* **1999**, *38*, 143–147. (b) Yamaguchi, N.; Gibson, H. W. *Chem. Commun.* **1999**, 789–790. Interwoven supramolecular polymers constructed in this fashion would serve as precursors for a novel interlocked macromolecular architecture, recently termed a 'figure 8 polyrotaxane' by Busch *et al.*, see: Hubin, T. J.; Kolchinski, A. G.; Vance, A. L.; Busch, D. H. *Adv. Supramol. Chem.* **1999**, *10*, 237–357.

25. (a) Ashton, P. R.; Parsons, I. W.; Raymo, F. M.; Stoddart, J. F.; White, A. J. P.; Williams, D. J.; Wolf, R. *Angew. Chem., Int. Ed.* **1998**, *37*, 1913–1916. (b) Yamaguchi, N.; Nagvekar, D. S.; Gibson, H. W. *Angew. Chem., Int. Ed.* **1998**, *37*, 2361–2364. (c) Mirzoian, A.; Kaifer, A. E. *Chem. Commun*. **1999**, 1603–1604. (d) Bülger, J.; Sommerdijk, N. A. J. M.; Visser, A. J. W. G.; van Hoek, A.; Nolte, R. J. M.; Engbersen, J. F. J.; Reinhoudt, D. N. *J. Am. Chem. Soc*. **1999**, *121*, 28–33. (e) Nielsen, M. B.; Hansen, J. G.; Becher, J. *Eur. J. Org. Chem.* **1999**, 2807–2815. (f) Jiménez, M. C.; Dietrich-Buchecker, C.; Sauvage, J.-P.; De Cian, A. *Angew. Chem., Int. Ed.* **2000**, *39*, 1295–1298.

26. Appropriately mono-substituted cyclo-oligosaccharides have been shown to crystallize to give arrays of this type in the solid state, see: (a) Hirotsu, K.; Higuchi, T.; Fujita, K.; Ueda, T.; Shinoda, A.; Imoto, T.; Tabushi, I. *J. Org. Chem*. **1982**, *47*, 1143-1144. (b) Mentzafos, D.; Terzis, A.; Coleman, A. W.; de Rango, C. *Carbohydr. Res*. **1996**, *282*, 125-135. (c) Liu, Y.; You, C.-C.; Zhang, M.; Weng, L.-H.; Wada, T.; Inoue, Y. *Org. Lett.* **2000**, *2*, 2761–2763.

27. Cyclic arrays are formed whenever chain termination of a propagating acyclic species occurs *via* intramolecular 'back-biting'. For examples, see: ref. 25a,c,f. In some less geometrically-demanding cases, the monomeric species is also capable of biting its own tail, to form an intramolecular self-

complexed species, see: ref. 25d,e, and Ashton, P. R.; Ballardini, R.; Balzani, V.; Boyd, S. E.; Credi, A.; Gandolfi, M. T.; Gómez-López, M.; Iqbal, S.; Philp, D.; Preece, J. A.; Prodi, L.; Ricketts, H. G.; Stoddart, J. F.; Tolley, M. S.; Venturi, M.; White, A. J. P.; Williams, D. J. *Chem. Eur. J.* **1997**, *3*, 152–170.

28. The term 'daisy chain' is used to describe an interwoven chain—usually made of flowers (hence 'daisy')—in which each unit acts as a 'donor' and an 'acceptor' for a threading interaction. The standard definition (*Webster's Third New International Dictionary*; Babcock-Gove, P., Ed.; Merriam–Webster: Springfield MA, 1993) of a 'daisy chain' is; '*a string of daisies with stems linked to form a chain, ... such a chain carried by chosen students at a class day or other celebration in some women's colleges.*'. Perhaps a much more lascivious definition can be found in the *Oxford Dictionary of Slang* (Ayto, J. Oxford University Press Inc.: New York, 1999), which relates the fact that the expression 'daisy chain' can be, '*applied to sexual activity involving three or more people*', and was first used for such a purpose *ca*. 1927! With regard to chemical systems, it should be noted that Busch and coworkers—not content with descriptions already used in the primary chemical literature—coined their own term for such a supramolecular polymeric architecture, calling it a 'figure 9 pseudopolyrotaxane', see: Hubin, T. J.; Busch, D. H. *Coord. Chem. Rev.* **2000**, *200-202*, 5–52.

29. Small cyclic daisy chain structures have been trapped kinetically upon post-assembly covalent modification of the corresponding complexes. For examples of dimers, see: (a) Jiménez, M. C.; Dietrich-Buchecker, C.; Sauvage, J.-P. *Angew. Chem., Int. Ed.* **2000**, *39*, 3284–3287. (b) Fujimoto, T.; Sakata, Y.; Kaneda, T. *Chem. Commun.* **2000**, 2143–2144. For a captured trimer, see: (c) Hoshino, T.; Miyauchi, M.; Kawaguchi, Y.; Yamaguchi, H.; Harada, A. *J. Am. Chem. Soc.* **2000**, *122*, 9876–9877. An alternative approach for the construction of these novel mechanically interlocked assemblies—which relies upon covalent, rather than noncovalent, oligo/polymerization —was communicated before any of the above reports, see: (d) Rowan, S. J.; Cantrill, S. J.; Stoddart, J. F.; White, A. J. P.; Williams, D. J. *Org. Lett.* **2000**, *2*, 759–762.

30. Daisy chain polyrotaxanes represent only one class of macromolecules with architectures reminiscent of rotaxanes. For a survey of possible linkages that constitute a polyrotaxane ensemble, see: (a) Amabilino, D. B.; Parsons, I. W.; Stoddart, J. F. *Trends Polym. Sci.* **1994**, *2*, 146–152. (b) Gibson, H. W.; Bheda, M. C.; Engen, P. T. *Prog. Polym. Sci.* **1994**, *19*, 843–945. (c) Raymo, F. M.; Stoddart, J. F. *Chem. Rev.* **1999**, *99*, 1643–1663. For specific examples of non-daisy chain polyrotaxane macro-structures, see: (d) Herrmann, W.; Schneider, M.; Wenz, G. *Angew. Chem., Int. Ed. Engl.* **1997**, *36*, 2511–2514. (e) Gong, C. G.; Gibson, H. W.; *Angew. Chem., Int. Ed.* **1998**, *37*, 310–314. (f) Harada, A. *Acta Polymer*. **1998**, 49, 3–17. (g) Park, K. M.; Heo, J.; Roh, S. G.; Jeon, Y. M.; Whang, D.; Kim, K. *Mol. Cryst. Liq. Crys. A* **1999**, *327*, 65–70. (h) Ooya, T.; Arizono, K.; Yui, N. *Polym. Adv. Technol.* **2000**, *11*, 642–651.

31. See Chapter 2 of this Thesis, and references therein.

32. Despite repeated efforts, the PF_6^- salt of $\mathbf{1}^+$ would not crystallize to give material of suitable quality for single crystal X-ray analysis. However, on changing to the $CF_3CO_2^-$ anion, good crystals were obtained easily.
33. Ashton, P. R.; Chrystal, E. J. T.; Glink, P. T.; Menzer, S.; Schiavo, C.; Spencer, N.; Stoddart, J. F.; Tasker, P. A.; White, A. J. P.; Williams, D. J. *Chem. Eur. J.* **1996**, *2*, 709–728.
34. DB24C8-sized macrocycles and phenyl-terminated secondary ammonium ions form threaded complexes at a rate slower than the ^{1}H NMR timescale. Consequently, all different species present in solution give rise to their own distinct set of NMR resonances. See: ref. 33 and Chapter 2 of this Thesis.
35. This observation is based upon ^{1}H NMR spectroscopic analyses of the numerous catechol-derived aromatic compounds that have been studied during the research that now constitutes this Thesis.
36. Despite studying space-filling molecular models of the different diastereoisomeric dimeric superstructures, it is difficult to produce a rationalization for which diastereoisomer should result in a greater shift for the signal associated with H_1, and which for H_3.
37. At concentrations greater than this one, **1**-H·PF_6 begins to precipitate only a few minutes after complete dissolution.
38. This model—for simplicity's sake—also assumes that only one stereoisomeric cyclic dimer, and only one stereoisomeric cyclic trimer are formed.
39. See Chapter 2 of this Thesis.
40. The conclusion that lower values of K_a (especially K_{a1}) than those observed in model systems fit better the experimental data observed here may reflect the fact that oligomerization of this self-complementary system always requires bringing together two positively charged species. This repulsive Coulombic effect may serve to reduce the overall affinity for two daisy chain monomers in comparison with the model two component system, in which a *cationic* thread is bound by a *neutral* macrocycle.
41. Baban, J. A.; Goodchild, N. J.; Roberts, B. P. *J. Chem. Soc., Perkin Trans. 2* **1986**, 157–161.
42. When complexed and uncomplexed species are equilibrating slowly on the ^{1}H NMR timescale, three different sets of resonances are observed, which arise from (1) the free crown ether host, (2) the uncomplexed guest, and (3) the 1:1 complex formed between the host and guest. See Chapter 2 of this Thesis for more detail.
43. See Chapter 2 of this Thesis for more examples.
44. In a slowly equilibrating complexation/decomplexation scenario, K_a values are determined as follows: integration of the peaks in the ^{1}H NMR spectrum associated with (1) free host, (2) free guest, and (3) 1:1 complex are measured, and by knowing accurately the concentrations of host and guest species that were dissolved initially, equilibrium concentrations can be determined. The K_a value is then given simply by dividing the equilibrium concentration of the 1:1 complex by the product of the equilibrium concentrations of the free host and guest species. To minimize errors in this study, numerous probe protons—associated with each of the three species present in

solution—were used to calculate K_a values in any one spectrum. These K_a values were simply averaged for each spectrum. Furthermore, at least three independent ^{1}H NMR spectroscopic analyses were performed for each host:guest system, and the subsequent K_a values were—once again—averaged. For leading references on this method, see Adrian, J. C.; Wilcox, C. S. *J. Am. Chem. Soc*. **1991**, *113*, 678–680.

45. Decomposition of the PF_6^- anion was also observed in another crown ether/secondary ammonium ion hexafluorophosphate salt binding experiment performed in a sealed NMR tube. Heiss, A. M., private comminication. It appears that a contributing factor is the presence of acidic impurities in $CDCl_3$, prompting an acid catalyzed decomposition. If, prior to use, the $CDCl_3$ is passed through a short column of basic alumina, no decomposition of the PF_6^- anion is observed. No decomposition of the PF_6^- anion was observed *in any other systems* investigated in this Chapter.

46. The doublet upfield of that one arising from the resonance of the PF_6^- anion has a coupling constant of ~950 Hz. This observation is consistent with the reported behavior of PF_5, which gives rise to only one doublet at this temperature (Lazzeretti, P.; Tossell, J. A. *J. Magn. Reson.* **1986**, *70*, 461–464), with a PF-coupling constant of ~920 Hz, see: Holmes, R. R. *Pentacoordinated Phosphorus*, Vol. 1; ACS Monograph 175; Washington D. C., 1980, pp. 104–105.

47. *Dictionary of Inorganic Compounds*, 1st Ed., Vol. 3; Chapman & Hall: London, 1992, pp. 3208.

48. NMR tubes were sealed as follows: (i) the sample-filled NMR tube was frozen in a Me_2CO/CO_2 bath, (ii) whilst, at this reduced temperature, a vacuum was applied to the top of the NMR tube, and finally (iii) a high temperature flame (glass-blowing torch) was used to melt the top of the NMR tube and thereby form a closed system (the partial vacuum makes it easier to seal the NMR tube). Consequently, the pressure inside the sealed NMR tube is less than atmospheric pressure.

49. Decomposition of the PF_6^- anion presumably results, initially, in the formation of F^-. This anion, however, is unlikely to be a non-participating one, and thus the observation that the F-substituted dibenzylammonium cation still threads through DB24C8, suggests that the new anion results as a product of the reaction of F^- with some other species in solution, or even the walls of the NMR tube. It should be noted, however, that no etching of the NMR tube was observed. Furthermore, no significant precipitation could be detected.

50. In general, most secondary ammonium ion hexafluorophosphate salts—as observed during the course of this research—are not soluble in water and, consequently, are isolated using this aqueous anion-exchange technique.

51. The kinetics of threading/dethreading in this particular system may be greater at 60 °C, but the thermodynamics of pseudorotaxane formation must also be favorable at this temperature to support this hypothesis. Although increasing the temperature in a [24]crown-8 daisy chain system (**1**-$H\cdot PF_6$) dissolved in CD_3CN has been shown (see Section 3.2.1) to decrease the propensity for aggregation, the association of these species in $MeNO_2$ is expected to be much stronger, based upon a model system, see: Cao, J.; Fyfe, M. C. T.; Stoddart, J. F.; Cousins, G. R. L.; Glink, P. T. *J. Org. Chem*. **2000**, *65*, 1937–1946.

52. The 'slippage' methodology was first exploited for rotaxane syntheses that were conducted in a statistical manner. In the absence of mutual recognition interactions between the ring and thread, formation of a rotaxane-like complex relied simply upon chance encounters between the components. For examples, see: (a) Harrison, I. T. *J. Chem. Soc., Chem. Commun.* **1972**, 231–232. (b) Agam, G.; Gravier, D.; Zilkha, A. *J. Am. Chem. Soc.* **1976**, *98*, 5206–5214 (c) Schill, G.; Beckmann, W.; Schweikert, N.; Fritz, H. *Chem. Ber.* **1986**, *119*, 2647–2655. The successful marriage—first reported in 1993 (see (d) Ashton, P. R.; Belohradsky, M; Philp, D.; Stoddart, J. F. *J. Chem. Soc., Chem. Commun.* **1993**, 1269–1274)—of template-directed approaches with slippage resulted in efficient noncovalent syntheses of rotaxane-like complexes. See also: (e) Raymo, F. M.; Stoddart J. F. *Pure Appl. Chem*. **1997**, *69*, 1987–1997. (f) Macartney, D. H. *J. Chem. Soc., Perkin Trans. 2* **1996**, 2775–2778. (g) Händel, M.; Plevoets, M.; Gestermann, S.; Vögtle, F. *Angew. Chem., Int. Ed. Engl.* **1997**, *36*, 1199–1201. (h) Ashton, P. R.; Ballardini, R.; Balzani, V.; Belohradsky, M.; Gandolfi, M. T.; Philp, D.; Prodi, L.; Raymo, F. M.; Reddington, M. V.; Spencer, N.; Stoddart, J. F.; Venturi, M.; Williams, D. J. *J. Am. Chem. Soc.* **1996**, *118*, 4931–4951. (i) Asakawa, M.; Ashton, P. R.; Ballardini, R.; Balzani, V.; Belohradsky, M.; Gandolfi, M. T.; Kocian, O.; Prodi, L.; Raymo, F. M.; Stoddart, J. F.; Venturi, M. *J. Am. Chem. Soc.* **1997**, *119*, 302–310. (j) Ashton, P. R.; Fyfe, M. C. T.; Schiavo, C.; Stoddart, J. F.; White, A. J. P.; Williams, D. J. *Tetrahedron Lett.* **1998**, *39*, 5455–5458. (k) Heim, C.; Affeld, A.; Nieger, M.; Vögtle, F. *Helv. Chim. Acta* **1999**, *82*, 746–759. (l) Fyfe, M. C. T.; Raymo, F. M.; Stoddart, J. F. In *Stimulating Concepts in Chemistry*; Shibasaki, M., Stoddart, J. F., Vögtle, F., Eds.; VCH-Wiley: Weinheim, 2000, pp. 211–220.

53. See Chapter 2 of this Thesis, and: Ashton, P. R.; Bartsch, R. A.; Cantrill, S. J.; Hanes, Jr., R. E.; Hickingbottom, S. K.; Lowe, J. N.; Preece, J. A.; Stoddart, J. F.; Talanov, V. S.; Wang, Z.-H. *Tetrahedron Lett*. **1999**, *40*, 3661–3664.

54. Mertens, I. J. A.; Wegh, R.; Jenneskens, L. W.; Vlietstra, E. J.; van der Kerk-van Hoof, A.; Zwikker, J. W.; Cleij, T. J.; Smeets, W. J. J.; Veldman, N.; Spek, A. L. *J. Chem. Soc., Perkin Trans. 2* **1998**, 725–735.

55. See Chapter 2 of this Thesis, and ref. 23j.

56. The solvent of choice was CD_3CN, as no meaningful ^1H or ^{19}F NMR spectroscopic results were obtained for CD_3NO_2 or CD_2Cl_2 solutions of **29**-H·PF_6.

57. The monomeric structure shown in Figure 3.47 can aggregate in many ways. Only two of these ways are shown. For example, the 'slipped' dimer could, in theory, aggregate with other 'slipped' dimer assemblies by utilizing any of the unsatisfied recognition sites.

58. The entropic cost associated with the loss of rotational and translational entropy on assembly, is proportional to the number of particles that go to form that assembly, see: Simanek, E. E.; Li, X.; Choi, I. S.; Whitesides, G. M. In *Comprehensive Supramolecular Chemistry*; Atwood, J. L.; Davies, J. E. D.; MacNicol, D. D.; Vögtle, F., Eds.; Pergamon: Oxford, 1996, pp. 595–621.

59. Krämer, R.; Lehn, J.-M.; Marquis-Rigault, A. *Proc. Natl. Acad. Sci. USA* **1993**, *90*, 5394–5398.

60. Chang, T.; Heiss, A. M.; Cantrill, S. J.; Fyfe, M. C. T.; Pease, A. R.; Rowan, S. J.; Stoddart, J. F.; White, A. J. P.; Williams, D. J. *Org. Lett*. **2000**, *2*, 2947–2950.

61. Poly[2]catenanes are also interlocked macromolecules that possess no continuous covalent backbone. For examples of these structures, and discussion of their properties, see: (a) Hamers, C.; Raymo, F. M.; Stoddart, J. F. *Eur. J. Org. Chem.* **1998**, 2109–2117. (b) Weidmann, J.-L.; Kern, J.-M.; Sauvage, J.-P.; Muscat, D.; Mullins, S.; Köhler, W.; Rosenauer, C.; Räder, H. J.; Martin, K.; Geerts, Y. *Chem. Eur. J.* **1999**, *5*, 1841–1851. (c) Muscat, D.; Köhler, W.; Räder, H. J.; Martin, K.; Mullins, S.; Müller, B.; Müllen, K.; Geerts, Y. *Macromolecules* **1999**, *32*, 1737–1745.

62. Performed in collaboration with Professor Stuart Rowan at the Department of Macromolecular Science, of Case Western Reserve University.

63. Perrin, D. D.; Armarego, W. F. L. *Purification of Laboratory Chemicals*; Pergamon: Oxford, 1989.

64. SHELXTL PC version 5.03, Siemens Analytical X-Ray Instruments, Inc., Madison, WI, 1994.

65. Copies of the crystallographic data can be obtained free of charge on application to CCDC, 12 Union Road, Cambridge CB12 1EZ, UK (Fax: (+44) 1223-336033; E-mail: teched@ccdc.cam. ac.uk).